Regulation and function of heparanase in the heart

by

FULONG WANG

B.Sc., Southeast University, 2009

M.Sc., University of Chinese Academy of Sciences, 2013

A DISSERTATION SUBMITTED IN PARTIAL FULFILLMENT OF

THE REQUIREMENTS FOR THE DEGREE OF

DOCTOR OF PHILOSOPHY

in

THE FACULTY OF GRADUATE AND POSTDOCTORAL STUDIES

(Pharmaceutical Sciences)

THE UNIVERSITY OF BRITISH COLUMBIA

(Vancouver)

December 2018

© Fulong Wang, 2018

The following individuals certify that they have read, and recommend to the Faculty of Graduate and Postdoctoral Studies for acceptance, the dissertation entitled:

Regulation and function of heparanase in the heart

submitted	Fulong Wang	in partial fulfillment of the requirements
the degree of	Doctor of Philosophy	
in	Pharmaceutical Sciences	

Examining Committee:

Brian Rodrigues, Pharmaceutical Sciences

Supervisor

Dan Luciani, Faculty of Medicine

Supervisory Committee Member

Bruce Verchere, Faculty of Medicine

Supervisory Committee Member

Lucy Marzban

University Examiner

Angela Devlin

University Examiner

Additional Supervisory Committee Members:

David Granville, Faculty of Medicine

Supervisory Committee Member

Corey Nislow, Pharmaceutical Sciences

Supervisory Committee Member

Abstract

Enzymatically-active heparanase (Hep^A) has been implicated as an essential metabolic adaptation in the heart following diabetes. However, the regulation of the enzymatically-inactive heparanase (Hep^L) remain poorly understood. We hypothesized that in response to high glucose (HG) and secretion of Hep^L from the endothelial cell (EC), Hep^L uptake and function can protect the cardiomyocyte by modifying its cell death signature. HG promoted both Hep^L and Hep^A secretion from EC, with subsequent uptake of Hep^L into cardiomyocytes. This occurred through a low-density lipoprotein receptor-related protein 1 (LRP1) dependent mechanism, as LRP1 inhibition significantly reduced uptake. Exogenous addition of Hep^L to rat cardiomyocytes produced a dramatically altered expression of apoptosis-related genes, and protection against HG and H_2O_2 induced cell death. Cardiomyocytes from acutely diabetic rats demonstrated a robust increase in LRP1 expression and levels of heparanase, a pro-survival gene signature, and limited evidence of cell death, observations that were not apparent following chronic and progressive diabetes. We also tested if overexpression of heparanase can protect the heart against chemically induced or ischemia/reperfusion (I/R) injury. Mice overexpressing heparanase (Hep-tg) displayed physiological cardiac hypertrophy and changes in expression of genes related to the stress response, immune response, cell death, and development. These transcriptomic alterations were associated with promotion of unfolded protein response (UPR), autophagy, and oxidative stress resistance in a pro-survival direction. The UPR activation was adaptive and not apoptotic, and together with mTOR inhibition, induced autophagy. Subjecting wild type mice to thapsigargin evoked a transition from adaptive

to apoptotic UPR, an effect attenuated in Hep-tg hearts. When exposed to I/R, infarct size and apoptosis were significantly lower in the Hep-tg heart, an effect reversed by inhibitors of UPR and autophagy. Our results highlight EC-to-cardiomyocyte transfer of heparanase to modulate the cardiomyocyte cell death signature. This mechanism was observed in the acutely diabetic heart, and its interruption following chronic diabetes may contribute towards the development of diabetic cardiomyopathy. Moreover, we established that the mechanisms by which heparanase promotes cell survival in cancer could be uniquely beneficial to the heart and exploited as a therapeutic target for the treatment of heart disease.

Lay Summary

Heparanase is an enzyme that contributes to the survival of cancer cells under harsh and stressful conditions like radioactive-therapy and chemotherapy and thus contributes towards the aggressiveness of cancer development. The heart cells, contrary to cancer cells, are vulnerable to different types of stresses. This, combined with the limited capability of this organ to regenerate new cells following cell death, leads to the prevalence of heart diseases. We explored the possibility of utilizing the properties of this enzyme to protect cardiac cells against cell death. We found out that heparanase, using its properties to promote cell survival, protected the heart cells against multiple stresses frequently seen in patients with ischemia and diabetes induced heart diseases, in both cell experiments and animal studies. This research could help devise new strategies to combat heart diseases.

Preface

This thesis is written by F. Wang and reviewed by Dr. Rodrigues. All the experiments in this thesis were designed and conceived by F. Wang under the supervision of Dr. Rodrigues. Studies in chapter 3 has been previously published (F. Wang, J. Jia, N. Lal, D. Zhang, A. P. Chiu, A. Wan, I. Vlodavsky, B. Hussein, B. Rodrigues. 2016. *High glucose facilitated endothelial heparanase transfer to the cardiomyocyte modifies its cell death signature*. **Cardiovascular Research**). F. Wang designed all the experiments and wrote the manuscript with Dr. Rodrigues. D. Zhang, B. Hussein, J. Jia, N. Lal, R. Shang, A. Wan, Y. Wang, and AP. Chiu participated in data analysis and manuscript editing. Dr. Vlodavsky provided the recombinant heparanase. Data in chapter 4 is currently submitted (Fulong Wang, Yanzhi Carolyn Jia, Dahai Zhang, Boris Trinajstic, Jocelyn Jia, Nathaniel Lal, Karn Puri, Rui Shang, Stephane Flibotte, Sunita Sinha, Purvi Trivedi, Dipsikha Biswas, Kathleen Macleod, Corey Nislow, Israel Vlodavsky, Thomas Pulinilkunnil, Bahira Hussein, and Brian Rodrigues. 2018. *Heparanase Overexpression Protects Mouse Heart against Chemical or Ischemia/Reperfusion Injury*. Submitted). D. Zhang, B. Hussein, J. Jia, N. Lal, R. Shang, A. Wan, Y. Wang, and AP. Chiu contributed in editing the manuscript. S. Flibotte and S. Sinha performed the RNAseq of ventricle and analyzed the data. YZ-C. Jia performed the echocardiology. Dr. Vlodavsky provided the heparanase transgenic mice. Dr. Pulinilkunnil assisted in conceiving some of the experiments and did part of the ischemia/reperfusion experiments. B. Hussein provided assistance with monitoring the animals, technical support and editing the manuscript. The study conforms to the guide for the care and use of laboratory animals published by the US National Institutes of Health, and was approved

by the Animal Care Committee in the University of British Columbia (Certificate No. A13-0250).

Table of Contents

List of Tables

List of Figures

List of Abbreviations and Acronyms

Acta1	Alpha-actin-1
AEBSF	4-(2-aminoethyl)benzenesulfonyl fluoride hydrochloride
AMPK	AMP-activated protein kinase
ADP	Adenosine diphosphate
AKT/PKB	Protein kinase B
ATF4	Activating transcription factor 4
ATF6α	Activating transcription factor 6 alpha
ATP	Adenosine triphosphate
Bax	BCL2 associated x
bCAECs	Bovine coronary artery endothelial cells
Bcl2	B-cell lymphoma 2
BiP	Binding-immunoglobulin protein
Calr	Calreticulin
CFLAR	CASP8 and fadd like apoptosis regulator
CHOP	CCAAT/enhancer-binding protein homologous protein
CNS	Central nervous system
Ctsl	Cathepsin L
CPM	Count per million
CPT	Carnitine palmitoyltransferase
CQ	Chloroquine
DE	Differentially expressed
ECs	Endothelial cells

ECM	Extracellular matrix
ECCM	Endothelial cell Conditioned medium
ER	Endoplasmic reticulum
ERK	Extracellular signal–regulated kinases
FC	Fold change
FDR	False discovery rate
FGF	Fibroblast growth factor
HAT	Histone acetyltransferase
Hep	Heparanase
Hep^{A}	Active heparanase
Hep^{L}	Latent heparanase
Hep-tg	Heparanase transgenic
HPSE	Heparanase
HS	Heparan sulfate
Hsp	Heat shock protein
HSPGs	Heparan sulfate proteoglycans
Ins	Insulin
I/R	Ischemia/Reperfusion
IRS	Insulin receptor substrate
JNK	c-Jun N-terminal kinases
LC3	MAP1LC3B
LDHA	Lactate dehydrogenase A
LPL	Lipoprotein lipase

LRP1	LDL receptor related protein
LV	Left ventricle
LVPW: s	Left ventricle posterior wall thickness: systolic
LVPW: d	Left ventricle posterior wall thickness: diastolic
LVAW: s	Left ventricle anterior wall thickness: systolic
LVAW: d	Left ventricle anterior wall thickness: diastolic
MAPK	Mitogen-activated protein kinase
mTOR	Mammalian target of rapamycin
Myh6	Myosin Heavy Chain 6
Myh7	Myosin Heavy Chain 7
M6PR	Mannose-6-phosphate receptor
NLS	Nuclear localization signal
Nppa	Natriuretic Peptide A
Nppb	Natriuretic Peptide B
PARP	Poly (ADP-Ribose) Polymerase
PERK	PRKR-Like Endoplasmic Reticulum Kinase
PI	Propidium iodide
PI3K	Phosphatidylinositol-3-OH kinase
PM	Plasma membrane
PKC	Protein kinase C
RAOEC	Rat aortic endothelial cells
RAP	Receptor-Associated Protein
RHMEC	Rat heart micro vessel endothelial cells

SLC2A1	Solute carrier family 2
STZ	Streptozotocin
S6K	Ribosomal protein S6 kinase beta-1
TG	Triglyceride
Thap	Thapsigargin
TNFα	Tumor necrosis factor α
TTC	Triphenyltetrazolium chloride
T1D	Type 1 diabetes
T2D	Type 2 diabetes
UPR	Unfolded protein response
VCAM1	Vascular cell adhesion molecule 1
VEGF	Vascular endothelial growth factor
WT	Wild type
XBP1	X-box binding protein 1
XBP1s	X-box binding protein 1, spliced
XBP1u	X-box binding protein 1, unspliced

Acknowledgements

I am glad to have this opportunity to express my appreciation to those who help me complete my PhD study and this thesis. These could not be achieved without the contribution and support from my supervisor, Dr. Brian Rodrigues, the committee group, my colleagues, as well as my beloved family. I firstly give my deepest appreciation to my Ph.D. supervisor, Dr. Brian Rodrigues, whose excellent work ethics and passionate personality greatly influenced me. His trust, encouragement and support without any holdback is the key to complete this thesis. Secondly, I sincerely thank all the members of my Ph.D. supervisory committee: Dr. Corey Nislow, Dr. Dan Luciani, Dr. David Granville, Dr. Bruce Verchere, who provided valuable input to my thesis. Special thanks are owed to Dr. Thomas Pulinilkunnil and his laboratory members Purvi Trivedi, Dipsikha Biswas for all the intelligent and technical support. In addition, I want to thank Dr. Vlodavsky for his generous gift of experimental animals and reagents, Dr. Stephane Flibotte and Dr. Sunita Sinha who carried out the RNA-seq part of work fascinatingly, Ms. Yanzhi Carolyn Jia from Dr. Kathleen Macleod's lab who helped me with the echocardiology. I have worked with a group of friendly and fascinating lab mates: Dr. Dahai Zhang, Ms. Bahira Hussein, Ms. Jocelyn Jia, Dr. Ying Wang, Boris Trinajstic, Mr. Nathaniel Lal, Ms. Rui Shang, Dr. Amy Pei-Ling Chiu, and Karn Puri, who support and care each other like a family. Lastly and most importantly, sincere thanks are given to my beloved family who are always behind me. Canadian Institutes of Health Research funded my research project.

Chapter 1: Introduction

1.1 Heparan sulfate proteoglycans (HSPGs)

Heparan sulfate proteoglycans are a group of glycoproteins that are widely distributed in the extracellular matrix (ECM) and cell surface, but are also present in the nucleus and cytosol [1]. Depending on the location and function, they are generally classified into the following 8 categories: 1) structural HSPGs that together with other ECM and cell surface components define basement membrane and ECM structure; 2) secretory HSPGs (serglycin) that help with packaging, structural maintenance, and secretory vesicle contents regulation; 3) reservoir HSPGs that bind, protect, and release various bioactive molecules such as cytokines, chemokines, growth factors, and morphogens (which add another layer of regulation of these molecules, as well as form a gradient that are essential in processes like cell differentiation during development, cancer metastasis, and immune cell recruitment and homing); 4) protease HSPGs that bind proteases and protease inhibitors and regulate their activity and function; 5) adhesion HSPGs that interact with cell adhesion receptors such as integrins to modulate cell-ECM and cell–cell interactions and cell motility; 6) coreceptor HSPGs that act as coreceptors for various tyrosine kinase-type growth factor receptors, lowering their activation threshold or regulating the duration of signaling reactions; 7) ligand HSPGs that work as endocytic receptors for clearance of bound ligands, which is especially important in lipoprotein metabolism and morphogen gradient formation during development; 8) nucleus HSPGs that regulate cell cycle, proliferation, transcription and transport of cargo to the nucleus

[1-4]. Altogether, HSPGs participate in a wide range of processes such as development, cancer progression and immune response, which emphasizes the importance of heparanase, the only known mammalian enzyme that can cleave heparan sulfate (HS).

1.2 Heparanase

Heparanase, a member of the glycoside hydrolase 79 (GH79) family of carbohydrate-processing enzymes, is an endoglycosidase (endo-β-d-glucuronidase) that cleaves the HS side chains of HSPGs into fragments of 10–20 sugar units [5]. Initially synthesized as a preproenzyme containing a signal peptide, heparanase is cleaved into a latent 65-kDa proheparanase (Hep^{L}) after removal of the signal sequence. A 6-kDa linker is subsequently removed by cathepsin L in acidic environment (mostly lysosomes), liberating an N-terminal 8-kDa subunit and a C-terminal 50-kDa subunit, which matures into a noncovalent heterodimer (active heparanase, Hep^{A}) [6]. The catalysis activity of heparanase is realized through hydrolysis of internal glucuronic acid (GlcUA) β1–4 N-sulfoglucosamine (GlcNS) linkages in HS [7]. The crystal structure of human heparanase reveals how an endo-acting binding cleft is exposed by proteolytic activation of latent proheparanase [5]. The cleft contains residues Glu343 and Glu225, a typical catalytic nucleophile and acid base required for retaining the catalytic mechanism [8]. The HS binding cleft of heparanase consists of basic side chains lined by Arg35, Lys158, Lys159, Lys161, Lys231, Arg272, Arg273, and Arg303, in accordance with the negatively charged HS [5].

Multiple receptors have been implicated in facilitating the uptake of secreted or exogenously added Hep^{L}, including the high-abundance, low-affinty HSPGs and the low-abundance, high-affinity mannose-6-phosphate receptor (M6PR) and LRP1 [9]. Following the rapid interaction with these cell surface receptors, heparanase is internalized through vesicles and processed into the active form (Hep^{A}) in lysosomes. This maturation procedure encompasses both the message delivery role of Hep^{L} and its involvement in processes related to vesicles and lysosomes. Indeed, heparanase was found to participate both in lysosomal processes such as autophagy [10] and vesicular processes such as formation, secretion, and function modulation of exsosomes [11-13]. Both processes contribute to the chemoresistance characteristics of tumor cells in anti-cancer therapy [10, 14]. The use of anti-cancer drugs can stimulate the production of exsomes usually referred as chemoexsomes. Heparanase was often found on the surface of the chemoexsomes and can shape the surrounding environment, which facilitates the migration of tumor cells and host cells [15].

Besides the HSPGs-dependent function, heparanase participate in a few processes independent of HSPGs. For example, both forms of heparanases promote transduction of multiple signalling pathways, including protein kinase B (Akt), extracellular signal-regulated kinase (Erk), steroid receptor co-activator (Src), signal transducer and activator of transcription (STAT), hepatocyte growth factor (HGF), insulin-like growth factor (IGF)-, and epidermal growth factor (EGF)-receptor signaling [16]. These activation of signaling pathways are mostly unrelated to the enzyme activity of heparanase, highlighting the importance of Hep^{L} in tumor migration.

The role of heparanase in tumor progression is also largely associated with its proangiogenic effect; vascular endothelial growth factor-A (VEGF-A), vascular endothelial growth factor-C (VEGF-C), cyclooxygenase-2 (COX-2), and matrix metallopeptidase 9 (MMP-9) can all be upregulated by heparanase [6]. Heparanase can also upregulate genes that are prothrombotic (i.e., tissue factor), proinflammatory [i.e., tumor necrosis factor α (TNFα), interleukin-1 (IL-1), IL-6], profibrotic [i.e., tumor growth factor β (TGF β)], mitogenic (i.e., HGF), osteolytic [receptor activator of nuclear factor kappa-B ligand (RANKL)], etc, in nontumor (host) cells including T lymphocytes, B lymphocytes, neutrophils, monocyte/macrophages, endothelial cells, osteoclasts, and fibroblasts. This makes it relevant in conditions such as acute and chronic inflammation, autoimmunity, atherosclerosis, tissue fibrosis, kidney dysfunction ocular surface dysfunction, viral infection, diabetes, and diabetic complications [17-28]. These functions are extensively involved in different pathological pathways, but may reflect an adaption mechanism and fulfill some homeostasis restoring functions, as illustrated in heparanase overexpression (Hep-tg) and knockout (Hep-ko) mouse models. While Hep-tg mice have higher food intake and body length, their body mass and fat mass are lower, with a more healthy fur color and activity (Hep-ko mice have the opposite phenotype) [29-31]. Indeed, notwithstanding the unfavourable effects of heparanase in cancer development (and the numerous studies that consider it a therapeutic target for cancer treatment) and other complications, overexpression of heparanase in mice (Hep-tg) exhibit a number of beneficial phenotypes. For example, Hep-tg mice have a reduced amyloid burden and are also more resistant to inflammation-induced amyloid build up in multiple organs,

especially the brain [32, 33]. In the skin, Hep-tg mice exhibit accelerated wound healing, which was related to effects on cell migration, proliferation, and angiogenesis [34]. Our recent study also reported that Hep-tg mice are resistant to chemical induced Type 1 diabetes and have an improved glucose homeostasis through multiple mechanisms [35].

1.3 Heart disease

1.3.1 Heart disease

Globally, cardiovascular disease is a leading cause of death. According to the World Health Organization, it is responsible for almost one third of all deaths, with coronary heart disease (CHD, also termed as ischemic heart disease, IHD) being the major instigator (12.8% of all deaths) [36]. Although typically considered a disease of developed countries, its incidence is also increasing in the developing world, as these countries experience a change in lifestyle that introduces novel risk factors for cardiovascular disease. Stemming usually from vascular dysfunction such as atherosclerosis, thrombosis or high blood pressure, heart function can eventually be compromised due to the loss of cardiomyocytes, resulting in heart disease frequently in the form of myocardial infarction. Although recent progress on therapies such as the administration of statins and the insertion of stents have reduced death rates considerably [37, 38], and the likelihood of stem cell and gene therapies around the corner [39-43], the mechanisms behind the pathophysiology of heart diseases are still not completely understood and clinically effective therapies underdeveloped.

1.3.2 Diabetic cardiomyopathy (DCM)

Although ischemic heart disease is the major cause of death in diabetic patients, an intrinsic defect in the cardiac muscle (cardiomyopathy) is also gaining recognition [44-46]. Thus, patients with Type 1 (T1D) and Type 2 (T2D) diabetes have also been diagnosed with reduced or low-normal diastolic function and left ventricular hypertrophy in the absence of vascular defects [47-50]. Similarly, evidence of cardiomyopathy is reported in animal models of T1D and T2D [51, 52]. As it is a complicated disorder, several factors have been associated with the development of cardiomyopathy. These include an accumulation of connective tissue and insoluble collagen with remodeling of the ECM, impaired sensitivity to various ligands (e.g., β-agonists), ER stress, oxidative stress, mitochondrial dysfunction, RAAS activation and abnormalities in proteins that regulate intracellular calcium [50, 53-55]. The view that alterations in cardiac metabolism can contribute towards the etiology of diabetic cardiomyopathy has also been proposed [56-60]. Unfortunately, as DCM is often underdiagnosed in asymptomatic patients, and no effective strategy for its prevention and treatment has been established, it is important to find new biomarkers and potentially new therapeutic targets.

1.3.3 Ischemic heart diseases

Ischaemic heart disease (IHD), defined as "*a condition in which imbalance between myocardial oxygen supply and demand, most often caused by atherosclerosis of the coronary arteries, results in myocardial hypoxia and accumulation of waste metabolites*" by Leonard S. Lilly (Pathophysiology of Heart Disease, 2007), is the most common form of

CVD and the single most frequent cause of death in the Western world. It is caused by reduced blood flow to the myocardium secondary to atherosclerotic narrowing of the coronary arteries. Coronary atherosclerosis is a chronic inflammatory process that affects the luminal surface of the coronary arteries and is usually associated with increased oxidative stress and luminal narrowing [61]. The patient is typically asymptomatic at rest but develops chest pain (angina pectoris) during sudden physical or emotional stress. Atherosclerotic plaques in the coronary artery may also provoke coronary vasospasm, producing angina at rest, or they may spontaneously rupture, triggering intravascular thrombosis that results in acute coronary syndrome [62]. The intravascular thrombosis may manifest itself either as recurrent episodes of angina at rest without myocardial injury, or acute myocardial infarction (AMI). Massive myocardial infarction usually directly leads to rapidly fatal cardiogenic shock, while minor myocardial injury may also be fatal by indirectly triggering lethal cardiac arrhythmias. Myocardial ischemia of less than 20 minutes duration results in reversible myocardial injury; however, more prolonged ischemia results in progressive irreversible myocardial injury by a “wave front” of cardiomyocyte death that begins in the subendocardium and extends transmurally over time toward the epicardium [63].

The deprivation of oxygen and nutrient supply leads to abrupt biochemical and metabolic changes within the myocardium, including oxidative phosphorylation uncoupling, mitochondrial membrane depolarization, ATP depletion, and inhibition of myocardial contractile function [64]. Oxygen deprivation switches cellular metabolism to anaerobic glycolysis and results in lactate accumulation and intracellular pH decrease to less than

7.0. The pH change in turn activates the Na^+-H^+ ion exchanger that extrudes protons from the cell in exchange for Na^+ entry, and $2Na^+$-Ca^{2+} ion exchanger that extrudes Na^+ out of the cell at the expense of Ca^{2+} overloading [65].

The major focus of acute therapy for AMI is rapid restoration of coronary blood flow, which can be achieved with percutaneous intervention with balloon angioplasty and stenting at the site of thrombotic occlusion. Although restoration of coronary blood flow is essential for the survival of ischemic tissue, the rapid restoration of oxygenated blood may induce cardiomyocyte death, a process known as ischemia reperfusion injury, by triggering a) a burst of reactive oxygen species (which can happen in the first several minutes of reperfusion from cardiomyocyte mitochondria and other cell types like endothelial cells and neutrophils); b) rapid restoration of physiological pH (by the washout of lactate and the activation of the Na^+-H^+ exchanger as well as the Na^+-HCO^- symporter, which causes cardiomyocyte death by permitting mitochondrial permeability transition pore (MPTP) opening and cardiomyocyte rigor hypercontracture); c) acute cellular calcium influx (exacerbated at the time of myocardial reperfusion due to disruption of the plasma membrane, oxidative stress-induced damage to the sarcoplasmic reticulum, and mitochondrial re-energization); and d) MPTP opening (which results in mitochondrial membrane depolarization and uncoupling of oxidative phosphorylation, leading to ATP depletion and cell death) [64].

1.4 Unfolded protein response (UPR) and heart disease

1.4.1 UPR

Under physiological conditions, chaperones, foldases, cofactors and enzymes mediate various post-translational modifications of newly synthesized proteins in the cytosol and endoplasmic reticulum (ER) to ensure correct folding and a quality control machinery that identifies misfolded proteins and facilitates their degradation via the proteasome, lysosome and autophagy pathways. These processes are essential for the maintenance of cellular homeostasis and prevents abnormal protein aggregation. However, for the ER to maintain its normal function under stress conditions such as abnormal metabolism, altered signaling activation, calcium imbalance, excessive oxidative stress, ischemia and reperfusion (ER stress) is challenging. Such conditions usually trigger a rapid and coordinated biochemical response that involves adaptive signalling pathways and gene expression changes, leading to modulation of protein folding, ER-associated degradation (ERAD), vesicular trafficking, autophagy, ER redox control, amino acid metabolism, lipid synthesis, and ER biogenesis. These would in effect reduce protein synthesis and increase chaperone production (which allows proper protein folding in the ER) and protein degradation, contributing to restoration of ER homeostasis and cell damage prevention [66]. This reaction is known as the unfolded protein response (UPR), an adaptation that can be viewed as a signal transduction pathway that involves two components: stress sensors at the ER membrane, and downstream transcription factors that reprogram gene expression toward stress mitigation or the induction of apoptosis when the stress is severe or prolonged [66]. The UPR target genes vary substantially depending on the

animal species, tissue context and the type of physiological or pathological perturbation that causes ER stress [66]. This variation might stem from the formation of different heterodimers between transcription factors, post-translational modifications and epigenetic changes [67]. The three main type-I transmembrane proteins that initiate the UPR are inositol-requiring protein 1α (IRE1α), activating transcription factor-6 α (ATF6α), and protein kinase RNA-like ER kinase (PERK).

IRE1α. IRE1α is the most evolutionarily conserved ER stress transducer, and contains both RNase (endoribonuclease) and kinase domains within its cytosolic region. Upon activation by release of binding-immunoglobulin protein (BiP, a key ER chaperone that constitutively binds to the luminal domains of the three sensors thus preventing their activation under basal conditions), IRE1α dimerizes and autotransphosphorylates, leading to IRE1α-mediated removal of a 26-nucleotide intron (by using RNase activity) from the mRNA of the transcription factor XBP1 [68]. The shift in reading frame of the XBP1 mRNA results in the formation of an active and stable transcription factor XBP1s (XBP1, spliced). XBP1s is generally viewed as prosurvival by inducing the expression of various genes that are involved in protein folding and quality control mechanisms, by activating the ERAD, and by promoting biogenesis of the ER and Golgi compartments (thus augmenting the ability of protein folding and secretion) [67]. IRE1α also mediates the degradation of a specific group of mRNAs and microRNAs through a process known as regulated IRE1α-dependent decay (RIDD), which alters expression of multiple proteins with various functions including stress mitigation, inflammation and apoptosis [69]. The kinase activity of IRE1α, on the other hand, is responsible for recruitment of several adaptor proteins

that mediate crosstalk with other stress pathways, including the mitogen-activated protein (MAP) kinase pathway, autophagy, and inflammatory pathways that involve nuclear factor-κB [67]. Overall, IRE1α has a dual role in the response to ER stress, mediating adaptation through XBP1s and mediating apoptosis via the MAP kinase pathway and RIDD.

ATF6α. ATF6α is expressed ubiquitously in the ER and contains a basic leucine zipper transcription factor domain in its cytosolic domain. Following ER stress, ATF6α is exported from the ER membrane to the Golgi apparatus. Out here, endopeptidase S1P and S2P cleave it into a fragment that translocates to the nucleus, and induces expression of XBP1 and other genes that are involved in ERAD and protein folding such as BiP, GRP94, protein disulphide isomerase, and CHOP [68]. Although ATF6 can induce expression of CHOP, there is no evidence to support its role in ER stress induced apoptosis. On the contrary, ATF6-mediated signals are generally viewed as a pure pro-survival branch of UPR that aims to resolve ER stress [70, 71].

PERK. The activation of PERK is responsible for protein synthesis inhibition. Dissociation of BiP from PERK also initiates the dimerization and autophosphorylation of this kinase and generates active PERK. On activation, PERK phosphorylates eukaryotic initiation factor 2 (eIF2), which leads to inhibition of general protein translation. This would help cell survival by decreasing the load of nascent proteins in the ER. Genetic or pharmacological blockade of PERK in mouse embryonic fibroblasts leads to protein accumulation in ER and increased cell death when challenged with ER stress-inducing agents [72]. However, phosphorylation of eIF2α selectively upregulates the translation of

certain genes, such as the transcription factor ATF4. ATF4 increases expression of genes that are involved in a wide range of processes, including redox control, amino acid metabolism, autophagy and protein folding and synthesis. However, when ER stress cannot be resolved, ATF4 also engages cell death pathways via induction of CHOP, reactive oxygen species and members of the apoptosis regulator BCL-2 family [67]. In addition, eIF2α phosphorylation also serves as a convergent point of several pathways (that when combined, is called integrated stress response), which is triggered by various stimuli, including viral infection, nutrient starvation and heme deficiency [73]. Overall, activation of PERK is initially protective but better known as an important element of the switch from pro-survival to pro-death signalling and an inducer of CHOP in the later stage of ER stress.

1.4.1 UPR and heart diseases

In the mammalian heart (which has only a transient capacity for cell renewal during the neonatal period), any injury in the adult will lead to compromised heart function and failure if protective mechanisms are absent or compromised. Thus, a diverse range of cellular stresses, including oxidative, osmotic, and mechanical stresses, together with inflammation and hypoxia, can lead to dysfunction of the endoplasmic reticulum (ER), impairing protein folding, and triggering the UPR [74]. Once initiated, cardiomyocytes can use UPR to reduce protein synthesis, increase chaperone production, and stimulate protein degradation, processes that overcome the accumulation of misfolded proteins and restore ER homeostasis and prevent cell damage [74]. However, this adaptation mechanism can also lead to cell death when UPR is protracted [75-77].

Diabetes is one disease that activates UPR in the heart [78, 79]. Following diabetes, factors such as downregulation of the glucose transporter 4 (GLUT4), generation of reactive oxygen species (ROS), alteration of Ca^{2+} levels, hyperinsulinemia and insulin resistance may all contribute to improper protein folding in cardiomyocytes. It has been shown that hyperglycemia, dyslipidemia, and inflammation may activate a combination of the three UPR branches and regulate different sets of signaling and gene expression, consequently leading to not only the effort to restore ER homeostasis, but the metabolism of excessive glucose, fatty acid and other metabolites [80-82].

However, diabetes and other conditions in the heart eventually converge to ischemic heart disease. Ischemia is known to upregulate a wide range of ER chaperones, especially BiP, which is also a sensor and regulator of UPR. BiP is a cardioprotective protein that promote correct protein folding and at the same time, quench the chronic pro-apoptotic signaling of the UPR [83, 84]. In most I/R models, XBP1, downstream of IRE1α, is an acute responder, knockdown of which leads to more severe I/R injury and increased cardiomyocyte death [85]. Other downstream pathways of IRE1α like JNK and RIDD, however, are activated after longer duration of I/R and leads to cell death [86, 87]. A similar situation happens for the PERK pathway: the main component contributing towards ischemic insults in the heart is the induction of CHOP, blockage of which diminish the I/R injury [88]. The ATF6α branch, which is also activated during ischemia but not reperfusion stage, seems a more “survival branch” in different studies, probably due to its interaction with XBP1, the induction of chaperones, the regulation of Ca^{2+} signaling

(through sarco/endoplasmic reticulum calcium ATPase 2, SERCA2), and the modulation of ROS [70, 71, 89, 90].

1.5 Heart disease and autophagy

1.5.1 Introduction

Autophagy is generally viewed, in physiological settings, as a protective mechanism that oversees the recycling of defective organelles and protein aggregates, ultimately contributing to the maintenance of cellular homeostasis, while abnormal up- or down-regulation of autophagy is a distinctive feature of various pathological states [91, 92]. Both excessive and impaired autophagy could lead to cellular destruction via apoptosis, and the complex interactions between autophagy and apoptosis are a subject of increasing attention [93-95]. Autophagy is a cellular degradation process in which cytoplasmic constituents are recycled by lysosomal enzymes for reuse [96]. In contrast to the ubiquitin-proteasome degradation system, during which specific protein substrates are selectively ubiquitinated for breakdown in the proteasome, the general autophagic process non-selectively degrades protein aggregates and defective organelles as part of a protective, homeostatic mechanism to maintain cell survival [97]. However, during autophagy, specific organelles and proteins can also be selectively targeted, mostly through p62, for breakdown by the autophagic process [98]. Mitophagy, one example of organelle-specific autophagy, is particularly important for the cardiomyocyte. In this process, defective or damaged mitochondria are primed for selective autophagic recognition via Pink1-Parkin signalling or by other mitophagy receptors, and are

subsequently degraded by acidic lysosomal hydrolases (for detailed reviews, see [99-102]).

The three classifications of autophagy are: a) microautophagy, in which cytoplasmic contents are directly engulfed by lysosomes, b) chaperone-mediated autophagy, in which chaperone proteins help protein substrates translocate across the lysosomal membrane, and c) macroautophagy, in which cytoplasmic substrates are sequestered inside autophagosomes and degraded by lysosomal enzymes [92, 103]. Of these, macroautophagy has been the most studied.

1.5.2 Processes of autophagy

Initially discovered by genetic screens performed in yeast, there are at present more than 30 known autophagy-related (Atg) genes that are confirmed in knockout mouse and mammalian cell models, in addition to genes related to this process (for a list of these genes and their relevant knockout mouse models, see review [91, 104]). These Atg genes initiate the nucleation step (Fig. 1.1B) of phagophore (isolation membrane) formation by activating the class III phosphoinositide 3-kinase (class III PI3K)/vacuolar protein sorting (Vps34) complex, which forms a multiprotein complex along with Beclin-1, Atg14, and Vps15 (Fig. 1.1A) [105]. Subsequently, two ubiquitin-like conjugation systems control the process of phagophore elongation [92, 106-108] (Fig. 1.1C-E). The first pathway (Fig. 1.1D) involves conjugation of ubiquitin-like protein Atg12 to Atg5, by way of successive reactions involving E1-like enzyme Atg7 and E2-like enzyme Atg10. The resulting Atg12-

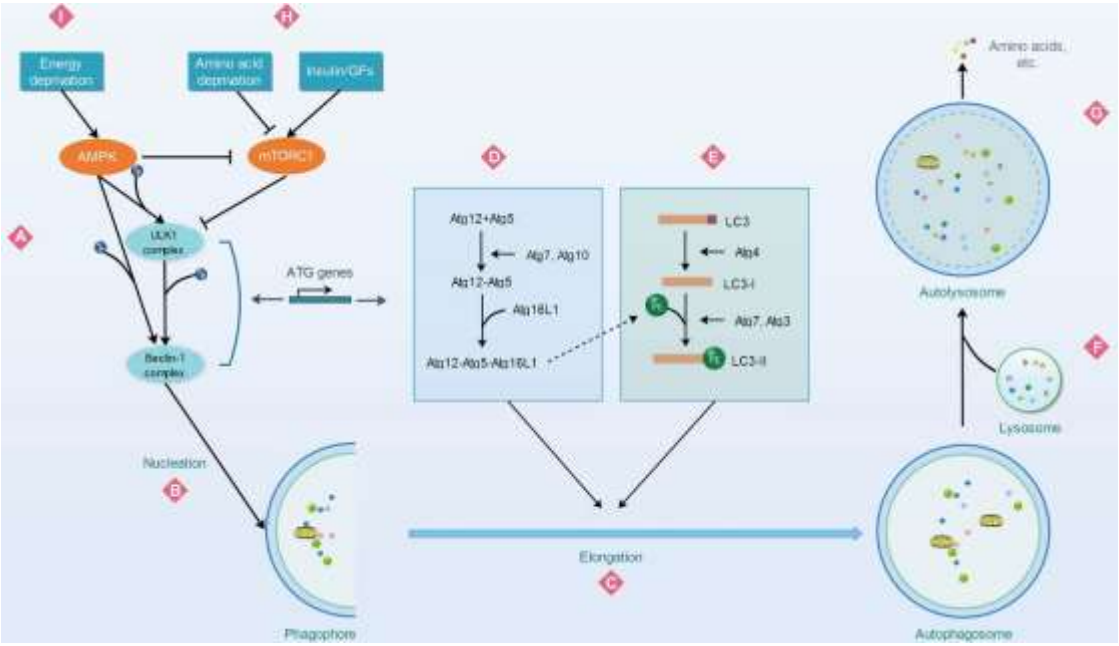

Figure 1.1. The macroautophagic process

(A) Mammalian target of rapamycin complex 1 (mTORC1), when activated by insulin and growth factors (GFs), inhibits the Unc-51–like autophagy activating kinase 1 (ULK1) complex to terminate autophagy. Amino acid deprivation directly inhibits mTORC1, releasing its block of the ULK1 complex, promoting autophagy. Adenosine monophosphate–activated kinase (AMPK), in response to energy deprivation and oxygen deprivation, is activated and inhibits mTORC1, in addition to activating the ULK1 complex directly through phosphorylation. (B) The activated ULK1 complex phosphorylates Beclin-1, which, along with autophagy-related (Atg)14/vacuolar protein sorting (Vps)15/class III phosphoinositide 3-kinase (PI3K)/Vps34, leads to nucleation. In addition, AMPK can directly activate Beclin-1 through phosphorylation. (C-E) Elongation of the phagophore (isolation membrane) is accomplished through 2 systems. (D) In the first pathway, Atg12-Atg5 associates with Atg16L1 to form the Atg12-Atg5-Atg16L1 complex, promoting the conjugation of phosphatidylethanolamine (PE) with light chain 3 (LC3)-I. (E) In the second pathway, LC3 is proteolytically processed to LC3-I and then to LC3-II after conjugation to PE. p62 links LC3-II and polyubiquitinated proteins inside the autophagosome. (F) Fusion of autophagosomes with lysosomes to form autolysosomes results in degradation of its contents, and (G) the amino acids and other building blocks generated are released into the cytoplasm for reuse by the cell. (H, I) The 2 master regulators of autophagy, AMPK and mTORC1, are subject to control by energy deprivation, amino acid deprivation, and insulin/growth factor signalling.

Atg5 conjugate, along with Atg16L1, forms the Atg12-Atg5-Atg16L1 complex, which initiates phagophore elongation both independently and also by promoting conjugation of microtubule-associated protein 1A/1B-light chain 3 (LC3-I; Atg8 in yeast) with phosphatidylethanolamine (PE), to form LC3-II. In the second pathway (Fig. 1.1E), LC3 undergoes proteolytic processing by Atg4 and conjugation to PE by E1-like Atg7 and E2-like Atg3 enzymes. The resulting amide bond is formed to the hydrophilic head of PE. Following nucleation by Atg genes and elongation by the Atg12-Atg5 and LC3 pathways, a double-membrane vesicular compartment - the autophagosome - is formed. In this process, cytosolic components, including damaged organelles, pathogenic material, and protein aggregates, become sequestered within autophagosomes. Fusion of autophagosomes with lysosomes results in the formation of autolysosomes (Fig. 1.1F), inside of which cargo are degraded by acidic hydrolases, and their breakdown products released into the cytosol for use in future anabolic reactions (Fig. 1.1G).

1.5.3 Regulation of autophagy

Regulation of autophagy is primarily accomplished through AMP-activated kinase (AMPK) and the mammalian target of rapamycin (mTOR) [107-109] (Fig. 1.1B). Under normal conditions, protein degradation by the proteasome is the major method used to supply amino acid building blocks for cellular functions [110]. During starvation, however, autophagy plays a more prominent role in amino acid generation [103]. Nutrient deprivation, with its associated reduction in amino acids and energy, in addition to reduced oxygen or growth factor signalling, increases autophagy. This occurs through inhibition of the serine/threonine protein kinase mTOR (Fig. 1.1H), which, as part of the

mTOR complex 1 (mTORC1), is a nutrient sensor and negative regulator of autophagy [97]. Under nutrient-rich conditions, mTORC1 is activated and suppresses the unc-51 like autophagy activating kinase 1 (ULK1) complex, terminating autophagy. In contrast, the serine/threonine kinase AMPK (Fig. 1.1I) is a highly conserved cellular energy sensor and positive regulator of autophagy. Hence, AMPK deletion or mutation in mice reduces their response to inducers of autophagy [111, 112]. AMPK is rapidly activated by a high AMP/ATP ratio as a result of exercise, nutrition deprivation, or ischemia, and maintains energy balance by decreasing pathways that use energy, and increasing those that produce energy, of which autophagy is included [113]. In response to low energy levels, AMPK activates ULK1 by phosphorylation. Activated ULK1 itself phosphorylates Beclin-1, thereby activating the Vps34-Beclin-1 complex and inducing autophagy.

1.5.4 Physiological and pathophysiological roles of autophagy

Autophagy has a role in maintaining homeostasis and, ultimately, in contributing to cell survival. Under normal conditions, autophagy participates in the recycling of cytosolic components as well as pathogen elimination. It has been established that a basal level of autophagy is beneficial for survival, and contributes to cellular homeostasis [94]. Insufficient autophagy leads to the accumulation of defective organelles and long-lived proteins, which can hinder cell survival and lead to apoptotic cell death, as evidenced in many Atg gene knockout mouse models [91]. On the other hand, while increased autophagy can be beneficial for cell survival in the short term, its excessive or chronic induction is linked to cell death and pathological states [93]. Past a certain threshold, autophagic destruction of organelles and cytosolic components can result in autophagy-

induced apoptosis [95]. One important determinant of cell survival is the level of mitochondrial stress - mild stress promotes adaptive autophagy, moderate stress activates apoptosis as a result of cytochrome c release from the mitochondrial intermembrane space, and extreme stress initiates necrosis due to ATP depletion [94, 114]. It is thus unsurprising that deviations from a basal level of autophagy are commonly observed in pathological conditions, as metabolic alterations feature prominently in the pathology of a variety of diseases [109]. For instance, elevation of autophagy in breast cancer cells may be instrumental in promoting tumour survival. In contrast, diabetes, obesity, and neurodegenerative diseases such as Alzheimer's disease are linked to autophagy inhibition [91]. It is evident that elucidating the pathophysiological roles of autophagy is necessary to further our understanding of the bioenergetic changes accompanying various disease states, and could potentially lead to the discovery of novel therapies.

1.5.5 The balance between autophagy and apoptosis

Inhibition of autophagy by both genetic manipulation and pharmacological inhibition increases apoptosis, likely due to an intracellular accumulation of protein aggregates and damaged cytoplasmic components [115]. For instance, in LAMP2 deficient cells, disrupted autophagosome-lysosome fusion leads to autophagosome accumulation and, consequently, cell death [116]. In addition to exhibiting disrupted autophagy in multiple organs, knockout of LAMP2 in mice also causes Danon disease, which counts fatal cardiomyopathy as one of its features [117]. In mice deficient in Atg5 or Atg7, mortality is observed within 1 day of delivery due to a disruption in the expected increase in

autophagy, which is normally observed immediately after birth [118, 119]. Additionally, mutant mice with neuron-specific depletion of Atg5 or Atg7 accumulate cytoplasmic protein aggregates and exhibit neurodegeneration [120, 121]. Furthermore, a deficiency of Atg5 in T cells increases the apoptosis of mature T cells in peripheral organs [122]. Finally, homozygous Beclin-$1^{-/-}$ embryonic stem cells also show a severely altered autophagic response, with Beclin-$1^{-/-}$ embryos undergoing mortality in early embryogenesis [123]. In contrast, when autophagy is appropriately induced, cell death can be reduced. For example, autophagy promoted by GAPDH can preserve cell survival even after apoptotic cytochrome c release [124]. Inhibition of mTOR, the "master negative regulator" of autophagy, can promote autophagy and consequently enable cell survival in several models of Huntington disease [125]. It should be noted that excessive autophagic destruction of cytoplasmic components and organelles leads to cell death. Hence, autophagic vacuoles are concurrently observed along with apoptotic and necroptotic vacuoles in multiple models [95].

One centralized mechanism that regulates the balance between autophagy and apoptosis is the interaction between anti-apoptotic Bcl-2 proteins (in most cases Bcl-2 and Bcl-X_L) and Beclin-1, a key component of the autophagy-promoting Beclin-1-Vps34-Vps15 complex that is subject to regulation by a variety of proteins [126] (Fig. 1.2). Upon autophagy induction, Beclin-1 binds to its partners and initiates autophagy (Fig. 1.2A). However, binding of anti-apoptotic Bcl-2 proteins to Beclin-1 disrupts this interaction, preventing autophagy (Fig. 1.2B). At the same time, this association of anti-apoptotic Bcl-2 proteins and Beclin-1 also abrogates the usual anti-apoptotic role of these Bcl-2

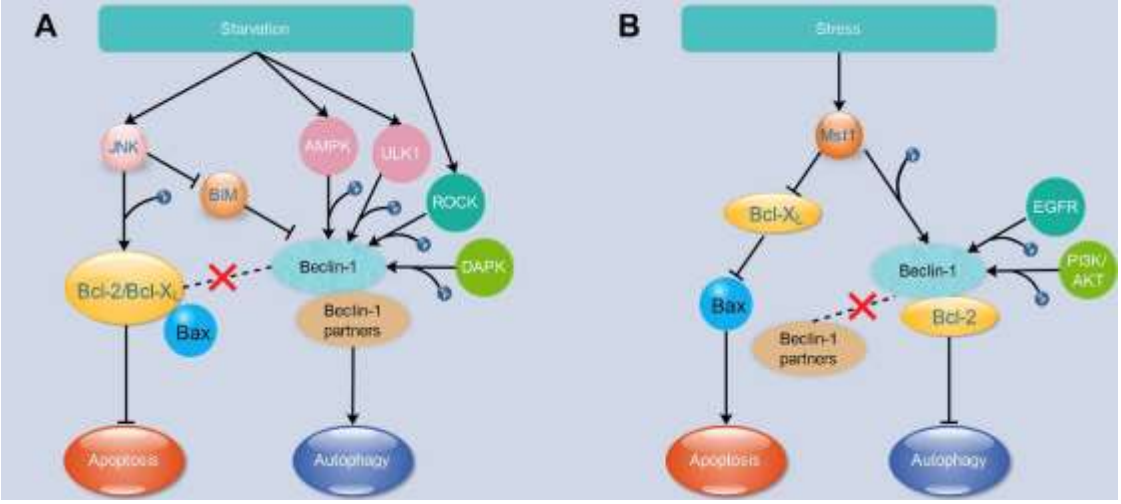

Figure 1.2. The balance between autophagy and apoptosis

A) The association between Beclin-1 and Bcl-2 can be disrupted by either phosphorylation at a specific locus, or by the competitive binding of other BH3 only proteins with Bcl-2/Bcl-XL. JNK can be phosphorylated and activated by different stimuli, especially starvation. Upon activation, JNK can either phosphorylate Bcl-2 at multiple sites, or alternatively phosphorylate Bim to thereby dissociate its inhibitory interaction with Beclin-1; both situations cause dissociation between Bcl-2 and Beclin-1 and lead to autophagy induction. Beclin-1 can also be phosphorylated by AMPK/ULK-1, ROCK1, and DAPK, all of which result in dissociation of Beclin-1 from Bcl-2 and increased autophagy. The interaction between Beclin-1 and Bcl-2 can also be disrupted by a replacement interaction between Bcl-2 and other BH3 only proteins. However, it should be noted that some of these interactions may also disrupt the binding of Bcl-2 to Bax, leading to apoptosis.

B) Phosphorylation of Beclin-1 at specific sites can promote the association of Beclin-1 and Bcl-2. Phosphorylation and activation of Mst1 can inhibit autophagy by phosphorylating Beclin-1 and promoting its interaction with Bcl-2. Concurrently, Mst1 phosphorylation can abrogate the inhibitory effect of Bcl-XL on apoptosis by phosphorylating Bcl-XL at Ser-14 and dissociating Bcl-XL from Bax. Beclin-1 is also subject to regulation by PI3K/Akt and EGFR, in both cases leading to inhibition of autophagy.

proteins. Thus, the relative concentration of anti-apoptotic Bcl-2 proteins and Beclin-1, in addition to their mutual interaction, constitutes a rheostat for autophagy and cell death [127]. In this regard, phosphorylation of Beclin-1 by Mst1 (on Ser-90) [128], EGFR (on Tyr-229, Tyr-233, and Tyr-352)[129], and the Class I PI3K-Akt axis (on Ser-295) [130] facilitates

the interaction between Beclin-1 and anti-apoptotic Bcl-2 proteins (in the case of the PI3K-Akt axis, the interaction is with 14-3-3 and vimentin intermediate filament proteins), thereby inhibiting autophagy (Fig. 1.2b). In contrast, phosphorylation of anti-apoptotic Bcl-2 proteins by JNK [131], and phosphorylation of Beclin-1 by AMPK [132], ULK1 [133] (both on Ser-14), ROCK1 [134] (on Thr-119), and DAPK (on Thr-119) [135], dissociates the binding between Bcl-2 and Beclin-1, promoting autophagy (Fig. 1.2a). The interaction between Beclin-1 and anti-apoptotic Bcl-2 proteins is also regulated by competitive binding between Beclin-1, other BH3-only proteins, anti-apoptotic Bcl-2 proteins, and other Bcl-2 family members [136-138]. For example, Bcl-2-interacting mediator of cell death (BIM) interacts with Beclin-1 and facilitates its interaction with dynein light chain 1 (DLC), thereby preventing autophagy [138] (Fig. 1.2a). JNK, which phosphorylates Bcl-2 and dissociates the interaction between Beclin-1 and Bcl-2, can also phosphorylate BIM and disrupt the BIM-Beclin-1 interaction, promoting autophagy induction [138] (Fig. 1.2a). It should be noted that other BH3-only proteins can also disrupt the interaction between Beclin-1 and Bcl-2 family proteins [139-141].

1.5.6 Autophagy in the heart

A series of studies have shown that autophagy is related to heart diseases, including dilated cardiomyopathy, valvular disease, and ischemic heart disease [142]. In fact, autophagic cell death has been detected more often than apoptotic cell death in multiple heart disease models [143]. For example, LAMP2 deficient mice showed abnormal cardiomyocyte ultrastructure and reduced contractility - characteristics related to Danon disease [144]. Loss of autophagy, through depletion of macrophage migration inhibitory

factor (MIF) [145] or myeloid cell leukemia 1 (MCL-1) [146], causes serious cardiomyopathy. Mortality in cardiac-specific Atg5-deficient mice, which display impaired sarcomere structure and dysfunctional mitochondria, is observed after 6 months [147]. Furthermore, temporal cardiac-specific ablation of Atg5 expression causes cardiac hypertrophy, left ventricular dilatation, and contractile dysfunction, and also results in disorganized sarcomere structure and mitochondrial misalignment and aggregation[148].

In contrast, GFP-LC3 transgenic mice showed increased numbers of autophagosomes (mitophagy), which is essential for mitochondria turnover and cardiomyocyte function [149]. In addition, multiple gene manipulation investigations demonstrated that increased autophagy is associated with decreased apoptosis and ameliorated heart dysfunction in different heart disease models [92, 104, 107, 109, 111, 113, 118, 128, 132, 150-199].

The heart is an organ that is particularly sensitive to oxygen deficiency and oxidative stress [190]. Oxygen deprivation is a key factor in the pathogenesis of various cardiac diseases, including heart failure and myocardial infarction [190]. Hypoxia generally induces autophagy in cardiomyocytes - a response that can be protective in some situations, but detrimental when out of control. One of the mechanisms by which hypoxia can promote autophagy is through the induction of BNIP3 and BNIP3L via hypoxia-inducible factor (HIF), which dissociates the interaction between Beclin-1 and Bcl-2/Bcl-X_L [139, 200]. The induction of autophagy attenuates hypoxia-induced cardiomyocyte apoptosis and improves cardiac function through a variety of mechanisms, particularly AMPK activation [154, 191-194, 201-205]. One possible caveat, however, is the use of an I/R model in some

of the above studies, for which the importance of oxidative stress is intensified. Nevertheless, autophagy activation has been observed in both ischemia/reperfusion and hypoxia alone, and can be either adaptive or maladaptive [195]. During diabetes or obesity, oxidative stress can be generated by glucolipotoxicity or cardiac ischemia [79, 196]. Although autophagy induction by gene overexpression has been shown to be protective against oxidative stress in the heart [181, 197], prolonged autophagy activation as a consequence of oxidative stress usually results in cardiomyocyte apoptosis and attendant heart disease [198, 199]. In addition, another study suggests that the activation of autophagy has a prosurvival function in the ischemic heart but represents exacerbated cardiomyocyte cell death during reperfusion [206].

1.6 UPR, autophagy, and heart disease

In almost all types of cardiac pathology, hypoxia, oxidative stress, UPR, autophagy, and mitochondrial dysfunction go hand in hand. As one of the solutions to remove the misfolded proteins in ER stress, autophagy is routinely activated and linked to all three branches of UPR. This is realized by upregulation of autophagy related genes and activation of upstream signaling of autophagy [207-209]. Several studies have shown that ischemic conditioning can protect the heart against I/R injury via sequentially activation of UPR and autophagy [210-213]. Mild ER stress induced by thapsigargin or tunicamycin can also elicit autophagy, and is protective against I/R in rat heart via upregulation of BiP, Akt, Bcl2, LC3-II, Beclin-1 and Atg5, suggesting new therapeutic targets in heart disease prevention [214].

Chapter 2: Materials and Methods

2.1 Animal care

This investigation conformed to the Guide for the Care and Use of Laboratory Animals published by the National Institutes of Health, the Canadian Council on Animal Care Guidelines, and the University of British Columbia (Animal Care Certificate A13-0098). Adult male Wistar rats (260-300 g) and C57BL/6J mice were purchased from Charles River Laboratories. Hep-tg mice were generated as previously described [35]. In brief, a constitutive β-actin promoter drives the expression of the human heparanase gene in a C57BL/6J genetic background. Hep-tg mice were previously crossed for 10 generations with C57BL/6J mice to produce a stable homozygous background. Male homozygous Hep-tg mice aged 12±1 week were used for all experiments.

2.2 Experimental animals

Streptozotocin (STZ) is a β-cell specific toxin used to induce diabetes [215]. Male Wistar rats (240-260 g) were injected intravenously with 55 mg/kg STZ. With this dose, the animals become hyperglycemic within 24 h. These animals, used as a model of poorly controlled Type 1 diabetes, were kept for 4 days (acute) or 6 weeks (chronic) before heart isolation.

2.3 Isolation of cardiomyocytes

Rats were euthanized using a 100 mg/kg intraperitoneal injection of sodium pentobarbital. Once toe pinch and corneal reflexes were lost, a thoracotomy was

performed prior to removal of the heart. Rat ventricular calcium-tolerant cardiomyocytes were prepared following previously described procedures [216]. Isolated rat cardiomyocytes were plated on laminin-coated culture dishes and allowed to settle for 3 h. Unattached cells were washed away prior to different treatment protocols.

2.4 Echocardiography

Six TG and WT mice (12 weeks of age) were assigned for echocardiography using the Vevo2100 Ultrasound System (VisualSonics Inc., Toronto, ON, Canada), and a high-frequency ultrasound probe. Briefly, animals were anesthetized with isoflurane (induction, 4.5%; maintenance, 2.0%; Baxter International Inc., Deerfield, IL, USA), and placed on a heated platform (THM100, Indus Instruments, Houston, TX, USA) to maintain body temperature at 36-37°C. Parasternal short axis M-Mode was used to visualize cardiovascular structure and assess cardiac function.

2.5 Endothelial cell (EC) culture

Representative macrovascular (rat aortic endothelial cells, RAOEC) and microvascular (rat heart micro vessel endothelial cells, RHMEC) EC were cultured at 37°C in a 5% CO_2 humidified incubator. Cells from the fifth to the eighth passages of 3 different starting batches, for each cell line, were used.

2.6 Ischemia/reperfusion in Isolated Hearts

Following heparin injection, mice were anesthetized with pentobarbital sodium (60 mg/kg, i.p.) and hearts rapidly excised. Isolated hearts were perfused with an oxygenated

Krebs Henseleit solution containing (in mM) NaCl 118, KCl 5, KH_2PO4 1.2, $MgSO_4$ 1.2, glucose 10, HEPES 24, and $CaCl_2$ 2, pH 7.4, at 37°C in a Langendorff system at a perfusion rate of 4 mL/min. To examine the signaling related to UPR and autophagy, hearts were subjected to 20 min intervals of stabilization, no flow global ischemia and reperfusion respectively, before being snap-frozen in liquid nitrogen. These intervals were extended to 40 min of ischemia and 60 min of reperfusion when apoptosis markers were determined. 4-(2-aminoethyl) benzenesulfonyl fluoride hydrochloride (AEBSF, 30 µM), an ATF6α inhibitor, was used to inhibit UPR. The drug was added to the perfusion buffer during the 20 min period of stabilization.

2.7 Evans blue/TTC staining

In some experiments, after 40 min ischemia and 60 min of reperfusion, hearts were perfused with 200 µl 0.5% Evans blue solution using an aortic cannula, and then frozen at -20°C for 20 min. A sharp scalpel was used to obtain transverse sections of the heart, which were incubated for 20 min in 1% triphenyl tetrazolium chloride (TTC) solution at 37°C. The slides were fixed for 10 min in 10% formalin, and then visualized for determination of infarct size [217].

2.8 RNA sequencing and analysis

RNA from seven WT and six Hep-tg mice was isolated using a RNeasy purification kit (Qiagen, Hilden, Germany). Sequencing libraries were prepared from 400 ng total RNA using the TruSeq Stranded mRNA Sample Preparation kit (Illumina, San Diego, CA). Samples were checked for quality using a Bioanalyzer and quantified using a Qubit

fluorometer. Libraries were then multiplexed and sequenced over one rapid run lane on the NextSeq 500 Sequencing System (Illumina), collecting a total of 409 million read pairs (2 x 75 nucleotide long). The number of read pairs per sample ranged from 14-75 million (median 21). Multiple analysis pipelines have been applied and their results combined. Briefly, for the alignment stage we used both STAR and HISAT2. We also used the pseudo aligners Kallisto and Salmon. Quantification was performed directly with STAR, Kallisto and Salmon or with RSEM and StringTie for the pipelines producing real alignments. In all cases the mouse reference genome and transcriptome were from version GRCm38 downloaded from the Ensembl web site (http://www.ensembl.org). In-house Perl scripts were used to sum the read counts at the transcript level for each gene and create a matrix comprising the read counts for all of the genes for all of the samples. Differential expression analysis was then performed on the data from that matrix using the R package DESeq2 and edgeR [218]. Each sample was assessed using the quality-control software RSeQC version 2.6.3 [219] and the PtR script from the trinity suite [220]. One potential outlier was detected when clustering the samples and therefore removed for the differential expression analysis. The output for each pipeline is a list of genes ranked by the *p*-value for differential expression after correction for multiple testing. A combined list was obtained by ranking the genes according to their median rank from the various analysis pipelines. Genes with differential expression not going in a consistent direction between pipelines were eliminated from that combined list. Network analysis and function categorization were conducted using STRING.

2.9 Treatments

To promote the secretion of heparanase, EC were incubated with high glucose (25 mM, HG). To test whether exogenous heparanase can be taken up into EC and cardiomyocytes, cells were treated with 500 ng/mL recombinant myc-tagged Hep^L (myc-Hep^L) for different time intervals. To elucidate the contribution of cell surface LRP1 towards heparanase uptake, we used RAP (200-400 nM, 1 h) or LRP1 neutralizing antibodies (20-40 mg/ml, 1 h) to inhibit LRP1. To inhibit LRP1 expression, siRNA specific for LRP1 was used in RAOEC. SST0001 (125 µg/ml, 4 h) was used to inhibit heparanase activity. To induce apoptosis, cardiomyocytes were incubated in HG (30 mM) for 48 h, or H_2O_2 (10 µM) for 12 h. To induce ER stress, animals were injected with either 0.3 or 2 mg/kg thapsigargin, and hearts collected after 48 h. Chloroquine treatment of mice (50 mg/kg; 4 h) was used to inhibit autolysosome formation, and markers of autophagy subsequently determined. The fasting-refeeding protocol included withdrawal of food (at 5 pm) for 16 h, followed by refeeding for 3 h, as described previously [221]. To test the effects of exogenous heparanase, isolated rat cardiomyocytes were treated with 500 ng/mL recombinant myc-tagged Hep^L (myc-Hep^L) for 12 h with or without addition of chloroquine. Mice were fasted for 6 h prior to an i.p. injection of 1 or 5 U/kg insulin (ALPCO, Salem, NH). 10 min post–insulin injection, the heart was isolated for Western blot determination of LC3.

2.10 Immunofluorescence

To visualize heparanase uptake into cardiomyocytes, cells were treated for 4 h with myc-Hep^L. Cells were washed with cold PBS and fixed with 4% formaldehyde solution. This was

followed by permeabilization with 0.2% Triton X-100 for 10 min and incubation with blocking buffer containing 5% goat serum for 1 h at room temperature. Incubation with primary antibodies was at 4°C overnight and secondary antibodies (Alexa Fluor, Santa Cruz Biotechnology) at room temperature for 1 h. To detect lysosome localization, LysoTracker Red was added 30 min before fixation. For determination of apoptosis, Annexin V (1:200) and propidium iodide (PI, 1:500) were used. Confocal Microscope LSM700 (Zeiss) was used for all the immunofluorescence work.

2.11 Autophagic flux detection

Rat cardiomyocytes were isolated and plated. Following treatment with myc-Hep^{L} for 12 h, autophagic flux was visualized using a CYTO-ID autophagy detection kit (ENZO, ENZ-51031-0050).

2.12 Nuclear isolation

Nuclear and cytosolic fractions were separated using the nuclear/cytosol fractionation kit from Thermo Fisher Scientific. To validate the purity of proteins, we used cytosolic (GAPDH) and nuclear (histone H3) protein markers to detect their predominance in cytosolic and nuclear fractions respectively.

2.13 Western blot

Western blot was done as described previously [222]. In some experiments using EC, cell culture media was concentrated with an Amicon centrifuge filter (Millipore) before the detection of heparanase protein.

2.14 Quantitative real-time PCR

Total RNA was isolated from EC, whole hearts, ventricle, or cardiomyocytes using TRIzol (Invitrogen). This was followed by extraction using chloroform and isopropanol, washing with ethanol, and dissolving in RNase-free water. RNA was reverse transcribed into cDNA using a mixture of dNTPs, oligo-(dT), and SuperScript II Reverse Transcriptase. cDNA was amplified by TaqMan probes (β-2 microglobulin, β-actin, heparanase, lrp1, tnfrsf10b, tnfsf10, tnfrsf11b, cflar, bcl-2, tradd, tnfsf1b, bad, caspase 7, caspase 8, atf4, gadd45, mtor, beclin-1, p62, xbp1s, xbp1u, and lc3) in triplicate, using a StepOnePlus Real-Time PCR system (Applied Biosystems). Gene expression was calculated by the comparative cycle threshold (ΔΔCT) method.

2.15 Apoptosis PCR microarrays

For the apoptosis PCR array (Qiagen), 300-1000 ng RNA was isolated using an RNeasy Mini Kit and cDNA were transcribed using the RT^2 First Strand Kit. The expression of 84 apoptosis-related genes was determined in control and Hep^L-treated rat cardiomyocytes.

2.16 Materials

RAOEC and RHMEC were obtained from Cell Applications and VEC technologies, respectively. STZ (S0130), D-Mannitol (M4125), thapsigargin (T9033) and chloroquine (C6628) were obtained from Sigma-Aldrich. Anti-LRP1 antibody (ab92544) was purchased from Abcam. Purified Hep^L was prepared as described previously [223]. LysoTracker (L-7528) was purchased from Life Technologies. For Western blots that detect only Hep^L, we used the heparanase (N-Term) antibody (ABIN786265), which preferentially recognizes

the 65 kDa Hep^L, from Aviva Systems Biology. For detection of Hep^A, we initially used mAb 130 (ANT-193), which can also detect Hep^L, from InSight (Rehovot, Israel). However, due to discontinuation of this antibody, we subsequently used HP3/17 (INS-26-0000), also from InSight (Rehovot, Israel). Receptor-Associated Protein (RAP, 03-62221) and the LRP1 neutralizing antibody (8G1) were from American Research Products and Millipore, respectively. Antibodies for TNFRSF10B (sc-19529), CFLAR (sc-5276) that recognizes both the full length and short isoforms, and TRAIL (sc-6079) were obtained from Santa Cruz Biotechnology. TNFRSF11B (PA5-19841) was from Thermo Fisher Scientific. Antibodies against Bip (ab21685), p62 (ab56416), p- IRE1α (ab48187) were purchased from Abcam, Calreticulin (ADI-SPA-600) from Stressgen, ATF6α (NBP1-40256) from Novus Biologicals, p-Beclin-1(Ser 15) (254515) from Abbiotec, heparanase (INS-26-0000) from InSight (Rehovot, Israel), β-Actin (sc-4778), JNK (sc-7345), p-JNK (sc-6254), CHOP (sc-7351), Bcl2 (sc-7382), Bax, p-PERK (sc-32577) and PERK (sc-377400) from Santa Cruz Biotechnology, Vinculin (13901), LC3A/B (4108), LC3B (2775), XBP-1s (12782), mTOR (2972), p-mTOR (Ser2448) (5536/2971), Beclin-1 (3495), AMPK (2532), p-AMPKα (Thr172) (2535), Caspase 3 (9962), PARP (9542), cleaved PARP (9545), S6K (2708), and p-S6K (9234) from Cell Signalling. SST0001 was a kind gift from Sigma-Tau Research Switzerland S.A. Antibodies for PARP (9542), caspase-3 (9662), and cleaved caspase-3 (9664) were purchased from Cell Signalling.

2.17 Statistical analysis

Values are means ± SE. Wherever appropriate, a nonparametric Mann-Whitney test (for comparison between two groups), or one/two-way ANOVA, followed by the Tukey test

(for comparison between multiple groups) was used to determine differences between group mean values. The level of statistical significance was set at *p<0.05, **p<0.01, or ***p<0.001.

Chapter 3: High Glucose Facilitated Endothelial Heparanase Transfer to the Cardiomyocyte Modifies its Cell Death Signature

3.1 Premise

In the heart, where contracting cardiomyocytes are incapable of regeneration, intrinsic mechanisms are available within the endothelial cell (EC) to protect the cardiomyocyte against cellular demise [224-227]. One conceivable cardioprotective protein, secreted exclusively from the EC in the heart, is heparanase [16, 228]. This endoglycosidase is initially synthesized as a latent (enzymatically inactive; Hep^{L}) 65 kDa proheparanase enzyme. Hep^{L} undergoes cellular secretion, which is followed by reuptake into lysosomes for proteolytic cleavage (removal of a 6 kDa linker peptide) [16]. Consequently, a 50 kDa polypeptide (enzymatically active; Hep^{A}) is formed that is ~100-fold more active than Hep^{L}.

In cancer biology, Hep^{A} degradation of heparan sulphate proteoglycan (HSPG) is associated with extracellular matrix and basement membrane disruption, facilitating tumour cell invasion [16, 229-231]. Following its nuclear entry, Hep^{A} also influences transcription by cleaving nuclear HSPG, mitigating the suppressive effect of heparan sulphate on histone acetyltransferase [232-236]. More recently, we established a novel role for Hep^{A} in modulating cardiac metabolism during diabetes [232, 237]. The above studies in cancer and diabetes fixated on the effects of Hep^{A}, incorrectly assuming that only the HSPG-hydrolyzing ability of heparanase was of importance. Intriguingly, Hep^{L} also has some remarkable properties, including its ability to activate signalling elements like

Erk1/2, PI3K-AKT, RhoA and Src, which in turn can contribute to changes in transcription [16]. Cancer cells use secreted Hep^{L} to alter gene expression (either through its cell signalling properties, or by its conversion to Hep^{A}) in neighbouring cells, preventing their cellular demise and promoting tumour growth [16, 238, 239]. In the heart, a similar paradigm would appear advantageous, with endothelial Hep^{L} protecting the cardiomyocyte against cell death. For this to happen, Hep^{L} needs to be secreted, followed by its subsequent binding and uptake into the cardiomyocyte. We hypothesized that, following its secretion from the EC, Hep^{L} uptake and function in the cardiomyocyte is protective against cell death. Results from this study suggest that HG increases heparanase secretion from EC, in addition to augmenting its uptake into the cardiomyocyte, where it has a favourable effect on the expression of apoptosis-related genes and limits the incidence of cell death. Occurrence of this EC-to-cardiomyocyte transfer of heparanase in the acutely diabetic heart, and the interruption of this process following chronic and progressive diabetes, may contribute towards the development of diabetic cardiomyopathy [49, 196, 240].

3.2 Macrovascular and microvascular EC secretion and reuptake of heparanase in response to high glucose

The concentration and activity of heparanase are elevated in the plasma and urine of diabetic patients [241]. We have also reported that HG can stimulate the secretion of both latent and active forms of heparanase from EC [242]. As EC behave differently based on their vessel type and environment [243], in this study, we compared the effects of HG on

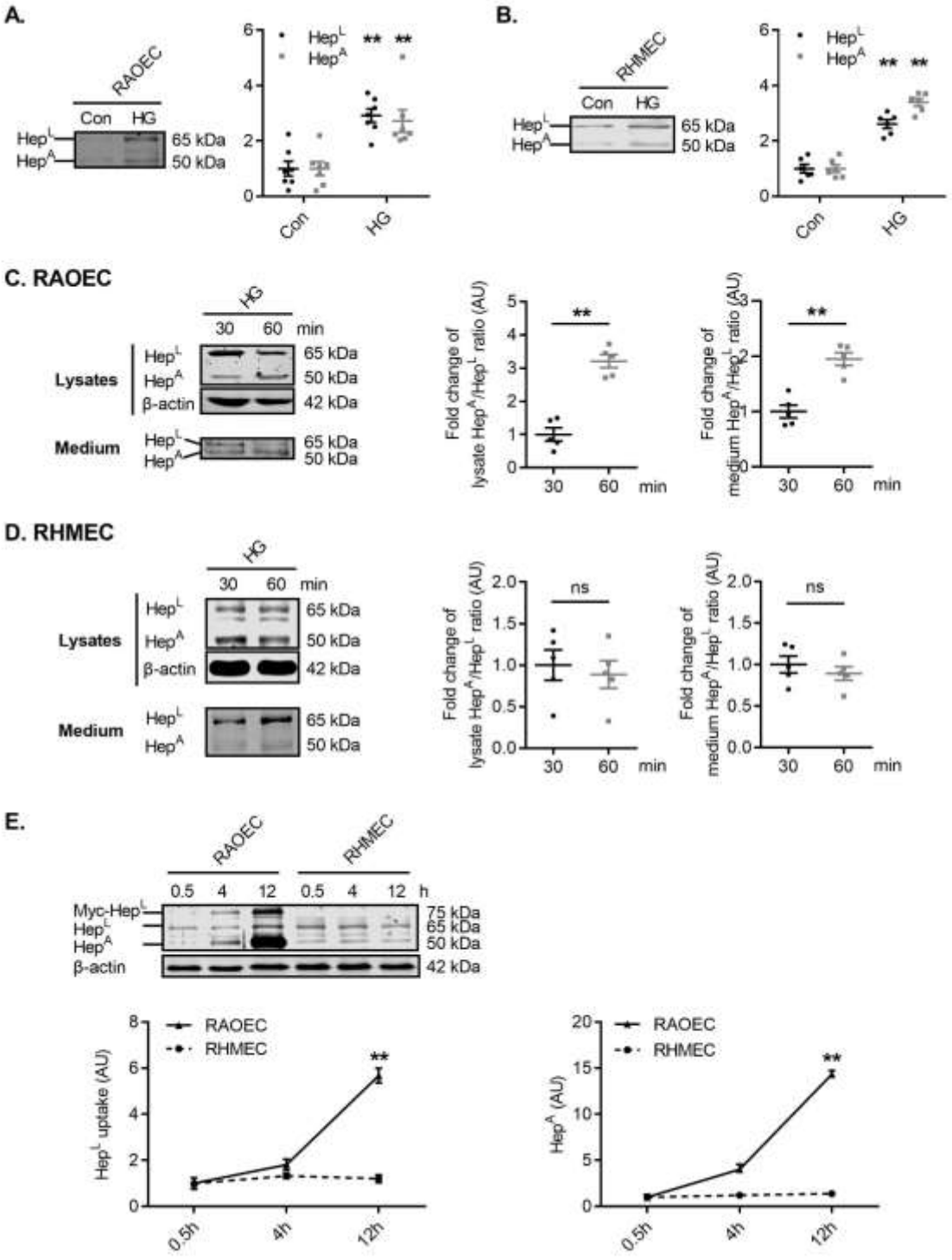

Figure 3.1. Heparanase secretion and reuptake into endothelial cells.

Rat aortic endothelial cells (RAOEC; passage 5-8) and rat heart microvessel endothelial cells (RHMEC, passage 5-8) were incubated in either 5.5 (normal glucose control; Con) or

25 mM (high glucose; HG) glucose for 30 min. Incubation medium was collected and used to determine latent (Hep^L) and active (Hep^A) heparanase secretion, n=6-7 (A and B). Data are presented as mean ± SEM (Student's t-test). $^{**}p<0.01$ compared to Con. RAOEC (C) and RHMEC (D) were incubated in 25 (HG) mM glucose for 30 or 60 min. Cell lysates and incubation medium were used to determine the intracellular and extracellular content of Hep^L and Hep^A, n=5, $^{**}p<0.01$. RAOEC and RHMEC were incubated with normal glucose and 500 ng/ml myc-Hep^L. Cell lysates were collected at indicated time points to measure the uptake of myc-Hep^L and its conversion to Hep^A, n=6 (E). Data are presented as mean ± SEM (Student's t-test). $^{**}p<0.01$ compared to RHMEC.

releasing Hep^L and Hep^A from macrovascular and microvascular EC. Incubation of RAOEC in HG promoted the release of both forms of heparanase into the incubation medium (Fig. 3.1A); Hep^A by purinergic receptor activation and lysosomal secretion [244], and Hep^L by activation of the serine/threonine protein kinase D (PKD), an enzyme involved in the fission of proteins destined for the cell surface (Supplementary Fig. 3.1). Similar results were observed when using RHMEC (Fig. 3.1B). The osmolarity control, mannitol, had no influence on heparanase release in either cell type (data not shown). After its cellular release, Hep^L must be taken back up into EC [16] for maturation into Hep^A. Hence, heparanase reuptake was also determined in EC subsequent to its release by HG. The decline in RAOEC lysate Hep^A at 30 min was followed by a substantial recovery at 60 min, resulting in an increase in the Hep^A/Hep^L ratio (Fig. 3.1C, left panel). Measurement of heparanase in the medium also demonstrated a higher Hep^A/Hep^L ratio over time (Fig. 3.1C, right panel), confirming the reuptake and processing of Hep^L into Hep^A, which was eventually secreted into the medium. Remarkably, unlike RAOEC, the reuptake and subsequent processing of Hep^L into Hep^A was not evident in RHMEC (Fig. 3.1D). To substantiate that only macrovascular, but not microvascular, EC can take up Hep^L, we

used EC incubated with recombinant myc-tagged latent heparanase (myc-Hep^{L}). In RAOEC, there was a robust time-dependent uptake of Hep^{L} and conversion into Hep^{A}, effects that were not apparent for RHMEC (Fig. 3.1E), suggesting that microvascular EC have a limited capacity for Hep^{L} reuptake.

3.3 LRP1 is important for Hep^{L} uptake

Multiple receptors have been implicated in facilitating the uptake of Hep^{L}, including the mannose-6-phosphate receptor, HSPG, and LRP1 [9]. We focused on LRP1 given its promiscuous role in the endocytosis of a number of different proteins [245, 246]. Of considerable interest was the observation that RAOEC demonstrated a robust expression of LRP1. This expression was not apparent in RHMEC (Fig. 3.2A and 3.2B), and could explain the disparate abilities of these two cell types to take up Hep^{L}. Using siRNA, we effectively reduced LRP1 expression in RAOEC (Fig. 3.2C bottom panel and 3.2D). As a consequence, myc-Hep^{L} uptake and conversion to Hep^{A} over 24 h was reduced in these cells compared to control (Fig. 3.2C top panel and 3.2E), validating the contribution of LRP1 in Hep^{L} uptake (schematic). In spite of LRP1 knockdown, some Hep^{L} was still detected, albeit at a level much lower as compared to control, and likely as a consequence of nonspecific binding of Hep^{L} to the endothelial cell surface. Simple binding to the cell surface exterior, with limited uptake, will fail to increase the amount of Hep^{A}, as shown in Fig. 3.2C. The essential role of LRP1 was further substantiated using the specific blocker RAP (an LRP1 chaperone) (Fig. 3.2F), and an LRP1 neutralizing antibody (Fig. 3.2G), both

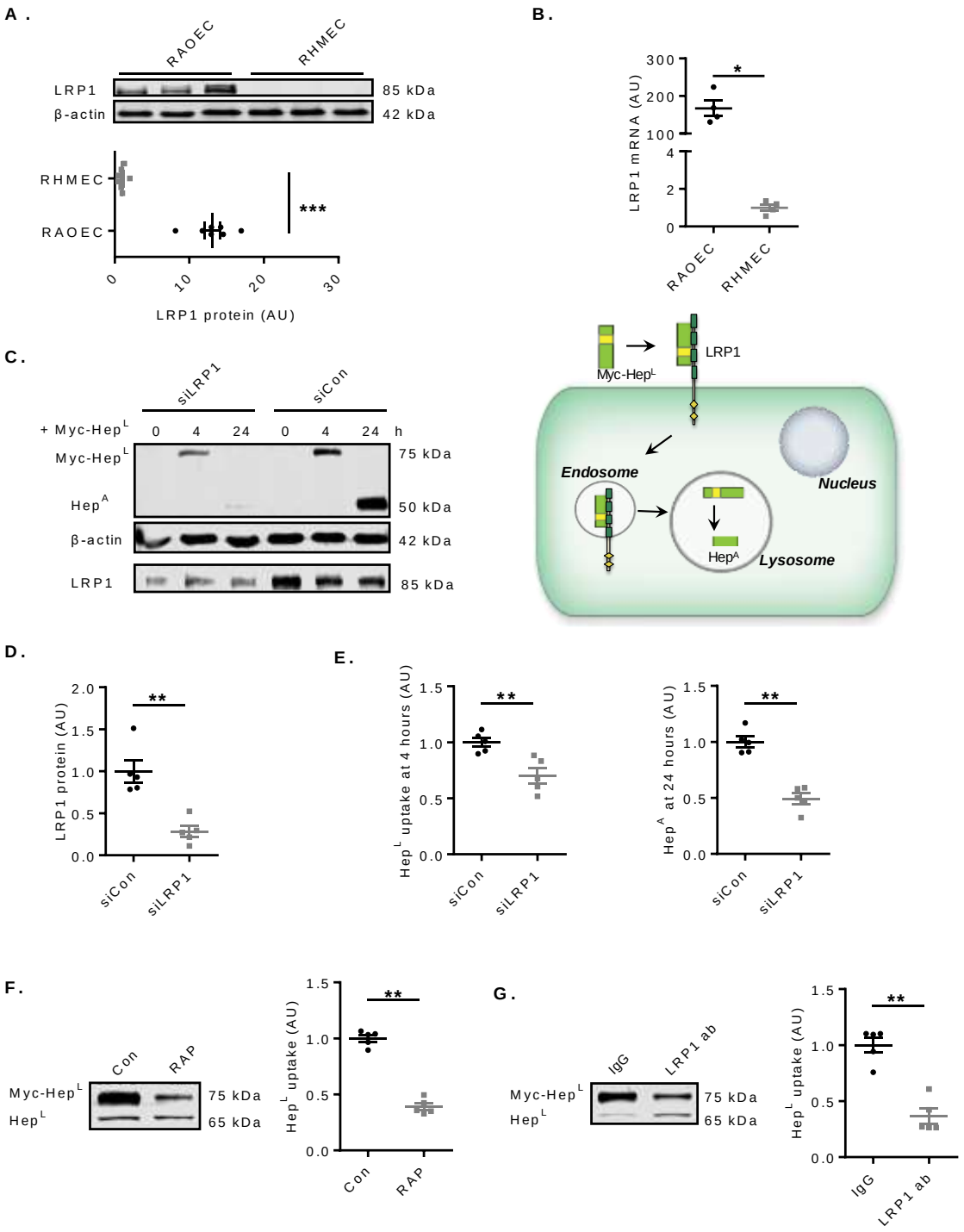

Figure 3.2. LRP1 is a key receptor for heparanase reuptake into endothelial cells.

RAOEC and RHMEC lysates were used to determine the expression of LRP1, n=7 and n=4 (A and B). In RAOEC, siRNA was used to silence LRP1, followed by determination of myc-Hep^{L} uptake and conversion to Hep^{A}, n=5 (C-E). RAOEC were pre-treated with or without 200 nM RAP (F) or 20 µg/ml LRP1 neutralizing antibody (G) for 1 h prior to incubation with

500 ng/ml myc-Hep^{L} for 4 h. Cell lysates were collected to determine Hep^{L} uptake, n=5. 20 µg/ml IgG was used as a control for the LRP1 neutralizing antibody experiment. Data are presented as mean ± SEM (Student's t-test). *p<0.05, **p<0.01, ***p<0.001.

of which reduced the uptake of Hep^{L} by RAOEC. Our data implicate LRP1 as an essential contributor in the endocytosis of Hep^{L} in EC.

3.4 Extracellular uptake determines presence of heparanase in cardiomyocytes

In the heart, EC outnumber cardiomyocytes by 3:1 [225]. Intriguingly, compared to EC, there is a negligible amount of heparanase gene expression in cardiomyocytes (Fig. 3.3A). We reasoned that the absence of a reuptake machinery in microvascular EC would lead to Hep^{L}, secreted from these cells, to be taken up into cells that are in close proximity; for example, the cardiomyocytes. Indeed, our results indicate that cardiomyocytes contain a significant amount of heparanase protein (Fig. 3.3B), suggesting that Hep^{L}, taken up from neighbouring microvascular EC, is converted to Hep^{A} in the cardiomyocyte lysosome. These results are supported by our previous work using EC co-cultured with cardiomyocytes [232]. The uptake and lysosomal localization of myc-Hep^{L} were further confirmed using immunofluorescence (Fig. 3.3C), whereas the nuclear presence of Hep^{A} was established using Western blot (Fig. 3.3D). Given the importance of LRP1 in EC Hep^{L} uptake, we determined and confirmed its expression in cardiomyocytes (Fig. 3.3E and 3.3F). In addition, and analogous to RAOEC, administration of either RAP or an LRP1 neutralizing antibody reduced the cardiomyocyte uptake of myc-Hep^{L} (Fig. 3.3G).

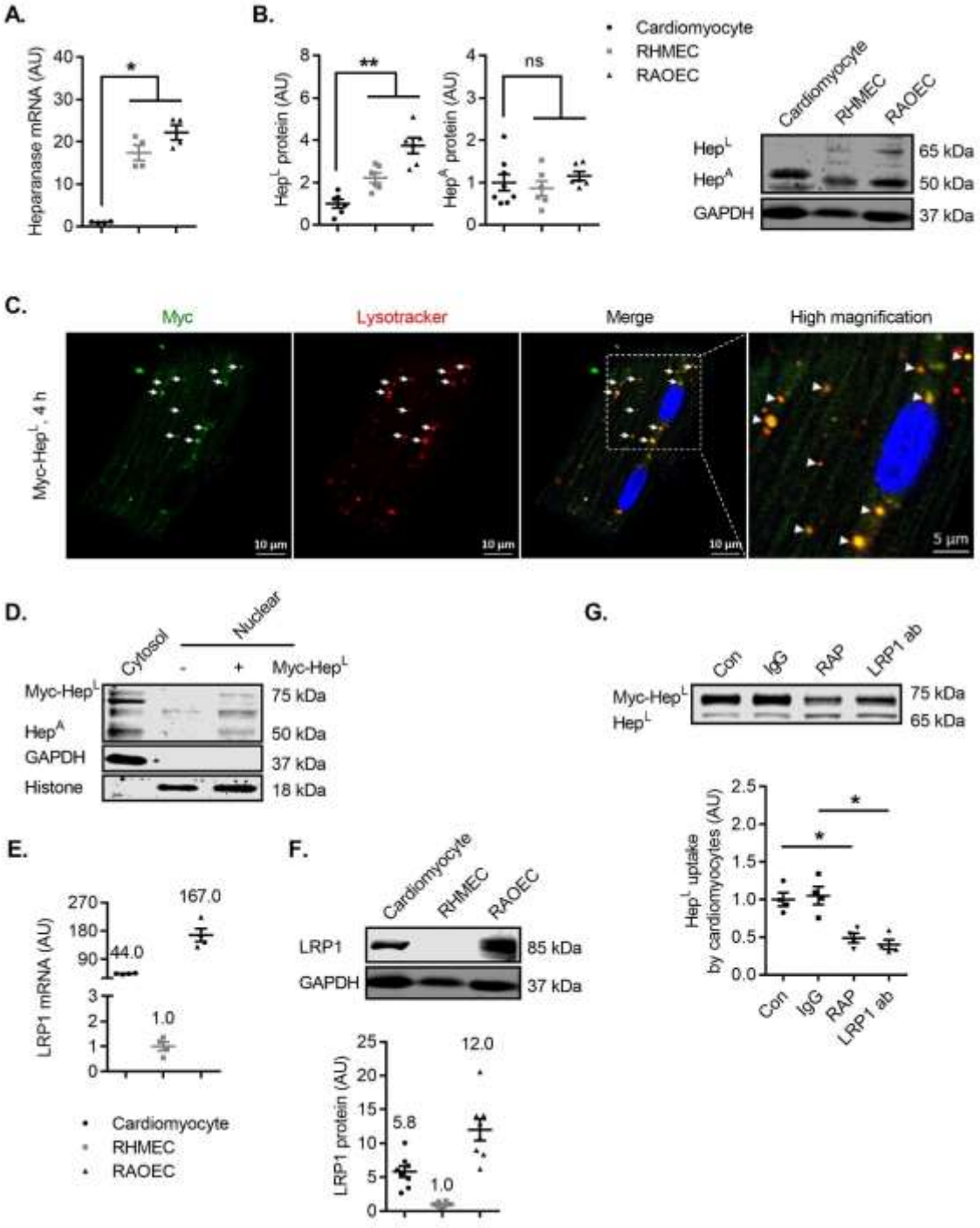

Figure 3.3. Cardiomyocytes are also capable of Hep^L uptake.

Cell lysates of primary rat cardiomyocytes, RAOEC or RHMEC were obtained for determination of heparanase mRNA (A) and protein (B), n=4-8. Cardiomyocytes seeded on coverslips were placed in a 6-well plate, and treated with 500 ng/ml myc-Hep^L prior to immunofluorescence staining examined under a confocal microscope. The merged image

of heparanase and lysosomes is described in the third (scale bar, 10 µm) and fourth (scale bar, 5 µm) panels from left (C) and are data from a representative experiment. Isolated myocytes were also treated with or without myc-Hep^L for 4 h. Following this incubation, nuclear and cytosolic fractions were isolated, and Hep^A protein levels determined by Western blot (D). Cell lysates of primary rat cardiomyocytes, RAOEC or RHMEC were obtained for determination of LRP1 mRNA (E) and protein (F), n=4 and n=8. In a different experiment, in cardiomyocytes incubated with HG, cells were pre-treated with or without 400 nM RAP or 40 µg/ml LRP1 neutralizing antibody for 1 h prior to incubation with 500 ng/ml myc-Hep^L for 4 h. Cell lysates were collected to determine Hep^L uptake, n=4 (G). 40 µg/ml IgG was used as a control for the LRP1 neutralizing antibody experiment. Data are presented as mean ± SEM (Student's t-test for A and one-way ANOVA for B and E-G). **p*<0.05, ***p*<0.01.

3.5 Hep^L modulates expression of apoptosis-related genes in cardiomyocytes

Entry of heparanase into the nucleus to regulate histone acetylation has been suggested as a mechanism modulating gene transcription and protection against apoptosis [233]. We hypothesized that, following its uptake into the cardiomyocyte, Hep^L can protect against cell death by influencing apoptosis-related genes. Using a rat apoptosis gene array in cardiomyocytes incubated with myc-Hep^L we found that, among the 70 genes that had well-defined functions and significant levels of expression, 15 out of 27 anti-apoptotic genes were upregulated, and 29 out of 43 pro-apoptotic genes were downregulated (Fig. 3.4A and 3.4B). Of the 18 genes that were significantly different (fold change >1.5) compared to control, 15 were in favour of cell survival (6 anti-apoptotic genes were upregulated; 9 pro-apoptotic genes were downregulated) (Fig. 3.4A and 3.4B; Supplementary Table 3.1). Further examining selective pro-apoptotic genes that were

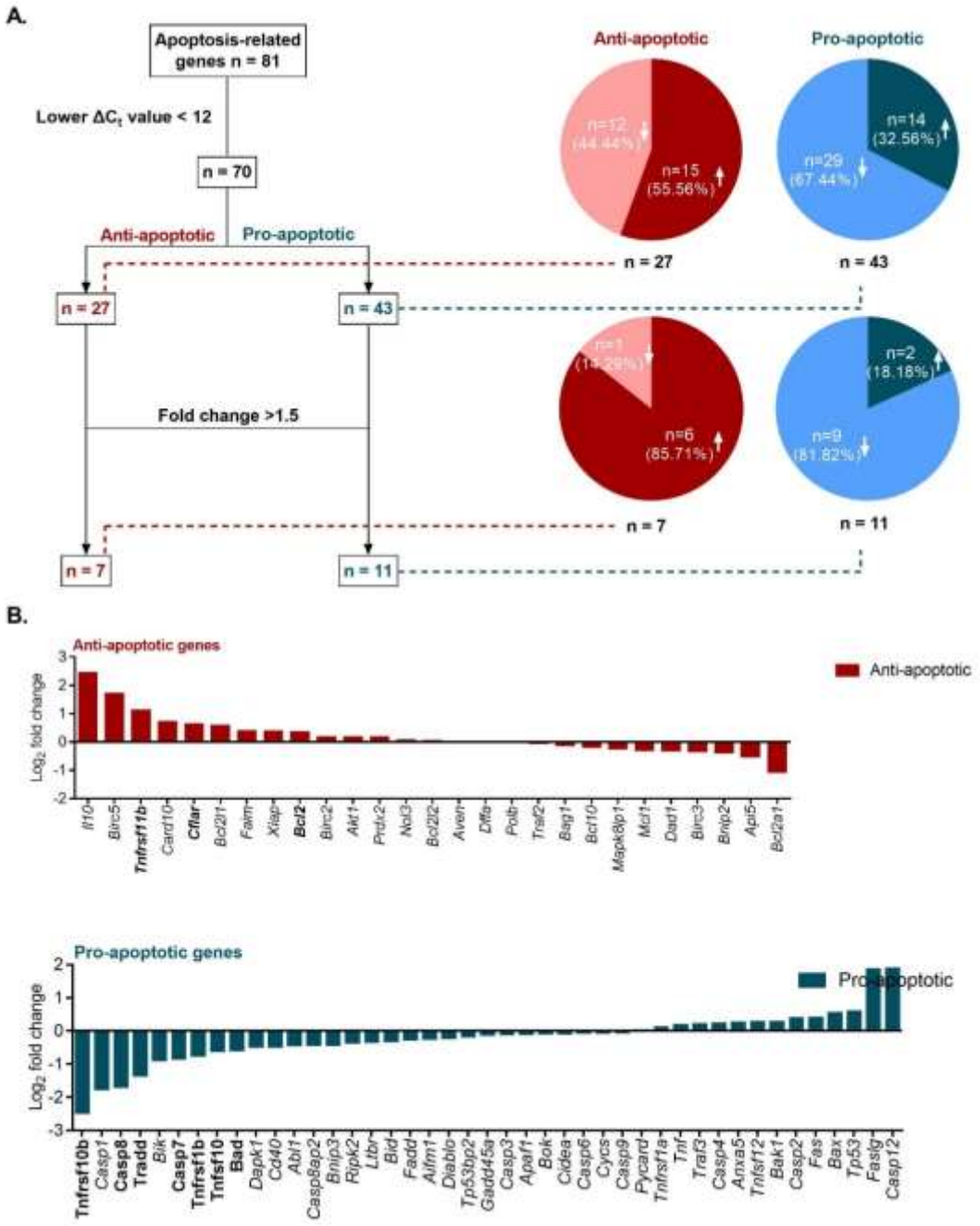

Figure 3.4. Expression of apoptosis-related genes in cardiomyocytes exposed to exogenous Hep^L.

Primary cardiomyocytes isolated from the adult rat heart were treated with or without 500 ng/mL myc-Hep^L for 12 h prior to RNA isolation and subsequent determination of 81 apoptosis-related genes using a PCR array (A and B).

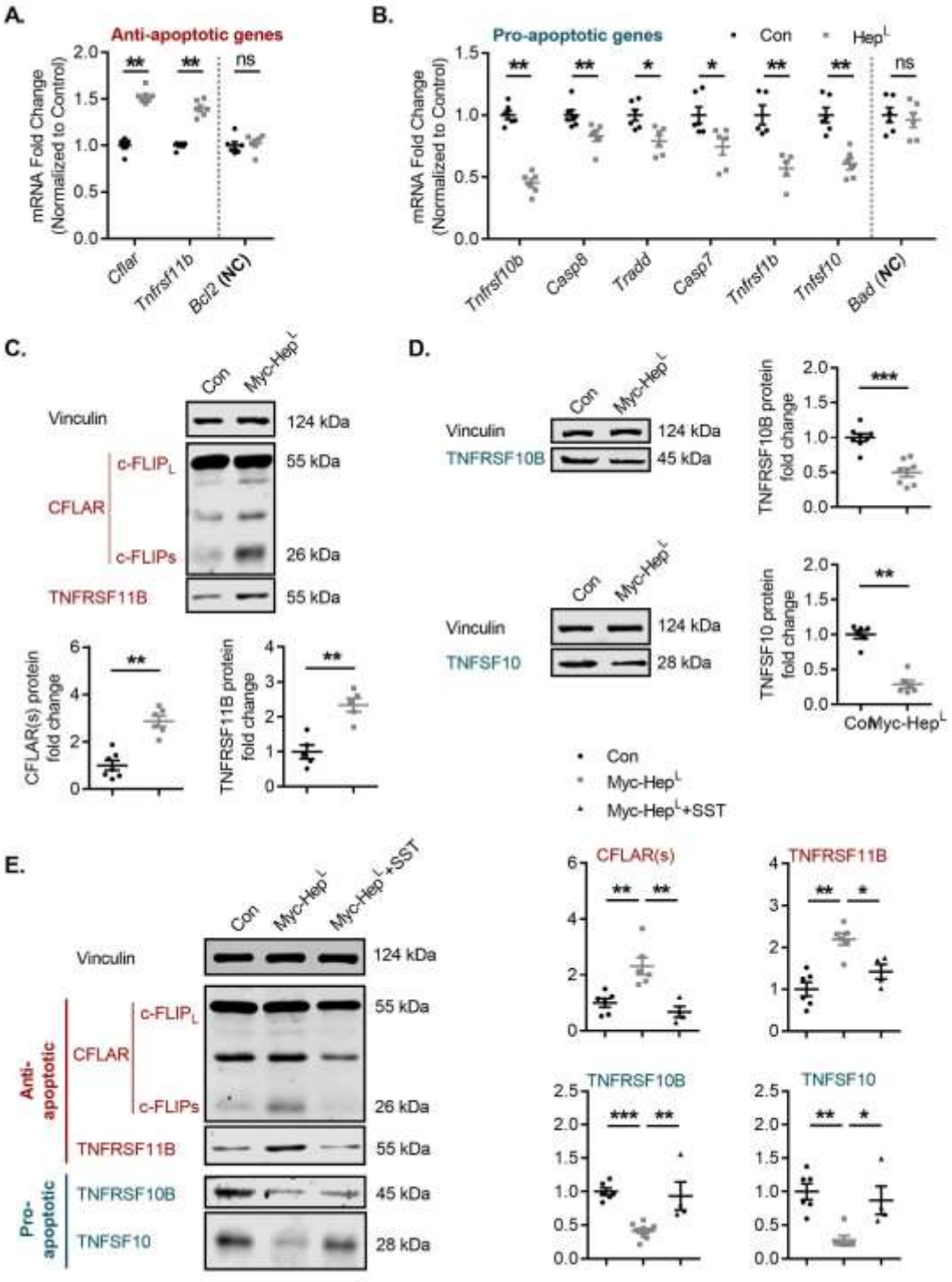

Figure 3.5. Inhibition of Hep^{A} abrogates changes in gene expression.

RT-PCR and Western blot were employed to confirm our results from the gene array using selected pro- and anti- apoptosis genes, n=5-8 (A-D). Vinculin was used as a loading control, NC-negative control. In a separate experiment, cardiomyocytes were pre-treated

with or without 125 µg/ml SST0001 for 4 h, prior to incubation with 500 ng/ml myc-Hep^{L} for 12 h, and the expression of selected genes determined, n=4-9 (E). Data are presented as mean ± SEM (Student's t-test for A-D and one-way ANOVA for E). *p<0.05, **p<0.01, ***p<0.001.

downregulated, and anti-apoptotic genes that were upregulated, results from the microarray were confirmed by quantitative real-time PCR (Fig. 3.5A and 3.5B) and Western blot (Fig. 3.5C and 3.5D). As SST0001, a specific heparanase inhibitor, reversed the effects of heparanase (Fig. 3.5E), our results suggest that heparanase can protect against apoptotic cell death.

3.6 Contrasting effects of diabetes on cardiomyocyte cell death signature

RAOEC incubated in HG demonstrate an increase in LRP1 expression (Supplementary Fig. 3.2), emphasizing the importance of HG in mediating its expression. Using a model of acute (4 day) diabetes, we assessed the impact of HG on whole heart and cardiomyocyte LRP1. Hearts from acute diabetic animals demonstrated augmented LRP1 expression (Fig. 3.6A). This effect likely contributed to a higher uptake of Hep^{L} and its subsequent conversion into Hep^{A}, which resulted in a higher Hep^{A}/Hep^{L} ratio (Fig. 3.6A). Extending this observation, cardiomyocytes isolated from animals with acute diabetes also exhibited higher LRP1 expression and intracellular heparanase content (Fig. 3.6B). The latter effect was unrelated to changes in heparanase gene expression (Fig. 3.6C). It should be noted that, unlike EC, when cardiomyocytes were exposed to HG, no change in LRP1 expression was observed, up to 48 h after incubation (data not shown). Nevertheless, we observed an increased uptake and lysosomal localization of heparanase at 4 h in cardiomyocytes

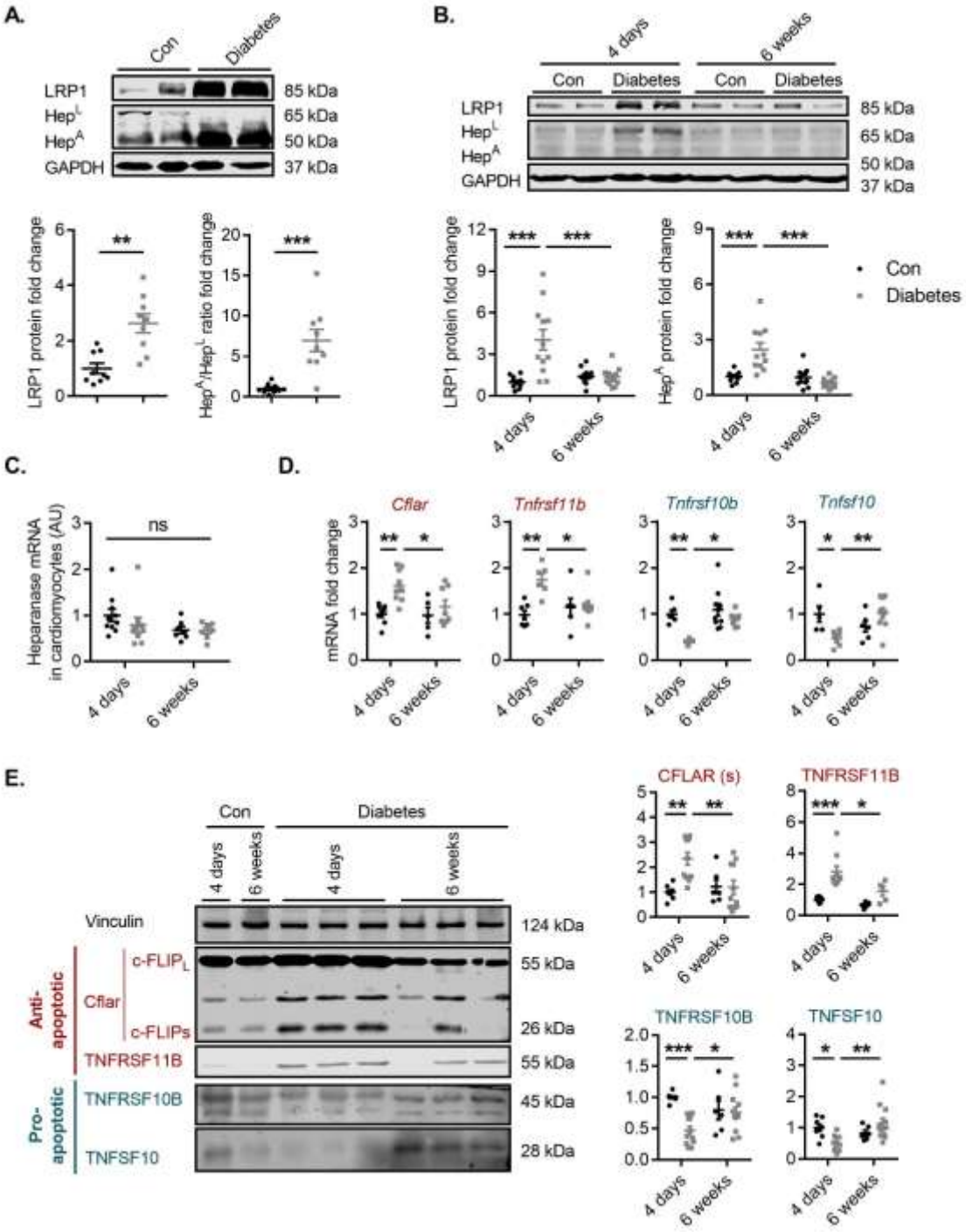

Figure 3.6. Acute and chronic effects of diabetes on cardiomyocyte cell death signature.

In animals made diabetic with STZ, hearts were obtained after 4 days of hyperglycemia and LRP1 protein and the Hep^A/Hep^L ratio determined, n=9 (A). Cardiomyocytes from acute (diabetes-4d) and chronic (diabetes-6w) diabetic animals were isolated for

determination of LRP1 and heparanase protein (B) and heparanase gene (C), n=10-12. Selected pro- and anti-apoptosis genes (D) and protein (E) were also evaluated in acute and chronic diabetic cardiomyocytes, n=5-11. Data are presented as mean ± SEM (Student's t-test). **p*<0.05, ***p*<0.01, ****p*<0.001.

incubated in HG (Supplementary Fig. 3.3A and B). As the inhibition of Src activation by PP2 abrogated this effect, this proto-oncogene, rather than augmented expression of LRP1, can be implicated in HG-mediated cardiomyocyte heparanase uptake *in vitro* (Supplementary Fig. 3.3C and D). Whether Src activation also has a contributory effect *in vivo* is currently unclear because its activation by HG was detected within 30 minutes *in vitro*, whereas diabetic animals are euthanized after 4 days of STZ. Of considerable significance was the observation that these effects on cardiomyocyte LRP1 and heparanase were abolished upon extending the duration of diabetes to 6 weeks (Fig. 3.6B), suggesting that cardiomyocyte LRP1 expression and heparanase uptake are affected in an opposite fashion depending on the duration of hyperglycemia. As apoptosis-related gene (Fig. 3.6D) and protein (Fig. 3.6E) expression and cleaved caspase 3 and PARP (Supplementary Fig. 3.4) followed a similar pattern predicated on the duration of diabetes, our data suggest that chronic diabetes nullifies the favourable effects of heparanase in cardiomyocytes.

3.7 HG and H_2O_2 induced cardiomyocyte cell death is attenuated by Hep^L

In HG, a greater production of ROS together with its disrupted detoxification causes cardiomyocyte cell death [247]**.** Given the effects of ROS on gene expression in cells

undergoing apoptosis, cardiomyocytes were incubated with HG in the presence or absence of heparanase. In HG, Hep^{L} caused a significant decrease in the Bax/Bcl-2 mRNA

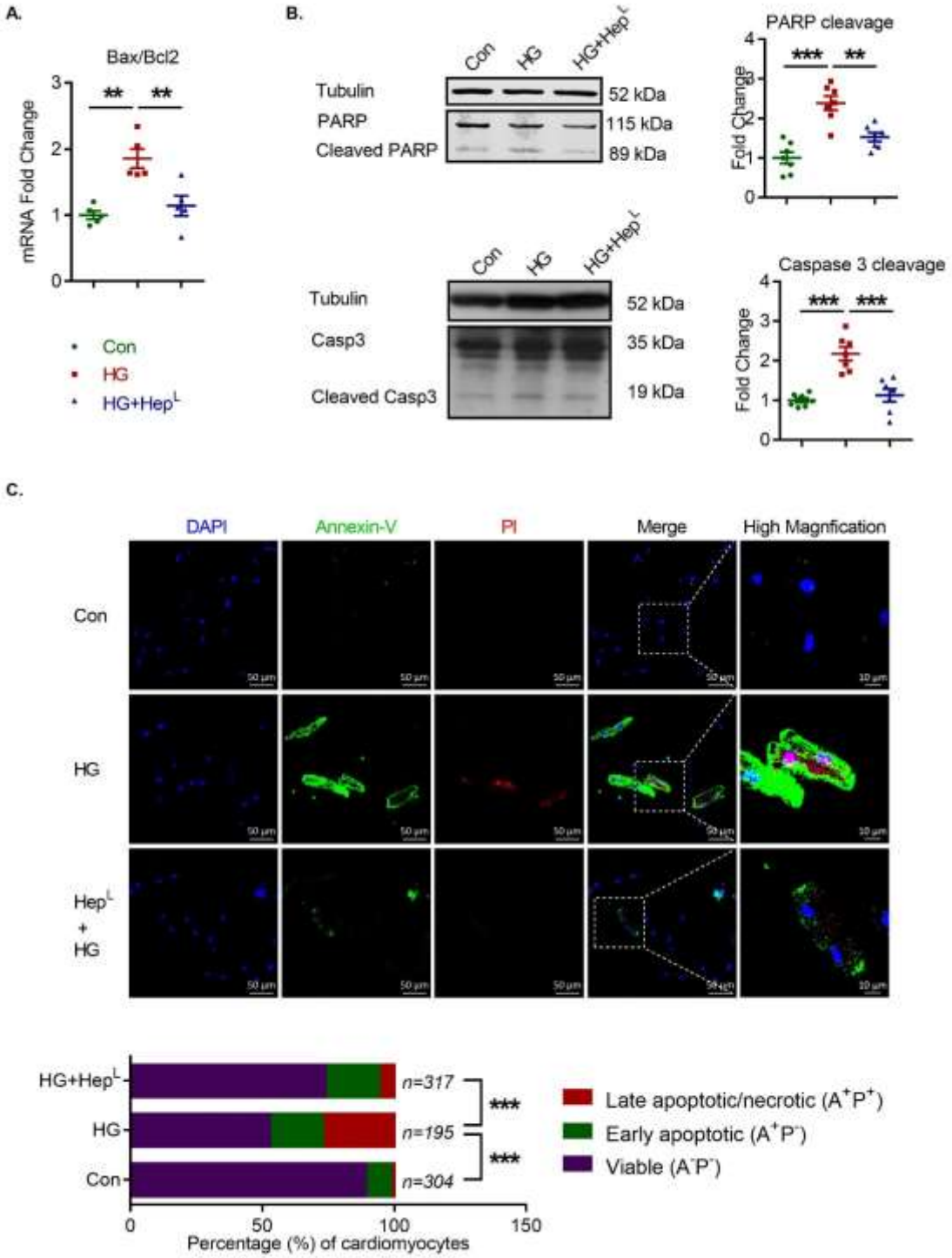

Figure 3.7. Hep^{L} protects cardiomyocytes from HG induced apoptosis.

Isolated rat cardiomyocytes were incubated with 30 mM glucose (HG) and/or 500 ng/mL myc-Hep^{L} for 12-48 h, n=6. After 12 h, the Bax/Bcl2 mRNA ratio was determined (A). PARP and caspase 3 cleavage were evaluated after 48 h (B), n=7. Annexin V/PI staining, as markers of apoptosis, were also determined after cardiomyocyte incubation with HG and/or myc-Hep^{L} (C), n=195-317 myocytes pooled from 4 independent experiments. The merged image of Annexin V/PI staining is described in the fourth panel (scale bar 50 µm), whereas a higher magnification image (scale bar 10 µm) is described in the fifth panel. Data are presented as mean ± SEM (one-way ANOVA). . **p<0.01, ***p<0.001.

ratio, a marker of cellular apoptosis (Fig. 3.7A). Cleaved PARP and caspase 3, apoptosis biomarkers that were augmented in cardiomyocytes treated with HG, were also significantly decreased upon heparanase addition (Fig. 3.7B). Importantly, the HG-induced decrease in the number of viable cardiomyocytes, as determined by Annexin V/Propidium Iodide staining, was improved by Hep^{L} (Fig. 3.7C). As these beneficial effects of Hep^{L} on apoptosis were reproduced in H_2O_2 induced oxidative stress (Supplementary Fig. 3.5), our data suggest that heparanase modulates the cell death signature and is protective against cardiomyocyte cell death.

3.8 Discussion

Under physiological conditions, the EC is responsible for secreting factors that support cardiomyocyte function [224-227]. Heparanase is one such example, having a unique responsibility to release cardiomyocyte cell surface HSPG-bound LPL to promote lipoprotein-TG breakdown. The resultant FA generated is then transported to the cardiomyocyte for oxidative energy generation [237]. In addition to liberating HSPG-bound proteins, heparanase, either by binding to putative cell-surface receptors, or

subsequent to its internalization and nuclear entry, has also been suggested to affect gene transcription [16, 233-236, 248, 249]. In cancer cells, this property of secreted heparanase can induce cell signalling and gene expression in both parent and adjacent cells, maintaining their survival and delaying demise [233, 238, 239, 250-252]. Our data suggest, for the first time, that HG promotes both the secretion of heparanase from EC as well as its uptake into cardiomyocytes, initiating pro-survival mechanisms to temper the consequences of hyperglycemia in the diabetic heart.

In EC, Hep^{A} resides in lysosomes [16] and hyperglycemia, a major complication of diabetes, is an effective stimulus for its secretion [244]. We have previously described a mechanism for this process, which includes purinergic receptor activation, as well as cortical and stress actin reorganization [244]. As EC are not all created equal and exhibit differences depending on their anatomical sites-such as arterial compared to venous architecture, or macro compared to their microvascular locations [243]-we compared the secretion of heparanase in RAOEC and RHMEC. Here we show that HG similarly affects the secretion of Hep^{L} from both EC cell types. Following its secretion, the EC has a capacity to reuptake Hep^{L} for lysosomal conversion to Hep^{A}. Interestingly, although both cell types had a similar capacity to secrete Hep^{L} in response to HG, only macrovascular EC were competent for its reuptake, an observation that was confirmed using myc-Hep^{L}. A receptor that has been implicated in Hep^{L} uptake is LRP1 [253]. Consistent with the differential uptake of Hep^{L} into the two cell types, only RAOEC showed a robust expression of LRP1. We further established that LRP1 is indispensable for Hep^{L} uptake into RAOEC by silencing the receptor using RAP or an LRP1 neutralizing antibody, both of

which decreased the uptake of Hep^L. Our data imply that the reuptake of Hep^L by macrovascular EC is dependent on LRP1, an uptake mechanism that is missing in microvascular EC. At present, the mechanism behind the differential LRP1 expression observed in macrovascular and microvascular endothelial cells is unclear, but could be related to shear stress, a stimulus that is known to change gene expression [254, 255]. The absence of this reuptake machinery in microvascular EC suggests that the Hep^L secreted from these cells is likely taken up, in the heart, by proximal cells. Given the proximity of cardiomyocytes (which do not express the heparanase gene) to microvascular EC, it is plausible to envision the exogenous uptake of EC-secreted heparanase into cardiomyocytes. In support of this theory, we detected both the latent and active forms of heparanase in isolated cardiomyocytes. This observation, coupled with the robust expression of LRP1 in cardiomyocytes, whose inhibition abrogates Hep^L uptake, indicates that transfer from exogenous sources determines the presence of heparanase in cardiomyocytes.

One implication of cardiomyocytes acquiring Hep^L is its subsequent intracellular conversion to Hep^A, followed by its nuclear entry to influence gene transcription. By cleaving nuclear HSPG, Hep^A mitigates the suppressive effect of heparan sulphate on histone acetyltransferase to activate gene expression [233]. Using an apoptosis PCR array, which detects both pro- and anti-apoptotic genes, we discovered that cardiomyocytes incubated with Hep^L downregulated pro-apoptotic genes (e.g., Tnfrsf10b, Tnfsf10), whereas anti-apoptotic genes (e.g., Cflar, Tnfrsf11b) were upregulated. As cardiomyocytes isolated from heparanase transgenic mice also showed a similar trend in

this gene expression pattern (unpublished data), our data imply that Hep^{L} displayed pro-survival effects on the cardiomyocyte by initiating a program that protects against apoptosis. This effect of heparanase on gene expression relies on its activity, as its inhibition by a specific heparanase inhibitor reversed its beneficial effects on gene expression. Additionally, the changes in gene expression induced by heparanase translated into protection against cardiomyocyte cell death, as confirmed by the reduction in the Bax/Bcl-2 mRNA ratio, cleaved PARP and caspase 3, and Annexin V/Propidium Iodide staining. In diabetes, hyperglycemia can provoke cardiomyocyte cell death and contribute to cardiomyopathy [49, 196, 240, 256]. However, it should be noted that it is the EC that is exposed to this metabolic alteration before the cardiomyocyte. As such, through their release of Hep^{L}, EC, as first responders to hyperglycemia, could precondition the cardiomyocyte against impending metabolic damage. For this to work, hyperglycemia also needs to increase Hep^{L} uptake into the cardiomyocyte. Indeed, we observed robustly increased LRP1 expression and levels of Hep^{A}, as well as a pro-survival gene signature in whole hearts and cardiomyocytes isolated from acutely diabetic animals. Hyperglycemia and its associated oxidative stress, which resembles hypoxia, and its attendant increase in HIF-1α, could be one explanation for LRP1 induction in short-term hyperglycemia. HIF-1α is a known factor that can induce LRP1 expression in cardiomyocytes [257] and in other cell types [258-261]. These effects were lost following chronic diabetes, and could contribute to the development of cardiomyopathy in these animals. The disappearance of LRP1, with prolonged duration of diabetes, may be related to a further attenuation of circulating insulin, as islets that escaped the initial insult by STZ

are later lost due to the combined features of hyperglycemia and hyperlipidemia (gluco-lipotoxicity). Interestingly, several studies have reported that LRP1 is downregulated in brains from chronically diabetic mice, an effect associated with sustained hyperglycemia and insulin deficiency in these animals [262, 263]. Confirmation of the beneficial effects of heparanase in the prevention of diabetic cardiomyopathy requires the induction of diabetes in mice that overexpress heparanase, experiments that are currently underway in our lab.

In summary, our data reveal a novel and complex role for EC in providing functional support to subjacent cardiomyocytes by communicating via soluble paracrine mediators. In this study, HG was a common stimulus for Hep^{L} secretion from the EC, in addition to promoting its uptake into the cardiomyocyte. The presence of heparanase in the cardiomyocyte dramatically changed the expression of apoptosis-related genes, providing an acute cardioprotective effect. Data obtained from these studies, suggesting a novel, favourable effect of Hep^{L} in the cardiomyocyte, will assist in devising novel therapeutic strategies to prevent or delay diabetic heart disease.

Chapter 4: Heparanase Protects the Heart against Chemical or Ischemia/Reperfusion Injury via Modulation of UPR and Autophagy

4.1 Premise

Heparan sulfate proteoglycans (HSPGs) are a class of macromolecules that constitute an important structural component, in addition to serving as a reservoir for signalling molecules [1]. More recently, HSPGs have also been reported to suppress histone acetyltransferase activity and consequently modulate gene expression [233]. Heparanase is the only known mammalian heparan sulfate-degrading enzyme (active heparanase, HepA). Its enzymatic action can elicit both physiological and pathophysiological responses [264]. An inactive precursor of the enzyme (latent heparanase, HepL), through non-enzymatic mechanisms, is involved in a number of signalling pathways including PI3K-Akt, ERK, RhoA, p38, and Src activation [21, 264]. Together, active and latent heparanase are known to participate in both unwanted consequences (heparanase upregulation by tumor cells leads to cancer progression) and favourable outcomes (such as wound healing and resistance to cell death) [34, 264].

Related to advancement of cancer, tumor cell production of heparanase can promote angiogenesis and protect cells against stress. It does so in several ways, by a) cleaving HSPGs and disrupting the extracellular matrix (ECM) to facilitate cell migration and invasiveness, b) shearing HSPGs to release attached growth factors and cytokines that

help with angiogenesis and cell survival, c) binding to putative cell surface receptors like LDL-related protein 1 and mannose-6-phosphate receptor to promote signalling related to cell migration, angiogenesis, and cell survival, and d) nuclear entry to regulate gene expression [6, 264].

Notwithstanding the ability of tumor cells to use heparanase for growth of cancer, the properties of heparanase to enable angiogenesis and cell survival in a non-cancer environment can be valuable. For example, transgenic overexpression of heparanase in mice (Hep-tg) exhibits a number of beneficial phenotypes. Hep-tg mice have a reduced amyloid burden and are also more resistant to inflammation-induced amyloid build up in multiple organs, especially in the brain [32, 33]. In the skin, Hep-tg mice exhibit accelerated wound healing, which is related to its effects to promote cell migration, proliferation, and angiogenesis [34]. Our recent study also reported that Hep-tg mice are resistant to chemically induced Type 1 diabetes, and have an improved glucose homeostasis through multiple mechanisms [35]. Additionally, we have described a protective function for heparanase in the acutely diabetic heart, where it conferred cardiomyocyte resistance to oxidative stress and apoptosis by provoking changes in gene expression [265].

The adult mammalian heart has no capacity for cell renewal and any injury will lead to compromised heart function and failure if protective mechanisms are absent or compromised. For example, under diverse pathological conditions like ischemia and diabetes, where there is dysfunction of the endoplasmic reticulum (ER) and impaired

protein folding, an intrinsic defensive mechanism is triggered called unfolded protein response (UPR). Once initiated, UPR can reduce protein synthesis, increase chaperone production (which allows proper protein folding in the ER), and stimulate protein degradation. This activation is sufficient to handle stress under physiological conditions, but is frequently insufficient under pathological conditions, including ischemic heart disease [74, 266, 267]. Furthermore, knock down of key UPR components usually leads to augmented cardiac infarction after ischemia/reperfusion (I/R), whereas overexpression of UPR regulators such as ATF6α or XBP1 has the opposite effect [267]. The protein degradation component of UPR is realized partly through autophagy, a process during which phagosomal engulfment of misfolded proteins and subsequent lysosomal fusion leads to their degradation [75, 207]. As a downstream executor of UPR, cardiac autophagy is also protective in I/R, especially in the ischemic stage [142, 206, 268]. Collectively, both UPR and autophagy restore ER homeostasis and prevent cell damage.

The organs that demonstrate the highest expression of heparanase following its global overexpression include the pancreas and the heart. Intriguingly, augmentation of heparanase in the pancreas is associated with an increase in autophagy [10], an outcome that could explain the resistance of this organ to the diabetogenic effects of streptozotocin, a beta-cell toxin [35]. We tested if overexpression of heparanase can defend the heart against chemically induced or ischemia/reperfusion (I/R) injury. Our data suggest that in Hep-tg mice, the heart exploits the pro-survival, anti-oxidative, and catabolic properties of heparanase to its advantage, protecting it against elements that would otherwise induce heart disease.

4.2 Hep-tg mice exhibit cardiac hypertrophy

In mice globally overexpressing heparanase, of all the different tissues evaluated, the heart demonstrated robust expression of both the Hep^{L} and Hep^{A} forms of heparanase (Supplementary Fig. 4.1). Of particular importance was the observation that when evaluated visually, hearts from Hep-tg mice appeared larger compared to those from WT animals (Fig. 4.1A). Hypertrophy was confirmed indirectly using heart weight/body weight and heart weight/tibia length ratios, both of which were higher in Hep-tg hearts (Fig. 4.1B). More directly using echocardiography, Hep-tg mice indeed displayed a larger left ventricular mass, with the posterior wall exhibiting the most significant increase in thickness (Fig. 4.1C). Interestingly, this evidence of cardiac hypertrophy was not reflected by alterations in cardiac function; ejection fraction, fractional shortening, and stroke volume were largely unaffected (Fig. 4.1D). Additional proof that the hypertrophy was likely adaptive is the evidence that the expression of genes associated with pathological remodelling (Fig. 4.1E), and hypertrophy-related signalling molecules like Akt and ERK (Fig. 4.1F), remain unchanged in Hep-tg hearts. Overall, our data provides evidence of physiological rather than pathological hypertrophy in Hep-tg hearts.

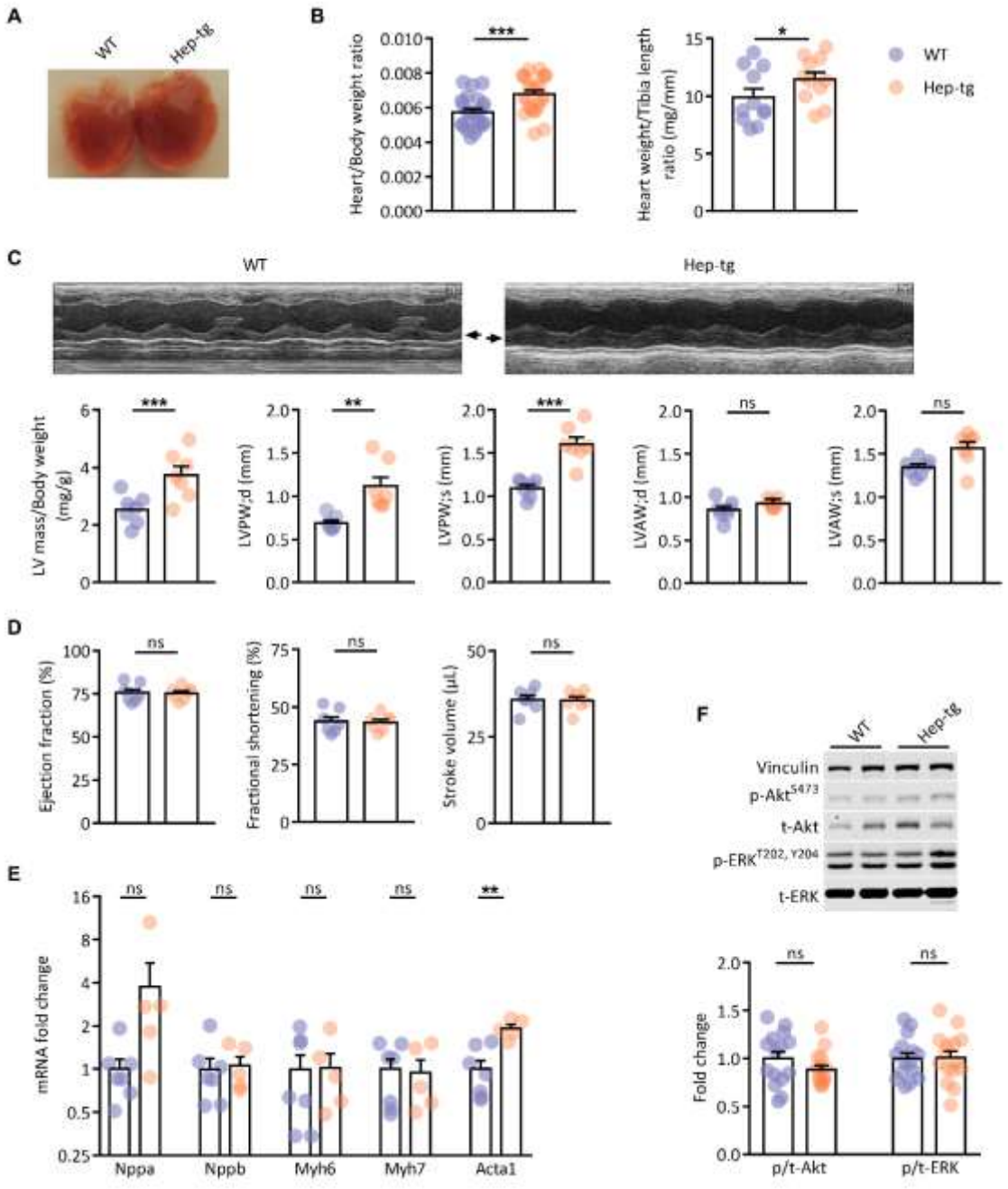

Fig 4.1. Cardiac morphology, function and hypertrophic gene expression in Hep-tg mice.

A: Representative image showing gross cardiac morphology. B: Heart weight/body weight ratio and heart weight/tibia length ratio; n=11-24. C: Representative M-mode image of wild type (WT) and heparanase transgenic (Hep-tg) heart using echocardiography. The arrow indicates posterior wall. D: Quantitative assessment of M-mode images describing left ventricular mass, wall thickness and function; n=7. E: mRNA of representative

hypertrophy markers; n=5-7. F: Protein expression of markers of hypertrophy; n=15. Data are presented as mean ± SEM (Student's t-test). *p<0.05, **p<0.01, ***p<0.001.

4.3 Heparanase overexpression alters the ventricular transcriptome

In our recent study using RNA-seq analysis of Hep-tg mice, we reported that the pancreatic islet transcriptome was greatly altered, with >2000 genes significantly differentially expressed in Hep-tg mice compared to control [35]. These effects could be partly explained by the nuclear entry and hydrolysis of HSPGs by Hep^{A}, which mitigated the suppressive effects of heparan sulphate on histone acetyltransferase, and which consequently activated gene expression [233]. In this study, we compared the ventricle transcriptome of WT and Hep-tg mice. Supplementary Tables 4.1 and 4.2 illustrate the 240 differentially regulated genes (padj < 0.05 and significant in at least 5 out of the 10 analysis pipelines used). When clustered according to function and ranked based on the false discovery rate (FDR), these genes were mostly related to the stress response (especially ER stress), immune response, cell death, and development (Fig. 4.2A). Additional analysis of these 240 genes revealed that the majority (80%) were upregulated (Fig. 4.2A, pie chart). Moreover, 64/240 genes are annotated as being related to modulation of cell survival, with the vast majority of these directed towards pro-survival mechanisms (Fig. 4.2B), encompassing genes related to UPR and autophagy, and those against oxidative stress (Fig. 4.2C and Supplementary Fig. 4.2). These data suggest that the reported property of heparanase in promoting cell survival in cancer progression could be uniquely beneficial in the heart, by protecting it against cellular stresses.

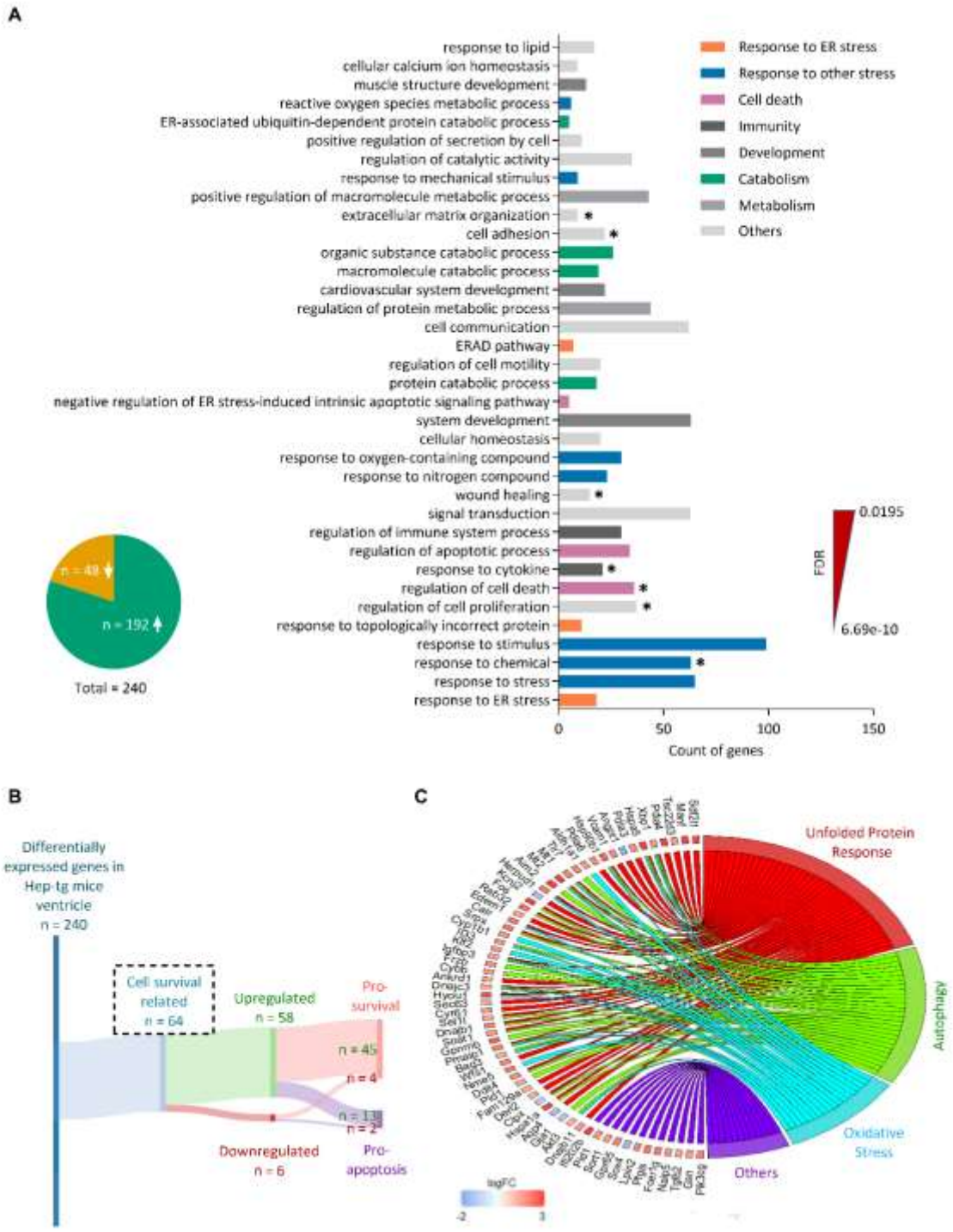

Fig 4.2. Ventricular transcriptome in hep-tg mice.

A: Ventricle RNA from WT (n=7) and Hep-tg (n=5) mice was sequenced, and differentially regulated genes (*padj* < 0.05 and significant in at least 5 out of the 10 analysis pipelines used) were clustered according to function and ranked based on FDR. The inset describes

the number of genes that were up- or down-regulated, *indicates that similar results have been obtained from other tissues isolated from Hep-tg mice. B: Of the 240 genes differentially regulated in Hep-tg mice ventricle, a Sankey diagram depicts the 64 cell-survival related genes. C: A Circos plot was used to link these 64 genes to 3 mechanisms that modulate cell survival. Expression level of genes involved in the pathways is indicated as a log2 fold change.

4.4 Activation of ATF6α by heparanase is a key initiator of adaptive UPR

In response to ER stress, the UPR is activated to salvage ER function (an adaptive response), the failure of which leads to apoptosis if the stress is prolonged [269]. Of the 240 differentially expressed genes in the Hep-tg ventricle, the ones that regulate UPR stood out as they exhibited the highest expression, fold change (Fig. 4.3A), and strongest interaction (Fig. 4.3B). Intriguingly, the genes related to adaptive UPR [e.g., Hspa5 (Grp78, Bip), Hsp90b1 (Grp94), Xbp1, Pdia3/4/6, Herpud1, Edem1, Calreticulin, Dnajc3 (p58IPK), Hyou1, Dnajc23 (Sec63, Erdj2), and Derlin-2], were upregulated, while classic markers for apoptotic UPR, including CHOP, Gadd34, Ero1α, and Trb3 were absent from the list (Fig. 4.4A). We confirmed these changes in gene expression by measuring selective proteins linked to adaptive (BiP, Calreticulin, and XBP1s) and apoptotic (CHOP and p-JNK) UPR markers in the ventricles (Fig. 4.4B) and whole hearts (Supplementary Fig. 4.3) of WT and Hep-tg mice. Additionally, we also evaluated the mechanisms that might contribute to changes in the UPR genes. Although both the IRE1α and PERK pathways were activated, the most robust change was observed with the cleavage of ATF6α (Fig. 4.4B), whose overexpression was recently reported to be cardioprotective [70]. To further ratify that it was the adaptive, but not apoptotic UPR that was activated, we also tested the mRNA

levels of Xbp1, Gadd34 and Atf4. While both forms of Xbp1 were higher, Gadd34, which is reflective of apoptotic UPR, remained unchanged in the Hep-tg mice ventricle. This latter effect occurred even in the presence of a modest increase in its upstream regulator, Atf4 (Fig. 4.4C). Altogether, these data suggest that heparanase overexpression in the heart can induce a pro-survival, adaptive UPR, without initiating apoptotic UPR activation (Fig. 4.4D).

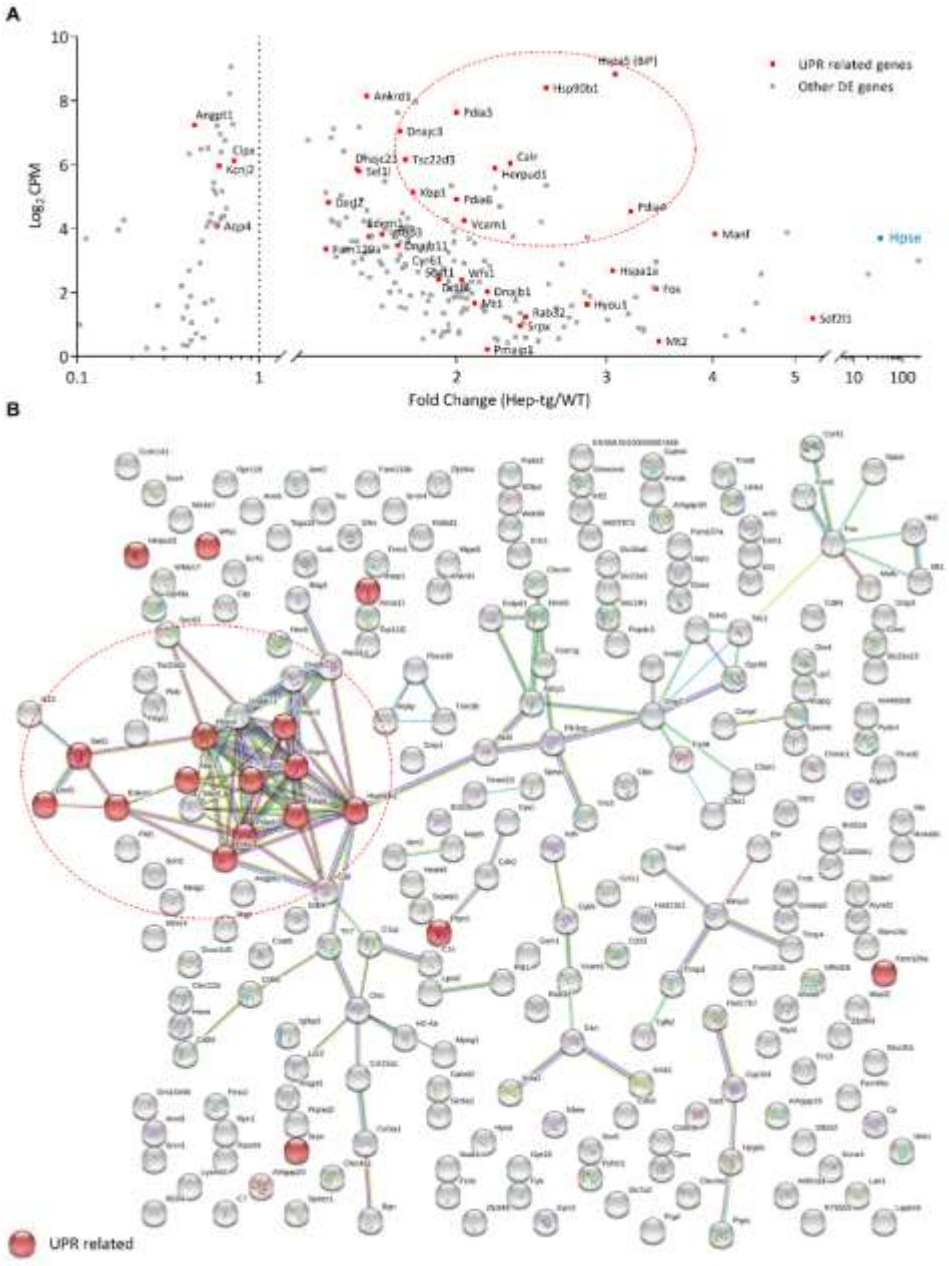

Fig 4.3. Expression profile and association network of differentially expressed genes highlighting those related to UPR.

A: Plot describing the profile of differentially expressed (DE) genes in Hep-tg mice. Red squares highlight the UPR related genes, and the red dotted line captures those UPR related genes that have the highest expression and fold change. CPM (count per million). B: Analysis of a protein-protein interaction network assembled from the RNA-seq data using String database (high confidence level). Highlighted by the red circles are genes related to UPR, whereas the dotted line establishes the tight functional connection between these genes.

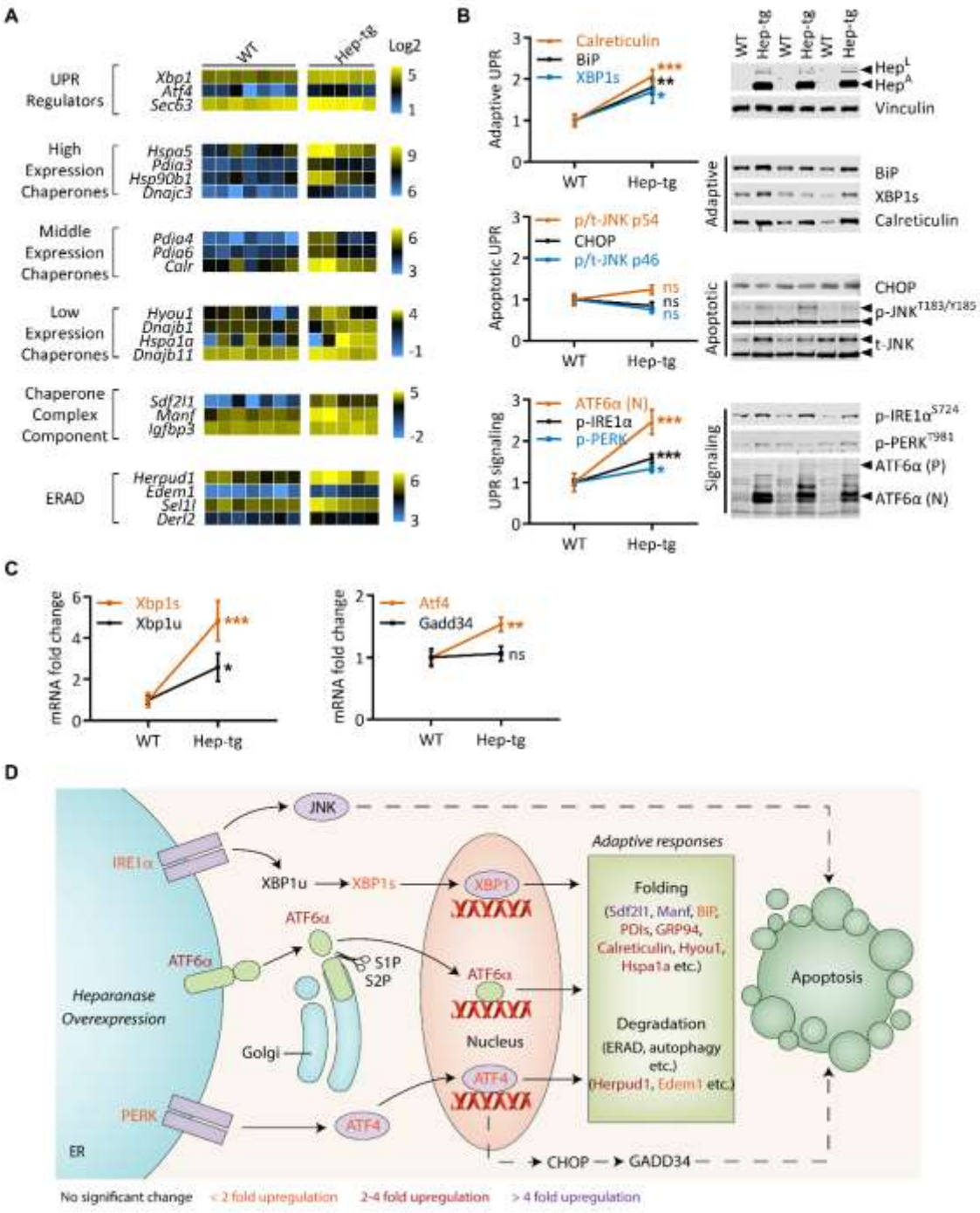

Fig 4.4. Unfolded protein response (UPR) in Hep-tg mice ventricle.

A: Heatmap of statistically significant UPR genes related to upstream regulation and protein folding/degradation. B: Representative protein expression of the adaptive and apoptotic arm of UPR confirmed using Western Blot (n=6-20). The figure also describes the signalling events involved in UPR activation. C: Confirmation of the RNA-seq data was achieved by RT-PCR (n=10-22). D: Summary of marker gene network in UPR showing both

the pro-survival and pro-apoptotic divisions. Data are presented as mean ± SEM (Student's t-test). *p<0.05, **p<0.01, ***p<0.001.

4.5 Heparanase promotes autophagy by UPR activation and mTOR inhibition

In the heart, activation of autophagy by mild ER stress has been implicated in cardiac protection [214]. To verify whether the adaptive UPR observed in Hep-tg mice ventricle can induce autophagy, we quantified the levels of LC3-II, a frequently used marker of autophagy, in both basal and chloroquine-treated conditions. In both circumstances, LC3-II was upregulated (Fig. 4.5A). Because these changes are likely a result of AMPK activation and/or mTOR inhibition, these two master regulator molecules were examined in Hep-tg mice ventricle. Although p-AMPK remained unchanged, p-mTOR was substantially downregulated (Fig. 4.5B). This loss of mTOR signaling was substantiated by evaluating its downstream target p-S6K, which was also reduced (Fig. 4.5B). As anticipated, using insulin to activate mTOR (Fig. 4.5C), or increasing insulin by feeding (Supplementary Fig 4.4C), reversed the increase in LC3-II observed in Hep-tg mice. Additional experiments indicated that other key components in autophagy activation, Beclin-1, p62 and LC3 were also upregulated in Hep-tg mice ventricles (Fig. 4.5D and E). All of these results in the Hep-tg ventricle were duplicated in whole hearts from these animals (Supplementary Fig. 4.4A) and in isolated cardiomyocytes exposed to recombinant latent heparanase (Myc-Hep^{L}, Supplementary Fig. 4.4B-D). It should be noted that following fasting, the process of autophagy is geared to provide the cell with energy. Intriguingly, although autophagy is increased in WT mice subjected to fasting, this catabolic process was further augmented in Hep-tg mice undergoing fasting (Supplementary Fig. 4.5), indicating an augmented capacity to respond to stimuli that induce autophagy. Taken together, our data suggest that heparanase promotes cardiac

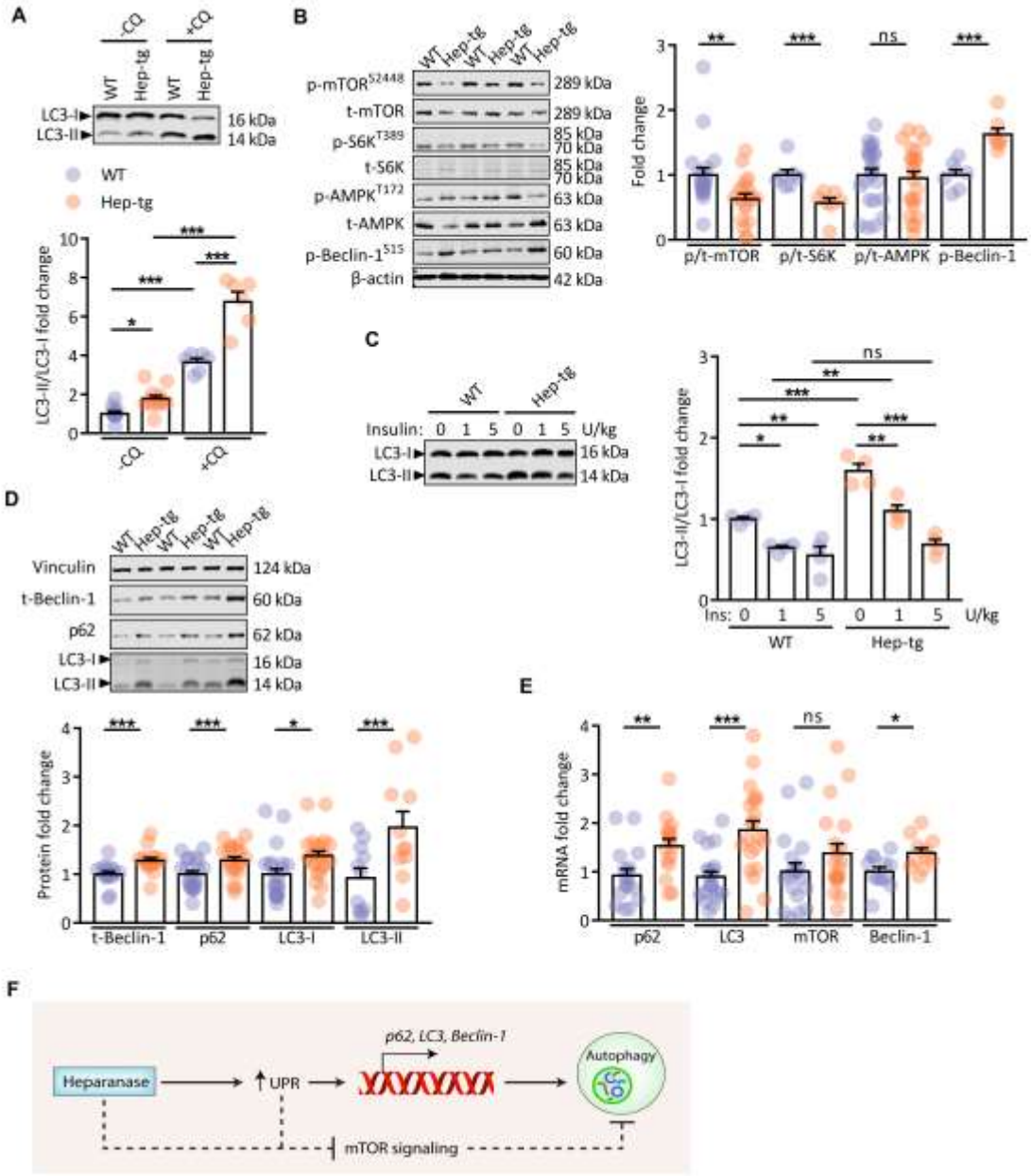

Fig 4.5. Heparanase promotes autophagy.

Western blot determination of A: autophagy marker LC3 in WT and Hep-tg mouse ventricle treated with or without chloroquine (CQ, 50 mg/kg for 4 h) (n=6-12); B: upstream regulators of autophagy (n=7-24): C: LC3 following an i.p. injection of insulin (1 U/kg or 5U/kg body weight) to 6-h–fasted mice; D: key proteins in the process of autophagy (n=11-23). E. RT-PCR was used to determine the transcription of autophagy related genes (n=11-21). F. Summary diagram describing the mechanism contributing towards augmentation of autophagy in Hep-tg mice ventricle. Data are presented as mean ± SEM

(Two-way ANOVA for A and C and Student's t-test for B, D, and E). *p<0.05, **p<0.01, ***p<0.001.

autophagy by both UPR activation and mTOR inhibition (Fig. 4.5F).

4.6 Overexpression of heparanase protects ventricles against high dose thapsigargin induced ER stress and apoptosis

Under severe or prolonged ER stress, the adaptive UPR is replaced by an apoptotic UPR [270]. We used two different doses (0.3 or 2 mg/kg) of thapsigargin to evaluate the transition from adaptive to apoptotic UPR. WT mice treated with the low dose of thapsigargin showed an increased expression of adaptive UPR markers, limited apoptotic UPR activation, augmented autophagy, and no significant increase in apoptosis (Fig. 4.6A), a situation resembling a form of cardiac preconditioning [210, 211]. The high dose thapsigargin in WT led to a loss of adaptive but an increase in apoptotic UPR, no additional increase in autophagy, and an increase in the apoptotic signal (Fig. 4.6A). Intriguingly, Hep-tg mice treated with high dose thapsigargin were resistant to transitioning from adaptive to apoptotic UPR. These animals continued to demonstrate a high level of adaptive UPR, a lower apoptotic UPR, a robust autophagy signal, and a substantially lower level of apoptosis (Fig. 4.6B). Overall, these results imply that the overexpression of heparanase preconditions the heart against severe ER stress.

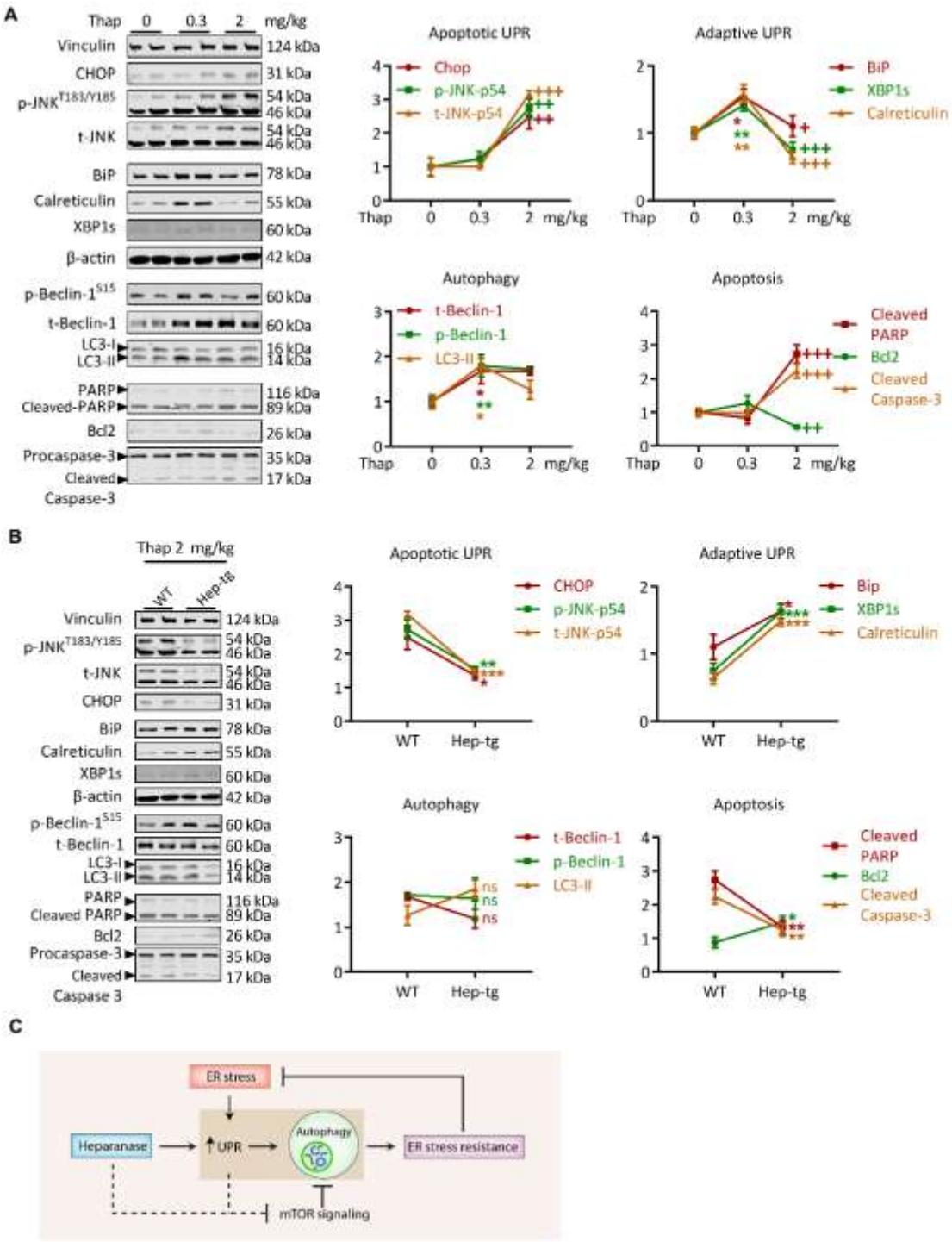

Fig 4.6. Heparanase stimulated UPR response and autophagy protect ventricular cells from ER stress induced apoptosis.

A. WT mice were injected with moderate (0.3 mg/kg) and high (2 mg/kg) doses of Thapsigargin (Thap) for 48 h and mice ventricle were collected and markers for UPR,

autophagy and apoptosis were measured by Western blot (n=6-13). $^{+}$Significantly different from 0.3 mg/kg Thap. *Significantly different from no drug. *p<0.05, **p<0.01, ***p<0.001; ^{+}p<0.05, ^{++}p<0.01, ^{+++}p<0.001. B: WT and Hep-tg mice were injected high (2 mg/kg) doses of Thapsigargin (Thap) for 48 h and mice ventricle were collected and markers for UPR, autophagy and apoptosis were measured by Western blot (n=6-13). Data are presented as mean ± SEM (Student's t-test). *p<0.05, **p<0.01, ***p<0.001.

4.7 Hearts from Hep-tg mice are resistant to I/R injury

Myocardial infarction following I/R is a leading cause of heart disease [271]. To test whether the preconditioning mimicking effects of heparanase overexpression protects the heart against I/R, we determined infarct size of WT and Hep-tg mouse hearts following I/R (40 min ischemia and 60 min reperfusion) using Evans blue/TTC double staining. Both the infarct size (% of area of risk, AAR) and AAR (% of total) were significantly lower in the Hep-tg hearts compared to WT (Fig. 4.7A). Analysis of cell death markers (Chop, PARP, and Caspase 3) following I/R confirmed a lower level of apoptosis in Hep-tg hearts (Fig. 4.7B). To investigate the participation of the UPR in apoptosis, we assessed early changes in apoptotic UPR markers following 20 min of I/R. Interestingly, the Hep-tg heart demonstrated a smaller increase in the apoptotic UPR markers like p-JNK and Chop compared to WT after I/R (Supplementary Fig. 4.6A). One downstream outcome of adaptive UPR is the activation of autophagy, which has been implicated in protecting the heart during ischemia [206]. No-flow ischemia for 20 min in WT mice increased LC3-II. Interestingly, this capability to augment LC3-II was still evident in the Hep-tg hearts, and thus these hearts demonstrated the highest amount of this autophagy marker (Supplementary Fig. 4.6A). Unlike adaptive UPR and autophagy, there was no evidence of the reperfusion injury salvage kinase (RISK) pathway being activated in Hep-tg heart as a mechanism to protect against I/R injury (Supplementary Fig. 4.6B). Collectively, our results indicate that the processes of adaptive UPR

and resultant autophagy are part of the mechanism by which heparanase offers protection against I/R injury.

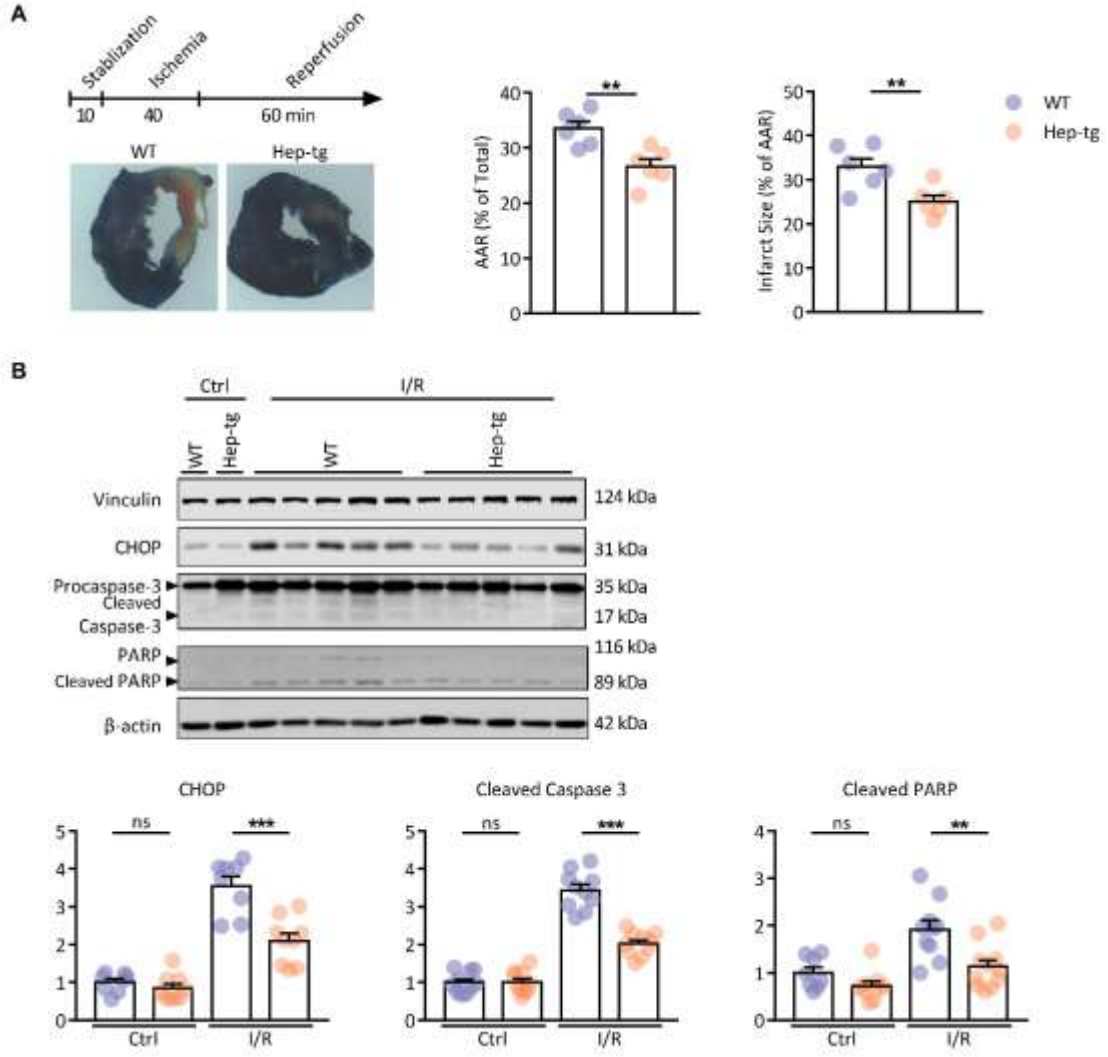

Fig 4.7. Heparanase overexpression protects the heart against I/R injury.

A: A representative image of WT and Hep-tg heart slices after I/R and Evans blue/TTC staining (left) and calculation of infarct sizes and AAR (right). B: Western blot was used to determine apoptosis markers in WT and Hep-tg mouse hearts with or without I/R (n=6-16). Data are presented as mean ± SEM (Student's t-test for A and Two-way ANOVA for B). *p<0.05, **p<0.01, ***p<0.001.

4.8 Impeding UPR or autophagy pharmacologically counteracts the favourable effect of heparanase in I/R

To corroborate that the protective effects of heparanase overexpression in I/R injury are realized through UPR and autophagy, we used inhibitors of these two processes prior to determining the infarct size of WT and Hep-tg hearts subjected to this insult. Both the UPR inhibitor AEBSF (which prevents ATF6α cleavage) and the autophagy inhibitor chloroquine (which causes accumulation of LC3-II), were effective at the concentrations and duration used in both groups of mice, as seen by a lower nuclear form of ATF6α and a higher LC3-II level (Fig. 4.8A). As anticipated, these agents reversed the protective effects of heparanase overexpression in I/R, as indicated by augmentation of the apoptosis markers (Fig. 4.8A), and a significant increase in infarct size (Fig. 4.8B). Our results imply that heparanase protects the heart against I/R injury, and does so through activation of UPR and autophagy.

4.9 Discussion

Heparanase is a protein whose enzymatic activity on cell surface HSPGs facilitates extracellular matrix reorganization, thus provoking the release of attached molecules such as growth factors, enzymes and cytokines [1]. This β-glucuronidase activity within the nucleus contributes to a significant change in the transcriptome [6, 264]. The non-enzymatic functions of heparanase include its participation in a number of signalling pathways [21, 264]. These characteristics of heparanase have been exploited to promote cell survival [264, 265]. Strikingly, this unique cell survival property of heparanase was exploited in hearts overexpressing heparanase, which demonstrated resistance to both chemical and I/R injury. Our data strengthen the novel idea that the heart can use heparanase as a candidate to combat stresses that would otherwise lead to heart disease.

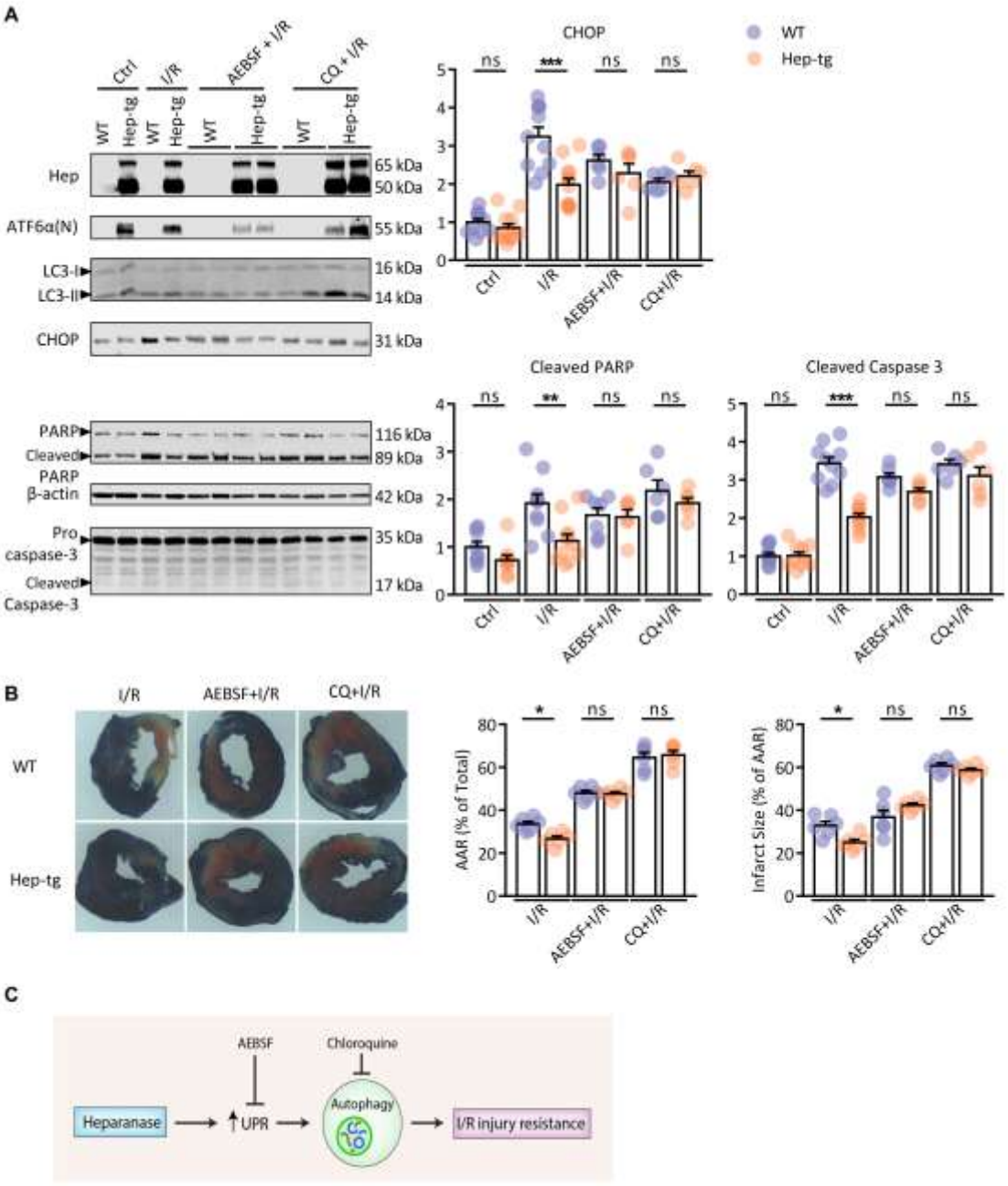

Fig 4.8. Inhibition of UPR or autophagy impairs the protective effect of heparanase.

Mice were injected with 50 mg/kg CQ for 4 h or isolated hearts perfused with 30 μM AEBSF for 20 min prior to 40 min global ischemia and 60 min reperfusion, and A: markers of apoptosis (n=8-16) measured and B: infarct size (n=6) calculated. C: Summary diagram describing that when UPR and autophagy are blocked by AEBSF and chloroquine, respectively, the protective effects of heparanase is abolished. Data are presented as mean ± SEM (Two-way ANOVA). *p<0.05, **p<0.01, ***p<0.001.

Following its entry into the nucleus, heparanase has been implicated in gene transcription by mitigating the suppressive effect of syndecan 1 on histone acetyltransferase activity or by modulating histone H3 methylation [264]. We have reported that in transgenic mice globally overexpressing heparanase, the pancreas and the heart were organs that demonstrated the highest expression of this protein. Interestingly, in these animals, the pancreatic islet transcriptome was greatly altered with >2000 genes differentially expressed compared to control [35]. In this study, hearts from Hep-tg mice also exhibited an altered transcriptome, albeit tempered (240 differentially regulated genes) compared to the pancreas. More specifically, and of considerable interest, was the impact that heparanase overexpression had on genes in the heart enriched for diverse functions including immunity, metabolism, cell death, and protection against cellular stresses. As the expression of genes related to UPR, oxidative stress, and autophagy were altered, our data suggest that in the heart, heparanase could be a novel pro-survival molecule.

In the heart, oxidative, osmotic, and mechanical stresses, together with inflammation and hypoxia can disturb ER homeostasis, disrupt protein folding and lead to cardiovascular diseases [74]. One strategy employed by cardiomyocytes to overcome the accumulation of misfolded proteins is the initiation of a process called UPR, an adaptation for cell survival, but which can also lead to cell death when UPR is protracted [75-77]. UPR is a complex signal transduction pathway initiated by the activation of three UPR stress sensors; PERK, IRE1α and ATF6α. Using transcriptional and non-transcriptional responses affecting pathways that impact protein folding, ER biogenesis, ER-associated degradation (ERAD), and autophagy, these sensors allow the heart to maintain its normal physiology [269]. In Hep-tg mice, a novel observation was the upregulation of a tightly clustered network of UPR genes that were directed towards the adaptive response. This included chaperones like BiP, Hsp90b1, Hyou1, protein disulfide isomerases (Pdia3, Pdia4, Pdia6), and

calreticulin that safeguard against protein misfolding, and genes linked to ERAD like Edem1, Herpud1, and Derlin2. Intriguingly, this activation of UPR occurred in the absence of any upregulation of genes associated with apoptosis; CHOP, Gadd34, Ero1α, and Trb3 all remained unchanged in hearts from Hep-tg mice. Further analysis suggested that these changes may be associated with alteration of the sensors that govern UPR activation. Indeed, PERK, IRE1α and ATF6α together with their downstream components ATF4, XBP1, and cleaved ATF6α were all activated, with ATF6α exhibiting the most robust change. It should be noted that ATF6α is generally recognized as a prominent protective branch of UPR [70, 272-282], and strategies to develop ATF6α specific activators have been proposed [283]. Indeed, studies have described the cardioprotective effect of ATF6α in I/R emphasizing the contribution of UPR signaling in safeguarding the heart [70]. Overall, our results uncover a potentially unique role of heparanase in adaptive UPR activation by ATF6α, that may offer the heart a defence against physiological or pathophysiological stresses.

In addition to the effects of UPR on inhibition of protein translation and activation of protein folding, augmentation of protein degradation by ERAD and autophagy is key to clear misfolded proteins and dysfunctional organelles in the stressed heart [208]. Hence, in the heart, both pharmacological and genetic manipulations that increase UPR also enhance autophagy [207]. In this study, two of the most common markers for activation of autophagy, p62 (an important adaptor for protein recruitment) and LC3-II (whose maturation is key for autophagosome formation) were induced in Hep-tg mouse hearts. Verification of autophagy in these mice was achieved using additional methods. The addition of chloroquine, an agent that increases the pH of lysosomes (and therefore inhibits fusion with autophagosomes), also led to a further increase of LC3-II in Hep-tg mice. Finally, the expression and phosphorylation of Beclin-1, a key mediator of autophagosome initiation, also increased, suggesting that upstream signalling in the regulation

of autophagy was activated. Two upstream regulators of Beclin-1 include AMPK (a positive regulator of autophagy) and mTOR (a negative regulator of autophagy) [91, 109]. In Hep-tg hearts, although there was no alteration in AMPK, a reduction in mTOR activation together with a decrease in S6K, its downstream target, was observed, suggesting that heparanase overexpression promotes autophagy by inactivating mTOR [209, 284]. Taken together, these results indicate that heparanase promotes autophagy in the heart by activating the UPR and inhibiting mTOR.

The role of heparanase in preventing apoptotic UPR is of some interest and was studied using two doses of thapsigargin. When changing from low to high dose, the function of this agent transits from inducing adaptive to apoptotic UPR [214]. Indeed, in our study, low dose thapsigargin induced adaptive UPR and subsequent autophagy markers, with no change in apoptotic UPR or apoptosis. Conversely, high dose thapsigargin had the opposite effect: we observed a robust drop in adaptive UPR markers and a considerable increase in apoptotic UPR and apoptosis. Intriguingly, in the Hep-tg animals exposed to high dose thapsigargin, the effects on apoptotic UPR and apoptosis were reversed. Here we show that in the equilibrium between adaptive and apoptotic UPR, heparanase overexpression favours the former over the latter, and could be a property that can be exploited in overcoming pathological stresses like I/R.

The favourable effects of UPR and autophagy has recently emerged as a new target to protect against I/R injury, with the extent and direction of UPR and autophagy determining cell survival or demise [76, 213]. Given the evidence that both processes are augmented in Hep-tg hearts, we subjected them to I/R. Intriguingly, in Hep-tg hearts exposed to no-flow ischemia followed by reperfusion, both the infarct size and AAR were significantly lower compared to WT. This protection against the stress of I/R was reflected by a limited change in markers of apoptosis, which exhibited a significant increase in WT hearts. Moreover, hearts from Hep-tg animals still

demonstrated stimulation of adaptive UPR and autophagy during ischemia, as well as an increased adaptive UPR during reperfusion. As impeding autophagy or UPR chemically abolished the resistance of Hep-tg hearts to I/R, our data imply that heparanase uses these two mechanisms to offer cardioprotection.

Notwithstanding these observations that suggest that the cardioprotective effects of heparanase materializes through UPR activation and autophagy, additional protective mechanisms could be proposed. In a previous report, heparinase (that can also cleave HS) increased protein synthesis and upregulated genes associated with cardiomyocyte hypertrophy (Nppa and Acta1) [285], an observation that was consistent with the physiological hypertrophy observed in the present study. Moreover, Hep-tg mice have been reported to have increased food consumption and higher body length, but reduced body weight and fat mass [31, 286], suggesting a beneficial energy balance, as evidenced by an upregulation of a cluster of genes related to catabolism.

In summary, our data reveal a novel and complex role for heparanase in providing the heart support against chemical or I/R injury via modulation of UPR and autophagy. Data obtained from this study should spur interest in devising novel therapeutic strategies that target heparanase biology to prevent or delay heart disease.

Chapter 5: Concluding Chapter

Heparanase is widely known as an endoglycosidase that contributes to the aggressiveness of cancer using both its enzymatic and non-enzymatic functions. Therefore, its consideration as a therapeutic target for cancer treatment has attracted a lot of attention [16, 23, 264]. In recent years, its emerging roles in chronic inflammation, diabetic nephropathy, bone osteolysis, thrombosis, atherosclerosis and other diseases have also been uncovered [25, 264, 287-289]. The introduction of Hep-tg and Hep-ko mice dramatically accelerated research on heparanase and revealed a number of beneficial phenotypes. For example, Hep-tg mice have a reduced amyloid burden and are also more resistant to inflammation-induced amyloid build up in multiple organs, especially the brain, suggestive of its application in neurodegenerative diseases [32, 33]. In the skin, Hep-tg mice exhibit accelerated wound healing, which was related to effects on cell migration, proliferation, and angiogenesis [34]. An additional "healthy" phenotype in the Hep-tg mice include a lean body mass (with a longer body length but less fat content) while consuming more food, suggestive of a modulated energy balance, with Hep-ko mice having the opposite effects [31, 34]. Our recent study also reported that Hep-tg mice are resistant to chemical induced Type 1 diabetes and have an improved glucose homeostasis by making cells more functionally efficient along with augmenting FGF21 and GLP1, useful changes for the management of diabetes [35]. In my paper, in which hearts from Hep-tg mice demonstrated a robust overexpression of both the latent and active heparanase, we observed a mild cardiac hypertrophy, without any heart function impairment. Other researchers have previously reported that HS, the target of

heparanase, can prevent hypertrophy. Moreover, heparinase (that can also cleave HS), by increasing protein synthesis and upregulating genes associated with hypertrophy (nppa and acta1), also promoted cardiac hypertrophy [285]. Therefore, it is not surprising that we observed an increased UPR in Hep-tg mouse heart as an adaptation to the increased protein synthesis and hypertrophy. Related to the activation of UPR, the prosurvival ATF6α branch was highly stimulated whereas the "apoptotic" PERK pathway was the least activated. It should be noted that ATF6α is generally recognized as a prominent protective branch of UPR [70, 272-282], and strategies to develop ATF6α specific activators have been proposed recently [283]. Indeed, studies have described the cardioprotective effect of ATF6α in I/R emphasizing the contribution of UPR signaling in safeguarding the heart [70]. My study for the first time establishes a link between heparanase and ATF6α. The implication behind this regulation in physiological and pathological conditions requires further investigation. Furthermore, it would be attractive to examine whether this activation is also present in certain types of cancer. The activation of UPR led to a comprehensive change in the downstream transcription factors and as a result, the upregulation of chaperones, ERAD, and autophagy. Promotion of UPR and autophagy strengthens the machinery to handle misfolded proteins that are generated under stress conditions in the heart like ischemia, that produce oxidative and ER stress. The finding that autophagy in Hep-tg heart is dramatically augmented following fasting adds to the list of research that heparanase may contribute to the energy balance. As autophagy augmentation by heparanase has been shown in other organs such as pancreas and also in cancer, the systematic changes that heparanase can cause (including ECM structure, signaling, and gene regulation) in different organs under physiological and

pathological conditions should be examined, especially in cancer, diabetes, and inflammatory diseases, where heparanase activation and function are most relevant.

In conditions like diabetes, the properties of heparanase may also be applicable to promoting benefit. In the WT heart, heparanase is highly expressed in EC but not cardiomyocytes. Following diabetes, the conversion from Hep^{L} to Hep^{A} in whole heart, together with an increased amount of heparanase in cardiomyocytes (in the absence of any changes in mRNA level) suggests an EC-cardiomyocyte transfer of heparanase. We found that this transfer relies heavily on the proximity of microvascular EC to cardiomyocytes, as well as the differential distribution and expression of LRP1 at the cell surface of cardiomyocytes and microvascular EC. Hyperglycemia in this sense not only facilitates the secretion of heparanase but also the uptake into cardiomyocytes. The transcription modulation role of heparanase mitigates the suppressive effect of HS on histone acetyltransferase, resulting in an upregulation of anti-apoptotic genes and downregulation of pro-apoptotic genes in cardiomyocytes. This gene alteration confers the cardiomyocyte resistance to oxidative stress caused by HG in both our *in vivo* and *in vitro* models. This upregulation of heparanase and its protective effect in the heart is only present in acute diabetes models but disappeared with chronic disease, suggesting that heparanase regulation is an acute adaptation to diabetes that is lost with disease progression. The major mechanism for this loss of adaptation may be related to the LRP1 expression modification at cardiomyocyte surface. The acute upregulation of LRP1 promotes the uptake of heparanase, but might at the same time take part in the lipid uptake by cardiomyocytes. As this lipid uptake also causes lipotoxicity, the LRP1

expression downregulation in chronic diabetic heart was supposed to protect the cardiomyocytes, but at the same time mitigates its effect on heparanase uptake. Overall, hyperglycemia is a cue of diabetes to secrete latent heparanase, which acts as a messenger that delivers the information from EC, the first responder of diabetes, to cardiomyocytes.

Another pathological condition that has an impact on heparanase is ischemia. It has been widely known that hypoxia is one factor that upregulates and activates heparanase and ischemic heart also sees a dramatic increase in both latent and active forms of heparanase [290-295]. As the proangiogenic, pro-survival, and pro-migration effects of heparanase are well established, it is not surprising that heparanase upregulation acts as an adaptation process that may be beneficial in the beginning but in some cases leads to catastrophic consequences in later stage of these conditions. Specifically, in the heart, the organ that frequently suffers from hypoxia due to the vascular pathogenesis but has limited capability to renew the impaired cardiomyocytes, the proangiogenic, pro-survival properties of heparanase is extremely welcome. Two remaining questions after this study are, 1). Whether heparanase can promote angiogenesis in the heart. Heparanase can promote angiogenesis in the development of cancer and in the wound healing in the skin. Angiogenesis in the heart may have the potential to protect the heart in certain situations such as I/R injury. 2). Would heparanase upregulation lead to detrimental effects in the heart in the later stage of heart diseases and if that is the case, what are the key components that contribute to this conversion. So far, most of the detrimental effects of heparanase has been reported in kidney disease, as heparanase enzyme activity destroys

the integrity of glomerular basement membrane and leads to the dysfunction of urinary system [21]. The current research focused on the cardiomyocyte, which has very low expression of heparanase but can take up heparanase from EC during pathological conditions. The biggest cluster of genes regulated by heparanase are related to stress response, which will help the cardiomyocyte handle stress better. However, the effects of heparanase in other cell types such as EC, fibroblast, and immune cells especially macrophage have not been well elucidated. A comprehensive study of the effect of heparanase in the whole heart would be helpful to answer these two questions.

In summary, as heparanase is consistently found to be relevant in all types of pathological conditions, the regulation, function, and dysfunction of heparanase may have some shared mechanisms spanning different diseases. Taking advantage of the known aspects of heparanase and elucidate their appliance in the heart would benefit not only the researches of cancer or heart disease, but provide therapeutic targets that are applicable to other diseases. Our study illustrated that the upregulation of heparanase and the transfer of heparanase (as a method of communication between cell types) are two adaptive regulation pathways that mobilize heparanase in the heart. However, the comprehensive understanding of regulation and function of heparanase in the heart would be desirable before appropriate therapeutic targets can be designed.

Reference

1. Sarrazin, S., W.C. Lamanna, and J.D. Esko, *Heparan sulfate proteoglycans.* Cold Spring Harb Perspect Biol, 2011. **3**(7).
2. Stewart, M.D. and R.D. Sanderson, *Heparan sulfate in the nucleus and its control of cellular functions.* Matrix Biol, 2014. **35**: p. 56-9.
3. Iozzo, R.V., *Heparan sulfate proteoglycans: intricate molecules with intriguing functions.* Journal of Clinical Investigation, 2001. **108**(2): p. 165-7.
4. Hacker, U., K. Nybakken, and N. Perrimon, *Heparan sulphate proteoglycans: the sweet side of development.* Nat Rev Mol Cell Biol, 2005. **6**(7): p. 530-41.
5. Vlodavsky, I., et al., *Mammalian heparanase: Gene cloning, expression and function in tumor progression and metastasis.* Nature Medicine, 1999. **5**(7): p. 793-802.
6. Vlodavsky, I., et al., *Heparanase: From basic research to therapeutic applications in cancer and inflammation.* Drug Resist Updat, 2016. **29**: p. 54-75.
7. Wu, L., et al., *Structural characterization of human heparanase reveals insights into substrate recognition.* Nat Struct Mol Biol, 2015. **22**(12): p. 1016-22.
8. Hulett, M.D., et al., *Identification of active-site residues of the pro-metastatic endoglycosidase heparanase.* Biochemistry, 2000. **39**(51): p. 15659-67.
9. Ben-Zaken, O., et al., *Low and high affinity receptors mediate cellular uptake of heparanase.* Int J Biochem Cell Biol, 2008. **40**(3): p. 530-42.
10. Shteingauz, A., et al., *Heparanase Enhances Tumor Growth and Chemoresistance by Promoting Autophagy.* Cancer Res, 2015. **75**(18): p. 3946-57.
11. Baietti, M.F., et al., *Syndecan-syntenin-ALIX regulates the biogenesis of exosomes.* Nat Cell Biol, 2012. **14**(7): p. 677-85.
12. David, G. and P. Zimmermann, *Heparanase tailors syndecan for exosome production.* Mol Cell Oncol, 2016. **3**(3): p. e1047556.
13. Roucourt, B., et al., *Heparanase activates the syndecan-syntenin-ALIX exosome pathway.* Cell Res, 2015. **25**(4): p. 412-28.
14. Abboud-Jarrous, G., et al., *Cathepsin L is responsible for processing and activation of proheparanase through multiple cleavages of a linker segment.* Journal of Biological Chemistry, 2008. **283**(26): p. 18167-18176.
15. Bandari, S.K., et al., *Chemotherapy induces secretion of exosomes loaded with heparanase that degrades extracellular matrix and impacts tumor and host cell behavior.* Matrix Biol, 2018. **65**: p. 104-118.
16. Ilan, N., M. Elkin, and I. Vlodavsky, *Regulation, function and clinical significance of heparanase in cancer metastasis and angiogenesis.* Int J Biochem Cell Biol, 2006. **38**(12): p. 2018-39.
17. Goldberg, R., et al., *Versatile role of heparanase in inflammation.* Matrix Biol, 2013. **32**(5): p. 234-40.
18. Li, R.W., et al., *Dramatic regulation of heparanase activity and angiogenesis gene expression in synovium from patients with rheumatoid arthritis.* Arthritis & Rheumatism, 2008. **58**(6): p. 1590-1600.
19. Garsen, M., et al., *Endothelin-1 Induces Proteinuria by Heparanase-Mediated Disruption of the Glomerular Glycocalyx.* Journal of the American Society of Nephrology, 2016. **27**(12): p. 3545-3551.

20. Gil, N., et al., *Heparanase Is Essential for the Development of Diabetic Nephropathy in Mice.* Diabetes, 2012. **61**(1): p. 208-216.
21. Rabelink, T.J., et al., *Heparanase: roles in cell survival, extracellular matrix remodelling and the development of kidney disease.* Nat Rev Nephrol, 2017. **13**(4): p. 201-212.
22. Mestre, A.M., et al., *Expression of the heparan sulfate-degrading enzyme heparanase is induced in infiltrating CD4+ T cells in experimental autoimmune encephalomyelitis and regulated at the level of transcription by early growth response gene.* Journal of Leukocyte Biology, 2007. **82**(5): p. 1289-1300.
23. Vlodavsky, I., et al., *Significance of heparanase in cancer and inflammation.* Cancer Microenviron, 2012. **5**(2): p. 115-32.
24. Parish, C.R., et al., *Unexpected new roles for heparanase in Type 1 diabetes and immune gene regulation.* Matrix Biol, 2013. **32**(5): p. 228-33.
25. Vlodavsky, I., et al., *Involvement of heparanase in atherosclerosis and other vessel wall pathologies.* Matrix Biol, 2013. **32**(5): p. 241-51.
26. Garsen, M., et al., *Heparanase Is Essential for the Development of Acute Experimental Glomerulonephritis.* The American Journal of Pathology, 2016. **186**(4): p. 805-815.
27. van den Hoven, M.J., et al., *Heparanase in glomerular diseases.* Kidney Int, 2007. **72**(5): p. 543-8.
28. Agelidis, A.M., et al., *Viral Activation of Heparanase Drives Pathogenesis of Herpes Simplex Virus-1.* Cell Reports, 2017. **20**(2): p. 439-450.
29. Sanderson, R.D., et al., *Heparanase regulation of cancer, autophagy and inflammation: new mechanisms and targets for therapy.* FEBS J, 2016.
30. Kundu, S., et al., *Heparanase Promotes Glioma Progression and Is Inversely Correlated with Patient Survival.* Molecular Cancer Research, 2016. **14**(12): p. 1243-1253.
31. Karlsson-Lindahl, L., et al., *Heparanase affects food intake and regulates energy balance in mice.* PLoS One, 2012. **7**(3): p. e34313.
32. Jendresen, C.B., et al., *Overexpression of heparanase lowers the amyloid burden in amyloid-beta precursor protein transgenic mice.* J Biol Chem, 2015. **290**(8): p. 5053-64.
33. Li, J.P., et al., *In vivo fragmentation of heparan sulfate by heparanase overexpression renders mice resistant to amyloid protein A amyloidosis.* Proc Natl Acad Sci U S A, 2005. **102**(18): p. 6473-7.
34. Zcharia, E., et al., *Heparanase accelerates wound angiogenesis and wound healing in mouse and rat models.* FASEB J, 2005. **19**(2): p. 211-21.
35. Zhang, D., et al., *Heparanase Overexpression Induces Glucagon Resistance and Protects Animals From Chemically Induced Diabetes.* Diabetes, 2017. **66**(1): p. 45-57.
36. Stewart, J., G. Manmathan, and P. Wilkinson, *Primary prevention of cardiovascular disease: A review of contemporary guidance and literature.* JRSM Cardiovascular Disease, 2017. **6**: p. 2048004016687211.
37. Chou, R., et al., *Statins for Prevention of Cardiovascular Disease in Adults: Evidence Report and Systematic Review for the US Preventive Services Task Force.* JAMA, 2016. **316**(19): p. 2008-2024.
38. Meads, C., et al., *Coronary artery stents in the treatment of ischaemic heart disease: a rapid and systematic review.* Health Technol Assess, 2000. **4**(23): p. 1-153.
39. Segers, V.F. and R.T. Lee, *Stem-cell therapy for cardiac disease.* Nature, 2008. **451**(7181): p. 937-42.
40. Dorobantu, M., et al., *Pursuing meaningful end-points for stem cell therapy assessment in ischemic cardiac disease.* World J Stem Cells, 2017. **9**(12): p. 203-218.

41. Tompkins, B.A., et al., *Preclinical Studies of Stem Cell Therapy for Heart Disease.* Circ Res, 2018. **122**(7): p. 1006-1020.
42. Rincon, M.Y., T. VandenDriessche, and M.K. Chuah, *Gene therapy for cardiovascular disease: advances in vector development, targeting, and delivery for clinical translation.* Cardiovasc Res, 2015. **108**(1): p. 4-20.
43. Rosik, J., et al., *Potential targets of gene therapy in the treatment of heart failure.* Expert Opin Ther Targets, 2018. **22**(9): p. 811-816.
44. Gilca, G.-E., et al., *Diabetic Cardiomyopathy: Current Approach and Potential Diagnostic and Therapeutic Targets.* Journal of Diabetes Research, 2017. **2017**: p. 1310265.
45. Francis, G.S., *Diabetic cardiomyopathy: fact or fiction?* Heart, 2001. **85**(3): p. 247-8.
46. Goraya, T.Y., et al., *Coronary atherosclerosis in diabetes mellitus: a population-based autopsy study.* J Am Coll Cardiol, 2002. **40**(5): p. 946-53.
47. Regan, T.J., et al., *Diabetic cardiomyopathy: experimental and clinical observations.* N J Med, 1994. **91**(11): p. 776-8.
48. Boudina, S. and E.D. Abel, *Diabetic cardiomyopathy, causes and effects.* Rev Endocr Metab Disord, 2010. **11**(1): p. 31-9.
49. Fang, Z.Y., J.B. Prins, and T.H. Marwick, *Diabetic cardiomyopathy: evidence, mechanisms, and therapeutic implications.* Endocr Rev, 2004. **25**(4): p. 543-67.
50. Jia, G., M.A. Hill, and J.R. Sowers, *Diabetic Cardiomyopathy: An Update of Mechanisms Contributing to This Clinical Entity.* Circ Res, 2018. **122**(4): p. 624-638.
51. Bugger, H. and E.D. Abel, *Rodent models of diabetic cardiomyopathy.* Dis Model Mech, 2009. **2**(9-10): p. 454-66.
52. Severson, D.L., *Diabetic cardiomyopathy: recent evidence from mouse models of type 1 and type 2 diabetes.* Can J Physiol Pharmacol, 2004. **82**(10): p. 813-23.
53. Shehadeh, A. and T.J. Regan, *Cardiac consequences of diabetes mellitus.* Clin Cardiol, 1995. **18**(6): p. 301-5.
54. Fein, F.S. and E.H. Sonnenblick, *Diabetic cardiomyopathy.* Prog Cardiovasc Dis, 1985. **27**(4): p. 255-70.
55. Dhalla, N.S., et al., *Subcellular remodeling and heart dysfunction in chronic diabetes.* Cardiovasc Res, 1998. **40**(2): p. 239-47.
56. An, D. and B. Rodrigues, *Role of changes in cardiac metabolism in development of diabetic cardiomyopathy.* Am J Physiol Heart Circ Physiol, 2006. **291**(4): p. H1489-506.
57. Taha, M. and G.D. Lopaschuk, *Alterations in energy metabolism in cardiomyopathies.* Ann Med, 2007. **39**(8): p. 594-607.
58. Sung, M.M., S.M. Hamza, and J.R. Dyck, *Myocardial metabolism in diabetic cardiomyopathy: potential therapeutic targets.* Antioxid Redox Signal, 2015. **22**(17): p. 1606-30.
59. Wan, A. and B. Rodrigues, *Endothelial cell-cardiomyocyte crosstalk in diabetic cardiomyopathy.* Cardiovasc Res, 2016. **111**(3): p. 172-83.
60. Chong, C.R., K. Clarke, and E. Levelt, *Metabolic Remodeling in Diabetic Cardiomyopathy.* Cardiovasc Res, 2017.
61. Stocker, R. and J.F. Keaney, Jr., *Role of oxidative modifications in atherosclerosis.* Physiol Rev, 2004. **84**(4): p. 1381-478.
62. Ayer, A., P. Macdonald, and R. Stocker, *CoQ(1)(0) Function and Role in Heart Failure and Ischemic Heart Disease.* Annu Rev Nutr, 2015. **35**: p. 175-213.
63. Reimer, K.A., et al., *The wavefront phenomenon of ischemic cell death. 1. Myocardial infarct size vs duration of coronary occlusion in dogs.* Circulation, 1977. **56**(5): p. 786-94.

64. Hausenloy, D.J. and D.M. Yellon, *Myocardial ischemia-reperfusion injury: a neglected therapeutic target.* J Clin Invest, 2013. **123**(1): p. 92-100.
65. Avkiran, M. and M.S. Marber, *Na(+)/H(+) exchange inhibitors for cardioprotective therapy: progress, problems and prospects.* J Am Coll Cardiol, 2002. **39**(5): p. 747-53.
66. Chow, C.Y., et al., *The genetic architecture of the genome-wide transcriptional response to ER stress in the mouse.* PLoS Genet, 2015. **11**(2): p. e1004924.
67. Hetz, C., E. Chevet, and S.A. Oakes, *Proteostasis control by the unfolded protein response.* Nat Cell Biol, 2015. **17**(7): p. 829-38.
68. Walter, P. and D. Ron, *The unfolded protein response: from stress pathway to homeostatic regulation.* Science, 2011. **334**(6059): p. 1081-6.
69. Maurel, M., et al., *Getting RIDD of RNA: IRE1 in cell fate regulation.* Trends Biochem Sci, 2014. **39**(5): p. 245-54.
70. Jin, J.K., et al., *ATF6 Decreases Myocardial Ischemia/Reperfusion Damage and Links ER Stress and Oxidative Stress Signaling Pathways in the Heart.* Circ Res, 2017. **120**(5): p. 862-875.
71. Doroudgar, S., et al., *Ischemia activates the ATF6 branch of the endoplasmic reticulum stress response.* J Biol Chem, 2009. **284**(43): p. 29735-45.
72. Harding, H.P., et al., *Perk is essential for translational regulation and cell survival during the unfolded protein response.* Mol Cell, 2000. **5**(5): p. 897-904.
73. Pakos-Zebrucka, K., et al., *The integrated stress response.* EMBO Rep, 2016. **17**(10): p. 1374-1395.
74. Groenendyk, J., et al., *Biology of endoplasmic reticulum stress in the heart.* Circ Res, 2010. **107**(10): p. 1185-97.
75. Zhang, C., et al., *Role of Endoplasmic Reticulum Stress, Autophagy, and Inflammation in Cardiovascular Disease.* Front Cardiovasc Med, 2017. **4**: p. 29.
76. Delbridge, L.M.D., et al., *Myocardial stress and autophagy: mechanisms and potential therapies.* Nat Rev Cardiol, 2017. **14**(7): p. 412-425.
77. Wang, F., J. Jia, and B. Rodrigues, *Autophagy, Metabolic Disease, and Pathogenesis of Heart Dysfunction.* Can J Cardiol, 2017.
78. Yang, L., et al., *Endoplasmic reticulum stress and protein quality control in diabetic cardiomyopathy.* Biochim Biophys Acta, 2015. **1852**(2): p. 209-18.
79. Varga, Z.V., et al., *Interplay of oxidative, nitrosative/nitrative stress, inflammation, cell death and autophagy in diabetic cardiomyopathy.* Biochim Biophys Acta, 2015. **1852**(2): p. 232-42.
80. Lakshmanan, A.P., et al., *The hyperglycemia stimulated myocardial endoplasmic reticulum (ER) stress contributes to diabetic cardiomyopathy in the transgenic non-obese type 2 diabetic rats: a differential role of unfolded protein response (UPR) signaling proteins.* Int J Biochem Cell Biol, 2013. **45**(2): p. 438-47.
81. Pulinilkunnil, T., et al., *Myocardial adipose triglyceride lipase overexpression protects diabetic mice from the development of lipotoxic cardiomyopathy.* Diabetes, 2013. **62**(5): p. 1464-77.
82. Zhang, K. and R.J. Kaufman, *From endoplasmic-reticulum stress to the inflammatory response.* Nature, 2008. **454**(7203): p. 455-62.
83. Glembotski, C.C., *Endoplasmic reticulum stress in the heart.* Circ Res, 2007. **101**(10): p. 975-84.
84. Ni, M. and A.S. Lee, *ER chaperones in mammalian development and human diseases.* FEBS Lett, 2007. **581**(19): p. 3641-51.

85. Wang, Z.V., et al., *Spliced X-box binding protein 1 couples the unfolded protein response to hexosamine biosynthetic pathway.* Cell, 2014. **156**(6): p. 1179-1192.
86. Urano, F., et al., *Coupling of stress in the ER to activation of JNK protein kinases by transmembrane protein kinase IRE1.* Science, 2000. **287**(5453): p. 664-6.
87. Han, D., et al., *IRE1alpha kinase activation modes control alternate endoribonuclease outputs to determine divergent cell fates.* Cell, 2009. **138**(3): p. 562-75.
88. Myoishi, M., et al., *Increased endoplasmic reticulum stress in atherosclerotic plaques associated with acute coronary syndrome.* Circulation, 2007. **116**(11): p. 1226-33.
89. Martindale, J.J., et al., *Endoplasmic reticulum stress gene induction and protection from ischemia/reperfusion injury in the hearts of transgenic mice with a tamoxifen-regulated form of ATF6.* Circ Res, 2006. **98**(9): p. 1186-93.
90. Toko, H., et al., *ATF6 is important under both pathological and physiological states in the heart.* Journal of Molecular and Cellular Cardiology, 2010. **49**(1): p. 113-120.
91. Levine, B. and G. Kroemer, *Autophagy in the pathogenesis of disease.* Cell, 2008. **132**(1): p. 27-42.
92. Mizushima, N. and M. Komatsu, *Autophagy: Renovation of Cells and Tissues.* Cell, 2011. **147**(4): p. 728-741.
93. Marino, G., et al., *Self-consumption: the interplay of autophagy and apoptosis.* Nature Reviews Molecular Cell Biology, 2014. **15**(2): p. 81-94.
94. Nikoletopoulou, V., et al., *Crosstalk between apoptosis, necrosis and autophagy.* Biochimica Et Biophysica Acta-Molecular Cell Research, 2013. **1833**(12): p. 3448-3459.
95. Maiuri, M.C., et al., *Self-eating and self-killing: crosstalk between autophagy and apoptosis.* Nature Reviews Molecular Cell Biology, 2007. **8**(9): p. 741-752.
96. Eskelinen, E.L. and P. Saftig, *Autophagy: A lysosomal degradation pathway with a central role in health and disease.* Biochimica Et Biophysica Acta-Molecular Cell Research, 2009. **1793**(4): p. 664-673.
97. Glick, D., S. Barth, and K.F. Macleod, *Autophagy: cellular and molecular mechanisms.* Journal of Pathology, 2010. **221**(1): p. 3-12.
98. Stolz, A., A. Ernst, and I. Dikic, *Cargo recognition and trafficking in selective autophagy.* Nature Cell Biology, 2014. **16**(6): p. 495-501.
99. Youle, R.J. and D.P. Narendra, *Mechanisms of mitophagy.* Nat Rev Mol Cell Biol, 2011. **12**(1): p. 9-14.
100. Saito, T. and J. Sadoshima, *Molecular Mechanisms of Mitochondrial Autophagy/Mitophagy in the Heart.* Circulation Research, 2015. **116**(8): p. 1477-1490.
101. Kobayashi, S. and Q.R. Liang, *Autophagy and mitophagy in diabetic cardiomyopathy.* Biochimica Et Biophysica Acta-Molecular Basis of Disease, 2015. **1852**(2): p. 252-261.
102. Lazarou, M., et al., *The ubiquitin kinase PINK1 recruits autophagy receptors to induce mitophagy.* Nature, 2015. **524**(7565): p. 309-14.
103. Mizushima, N., *Autophagy: process and function.* Genes & Development, 2007. **21**(22): p. 2861-2873.
104. Kubli, D.A. and A.B. Gustafsson, *Cardiomyocyte health: adapting to metabolic changes through autophagy.* Trends in Endocrinology and Metabolism, 2014. **25**(3): p. 156-164.
105. Levine, B. and G. Kroemer, *SnapShot: Macroautophagy.* Cell, 2008. **132**(1): p. 162-U14.
106. Shibutani, S.T., et al., *Autophagy and autophagy-related proteins in the immune system.* Nature Immunology, 2015. **16**(10): p. 1014-1024.
107. Noda, N.N. and F. Inagaki, *Mechanisms of Autophagy.* Annual Review of Biophysics, Vol 44, 2015. **44**: p. 101-122.

108. He, C.C. and D.J. Klionsky, *Regulation Mechanisms and Signaling Pathways of Autophagy.* Annual Review of Genetics, 2009. **43**: p. 67-93.
109. Kaur, J. and J. Debnath, *Autophagy at the crossroads of catabolism and anabolism.* Nature Reviews Molecular Cell Biology, 2015. **16**(8): p. 461-472.
110. Todde, V., M. Veenhuis, and I.J. van der Klei, *Autophagy: Principles and significance in health and disease.* Biochimica Et Biophysica Acta-Molecular Basis of Disease, 2009. **1792**(1): p. 3-13.
111. Xie, Z.L., et al., *Improvement of Cardiac Functions by Chronic Metformin Treatment Is Associated With Enhanced Cardiac Autophagy in Diabetic OVE26 Mice.* Diabetes, 2011. **60**(6): p. 1770-1778.
112. Bujak, A.L., et al., *AMPK Activation of Muscle Autophagy Prevents Fasting-Induced Hypoglycemia and Myopathy during Aging.* Cell Metabolism, 2015. **21**(6): p. 883-890.
113. Bairwa, S.C., N. Parajuli, and J.R. Dyck, *The role of AMPK in cardiomyocyte health and survival.* Biochim Biophys Acta, 2016.
114. Nishida, K., O. Yamaguchi, and K. Otsu, *Crosstalk between autophagy and apoptosis in heart disease.* Circulation Research, 2008. **103**(4): p. 343-351.
115. Boya, P., et al., *Inhibition of macroautophagy triggers apoptosis.* Mol Cell Biol, 2005. **25**(3): p. 1025-40.
116. Gonzalez-Polo, R.A., et al., *The apoptosis/autophagy paradox: autophagic vacuolization before apoptotic death.* Journal of Cell Science, 2005. **118**(14): p. 3091-3102.
117. Tanaka, Y., et al., *Accumulation of autophagic vacuoles and cardiomyopathy in LAMP-2-deficient mice.* Nature, 2000. **406**(6798): p. 902-6.
118. Kuma, A., et al., *The role of autophagy during the early neonatal starvation period.* Nature, 2004. **432**(7020): p. 1032-1036.
119. Komatsu, M., et al., *Impairment of starvation-induced and constitutive autophagy in Atg7-deficient mice.* J Cell Biol, 2005. **169**(3): p. 425-34.
120. Hara, T., et al., *Suppression of basal autophagy in neural cells causes neurodegenerative disease in mice.* Nature, 2006. **441**(7095): p. 885-889.
121. Komatsu, M., et al., *Loss of autophagy in the central nervous system causes neurodegeneration in mice.* Nature, 2006. **441**(7095): p. 880-4.
122. Pua, H.H., et al., *A critical role for the autophagy gene Atg5 in T cell survival and proliferation.* Journal of Experimental Medicine, 2007. **204**(1): p. 25-31.
123. Yue, Z., et al., *Beclin 1, an autophagy gene essential for early embryonic development, is a haploinsufficient tumor suppressor.* Proc Natl Acad Sci U S A, 2003. **100**(25): p. 15077-82.
124. Colell, A., et al., *GAPDH and autophagy preserve survival after apoptotic cytochrome c release in the absence of caspase activation.* Cell, 2007. **129**(5): p. 983-97.
125. Ravikumar, B., et al., *Inhibition of mTOR induces autophagy and reduces toxicity of polyglutamine expansions in fly and mouse models of Huntington disease.* Nature Genetics, 2004. **36**(6): p. 585-595.
126. Funderburk, S.F., Q.J. Wang, and Z.Y. Yue, *The Beclin 1-VPS34 complex - at the crossroads of autophagy and beyond.* Trends in Cell Biology, 2010. **20**(6): p. 355-362.
127. Pattingre, S., et al., *Bcl-2 antiapoptotic proteins inhibit Beclin 1-dependent autophagy.* Cell, 2005. **122**(6): p. 927-939.
128. Maejima, Y., et al., *Mst1 inhibits autophagy by promoting the interaction between Beclin1 and Bcl-2.* Nature Medicine, 2013. **19**(11): p. 1478-1488.
129. Wei, Y.J., et al., *EGFR-Mediated Beclin 1 Phosphorylation in Autophagy Suppression, Tumor Progression, and Tumor Chemoresistance.* Cell, 2013. **154**(6): p. 1269-1284.

130. Wang, R.C., et al., *Akt-Mediated Regulation of Autophagy and Tumorigenesis Through Beclin 1 Phosphorylation.* Science, 2012. **338**(6109): p. 956-959.
131. Wei, Y., et al., *JNK1-mediated phosphorylation of Bcl-2 regulates starvation-induced autophagy.* Mol Cell, 2008. **30**(6): p. 678-88.
132. He, C.Y., et al., *Dissociation of Bcl-2-Beclin1 Complex by Activated AMPK Enhances Cardiac Autophagy and Protects Against Cardiomyocyte Apoptosis in Diabetes.* Diabetes, 2013. **62**(4): p. 1270-1281.
133. Russell, R.C., et al., *ULK1 induces autophagy by phosphorylating Beclin-1 and activating VPS34 lipid kinase.* Nature Cell Biology, 2013. **15**(7): p. 741-750.
134. Gurkar, A.U., et al., *Identification of ROCK1 kinase as a critical regulator of Beclin1-mediated autophagy during metabolic stress.* Nature Communications, 2013. **4**.
135. Zalckvar, E., et al., *DAP-kinase-mediated phosphorylation on the BH3 domain of beclin 1 promotes dissociation of beclin 1 from Bcl-X-L and induction of autophagy.* Embo Reports, 2009. **10**(3): p. 285-292.
136. Maiuri, M.C., et al., *Functional and physical interaction between Bcl-X-L and a BH3-like domain in Beclin-1.* Embo Journal, 2007. **26**(10): p. 2527-2539.
137. Malik, S.A., et al., *BH3 mimetics activate multiple pro-autophagic pathways.* Oncogene, 2011. **30**(37): p. 3918-3929.
138. Luo, S.Q., et al., *Bim Inhibits Autophagy by Recruiting Beclin 1 to Microtubules.* Molecular Cell, 2012. **47**(3): p. 359-370.
139. Bellot, G., et al., *Hypoxia-Induced Autophagy Is Mediated through Hypoxia-Inducible Factor Induction of BNIP3 and BNIP3L via Their BH3 Domains.* Molecular and Cellular Biology, 2009. **29**(10): p. 2570-2581.
140. Elgendy, M., et al., *Oncogenic Ras-induced expression of Noxa and Beclin-1 promotes autophagic cell death and limits clonogenic survival.* Mol Cell, 2011. **42**(1): p. 23-35.
141. Kang, R., et al., *The Beclin 1 network regulates autophagy and apoptosis.* Cell Death Differ, 2011. **18**(4): p. 571-80.
142. Gustafsson, A.B. and R.A. Gottlieb, *Autophagy in Ischemic Heart Disease.* Circulation Research, 2009. **104**(2): p. 150-158.
143. Knaapen, M.W.M., et al., *Apoptotic versus autophagic cell death in heart failure.* Cardiovascular Research, 2001. **51**(2): p. 304-312.
144. Stypmann, J., et al., *LAMP-2 deficient mice show depressed cardiac contractile function without significant changes in calcium handling.* Basic Research in Cardiology, 2006. **101**(4): p. 281-291.
145. Xu, X., R. Bucala, and J. Ren, *Macrophage migration inhibitory factor deficiency augments doxorubicin-induced cardiomyopathy.* J Am Heart Assoc, 2013. **2**(6): p. e000439.
146. Thomas, R.L., et al., *Loss of MCL-1 leads to impaired autophagy and rapid development of heart failure.* Genes Dev, 2013. **27**(12): p. 1365-77.
147. Taneike, M., et al., *Inhibition of autophagy in the heart induces age-related cardiomyopathy.* Autophagy, 2010. **6**(5): p. 600-6.
148. Nakai, A., et al., *The role of autophagy in cardiomyocytes in the basal state and in response to hemodynamic stress.* Nat Med, 2007. **13**(5): p. 619-24.
149. Mizushima, N., et al., *In vivo analysis of autophagy in response to nutrient starvation using transgenic mice expressing a fluorescent autophagosome marker.* Molecular Biology of the Cell, 2004. **15**(3): p. 1101-1111.
150. Gupta, M.K., et al., *UBC9-Mediated Sumoylation Favorably Impacts Cardiac Function in Compromised Hearts.* Circ Res, 2016. **118**(12): p. 1894-905.

151. Zhang, S., et al., *PDCD5 protects against cardiac remodeling by regulating autophagy and apoptosis.* Biochem Biophys Res Commun, 2015. **461**(2): p. 321-8.
152. Yan, C.H., et al., *CREG1 ameliorates myocardial fibrosis associated with autophagy activation and Rab7 expression.* Biochim Biophys Acta, 2015. **1852**(2): p. 353-64.
153. Ma, X., et al., *Regulation of the transcription factor EB-PGC1alpha axis by beclin-1 controls mitochondrial quality and cardiomyocyte death under stress.* Mol Cell Biol, 2015. **35**(6): p. 956-76.
154. Sun, L.J., et al., *Overexpression of Rcan1-1L Inhibits Hypoxia-Induced Cell Apoptosis through Induction of Mitophagy.* Molecules and Cells, 2014. **37**(11): p. 785-794.
155. Grundy, S.M., et al., *Diabetes and cardiovascular disease: a statement for healthcare professionals from the American Heart Association.* Circulation, 1999. **100**(10): p. 1134-46.
156. Ruderman, N.B., et al., *AMPK, insulin resistance, and the metabolic syndrome.* J Clin Invest, 2013. **123**(7): p. 2764-72.
157. Trivedi, P.C., et al., *Glucolipotoxicity diminishes cardiomyocyte TFEB and inhibits lysosomal autophagy during obesity and diabetes.* Biochim Biophys Acta, 2016.
158. Yang, L., et al., *Defective Hepatic Autophagy in Obesity Promotes ER Stress and Causes Insulin Resistance.* Cell Metabolism, 2010. **11**(6): p. 467-478.
159. Sciarretta, S., et al., *Rheb is a Critical Regulator of Autophagy During Myocardial Ischemia Pathophysiological Implications in Obesity and Metabolic Syndrome.* Circulation, 2012. **125**(9): p. 1134-U166.
160. Lim, Y.M., et al., *Systemic autophagy insufficiency compromises adaptation to metabolic stress and facilitates progression from obesity to diabetes.* Nat Commun, 2014. **5**: p. 4934.
161. Xu, X.H., et al., *Akt2 knockout preserves cardiac function in high-fat diet-induced obesity by rescuing cardiac autophagosome maturation.* Journal of Molecular Cell Biology, 2013. **5**(1): p. 61-63.
162. Cao, L., et al., *CARD9 knockout ameliorates myocardial dysfunction associated with high fat diet-induced obesity.* J Mol Cell Cardiol, 2016. **92**: p. 185-95.
163. Kobayashi, S., et al., *Suppression of autophagy is protective in high glucose-induced cardiomyocyte injury.* Autophagy, 2012. **8**(4): p. 577-592.
164. Xie, Z., C. He, and M.H. Zou, *AMP-activated protein kinase modulates cardiac autophagy in diabetic cardiomyopathy.* Autophagy, 2011. **7**(10): p. 1254-5.
165. Pfisterer, S.G., et al., *Ca2+/Calmodulin-Dependent Kinase (CaMK) Signaling via CaMKI and AMP-Activated Protein Kinase Contributes to the Regulation of WIPI-1 at the Onset of Autophagy.* Molecular Pharmacology, 2011. **80**(6): p. 1066-1075.
166. Ghislat, G., et al., *Withdrawal of Essential Amino Acids Increases Autophagy by a Pathway Involving Ca2+/Calmodulin-dependent Kinase Kinase-beta (CaMKK-beta).* Journal of Biological Chemistry, 2012. **287**(46): p. 38625-38636.
167. Liang, J.Y., et al., *The energy sensing LKB1-AMPK pathway regulates p27(kip1) phosphorylation mediating the decision to enter autophagy or apoptosis.* Nature Cell Biology, 2007. **9**(2): p. 218-U125.
168. Das, A., et al., *Mammalian target of rapamycin (mTOR) inhibition with rapamycin improves cardiac function in type 2 diabetic mice: potential role of attenuated oxidative stress and altered contractile protein expression.* J Biol Chem, 2014. **289**(7): p. 4145-60.
169. Efeyan, A., et al., *Regulation of mTORC1 by the Rag GTPases is necessary for neonatal autophagy and survival.* Nature, 2013. **493**(7434): p. 679-83.

170. Hosokawa, N., et al., *Nutrient-dependent mTORC1 association with the ULK1-Atg13-FIP200 complex required for autophagy.* Mol Biol Cell, 2009. **20**(7): p. 1981-91.
171. Zhang, M., et al., *MST1 coordinately regulates autophagy and apoptosis in diabetic cardiomyopathy in mice.* Diabetologia, 2016.
172. Guo, Y., et al., *A novel protective mechanism for mitochondrial aldehyde dehydrogenase (ALDH2) in type i diabetes-induced cardiac dysfunction: role of AMPK-regulated autophagy.* Biochim Biophys Acta, 2015. **1852**(2): p. 319-31.
173. Yamamoto, S., et al., *Activation of Mst1 causes dilated cardiomyopathy by stimulating apoptosis without compensatory ventricular myocyte hypertrophy.* Journal of Clinical Investigation, 2003. **111**(10): p. 1463-1474.
174. Li, W., et al., *ZLN005 protects cardiomyocytes against high glucose-induced cytotoxicity by promoting SIRT1 expression and autophagy.* Exp Cell Res, 2016. **345**(1): p. 25-36.
175. Munasinghe, P.E., et al., *Type-2 diabetes increases autophagy in the human heart through promotion of Beclin-1 mediated pathway.* Int J Cardiol, 2016. **202**: p. 13-20.
176. Munasinghe, P.E., et al., *Data supporting the activation of autophagy genes in the diabetic heart.* Data Brief, 2015. **5**: p. 269-75.
177. Xu, X. and J. Ren, *Macrophage migration inhibitory factor (MIF) knockout preserves cardiac homeostasis through alleviating Akt-mediated myocardial autophagy suppression in high-fat diet-induced obesity.* Int J Obes (Lond), 2015. **39**(3): p. 387-96.
178. Kandadi, M.R., et al., *Deletion of protein tyrosine phosphatase 1B rescues against myocardial anomalies in high fat diet-induced obesity: Role of AMPK-dependent autophagy.* Biochim Biophys Acta, 2015. **1852**(2): p. 299-309.
179. Glazer, H.P., et al., *Hypercholesterolemia is associated with hyperactive cardiac mTORC1 and mTORC2 signaling.* Cell Cycle, 2009. **8**(11): p. 1738-1746.
180. Guo, R., et al., *Adiponectin knockout accentuates high fat diet-induced obesity and cardiac dysfunction: Role of autophagy.* Biochimica Et Biophysica Acta-Molecular Basis of Disease, 2013. **1832**(8): p. 1136-1148.
181. Liang, L., et al., *Antioxidant catalase rescues against high fat diet-induced cardiac dysfunction via an IKK beta-AMPK-dependent regulation of autophagy.* Biochimica Et Biophysica Acta-Molecular Basis of Disease, 2015. **1852**(2): p. 343-352.
182. Inoki, K., et al., *TSC2 is phosphorylated and inhibited by Akt and suppresses mTOR signalling.* Nature Cell Biology, 2002. **4**(9): p. 648-657.
183. Wang, L.F., et al., *PRAS40 regulates mTORC1 kinase activity by functioning as a direct inhibitor of substrate binding.* Journal of Biological Chemistry, 2007. **282**(27): p. 20036-20044.
184. Riehle, C., et al., *Insulin receptor substrate signaling suppresses neonatal autophagy in the heart.* Journal of Clinical Investigation, 2013. **123**(12): p. 5319-5333.
185. He, C.C., et al., *Exercise-induced BCL2-regulated autophagy is required for muscle glucose homeostasis.* Nature, 2012. **481**(7382): p. 511-U126.
186. He, C.C., R. Sumpter, and B. Levine, *Exercise induces autophagy in peripheral tissues and in the brain.* Autophagy, 2012. **8**(10): p. 1548-1551.
187. Gu, C.H., et al., *Exercise Training Improves Ischaemic Tolerance of the Senescent Heart by Ampk-Autophagy Cascade.* Heart, 2012. **98**: p. E54-E55.
188. Bhuiyan, M.S., et al., *Enhanced autophagy ameliorates cardiac proteinopathy.* Journal of Clinical Investigation, 2013. **123**(12): p. 5284-5297.
189. Lira, V., et al., *Loss of Ulk1 in skeletal muscle and heart prevents exercise protection against dietinduced insulin resistance.* Faseb Journal, 2015. **29**.

190. Giordano, F.J., *Oxygen, oxidative stress, hypoxia, and heart failure.* Journal of Clinical Investigation, 2005. **115**(3): p. 500-508.
191. Zhang, J., et al., *Overexpression of BAG3 Attenuates Hypoxia-Induced Cardiomyocyte Apoptosis by Inducing Autophagy.* Cell Physiol Biochem, 2016. **39**(2): p. 491-500.
192. Zhang, M., et al., *Polydatin protects cardiomyocytes against myocardial infarction injury by activating Sirt3.* Biochim Biophys Acta, 2016.
193. Xiao, Q., et al., *AMP-activated protein kinase-dependent autophagy mediated the protective effect of sonic hedgehog pathway on oxygen glucose deprivation-induced injury of cardiomyocytes.* Biochemical and Biophysical Research Communications, 2015. **457**(3): p. 419-425.
194. Maeda, H., et al., *Intermittent-hypoxia induced autophagy attenuates contractile dysfunction and myocardial injury in rat heart.* Biochimica Et Biophysica Acta-Molecular Basis of Disease, 2013. **1832**(8): p. 1159-1166.
195. Nishida, K., et al., *The role of autophagy in the heart.* Cell Death Differ, 2009. **16**(1): p. 31-8.
196. Boudina, S. and E.D. Abel, *Diabetic cardiomyopathy revisited.* Circulation, 2007. **115**(25): p. 3213-23.
197. Hamacher-Brady, A., N.R. Brady, and R.A. Gottlieb, *Enhancing macroautophagy protects against ischemia/reperfusion injury in cardiac myocytes.* Journal of Biological Chemistry, 2006. **281**(40): p. 29776-29787.
198. Mei, Y., et al., *Autophagy and oxidative stress in cardiovascular diseases.* Biochimica Et Biophysica Acta-Molecular Basis of Disease, 2015. **1852**(2): p. 243-251.
199. Ouyang, C.H., J.Y. You, and Z.L. Xie, *The interplay between autophagy and apoptosis in the diabetic heart.* Journal of Molecular and Cellular Cardiology, 2014. **71**: p. 71-80.
200. Gui, L., B.T. Liu, and G. Lv, *Hypoxia induces autophagy in cardiomyocytes via a hypoxia-inducible factor 1-dependent mechanism.* Experimental and Therapeutic Medicine, 2016. **11**(6): p. 2233-2239.
201. Chen, D., et al., *HO-1 Protects against Hypoxia/Reoxygenation-Induced Mitochondrial Dysfunction in H9c2 Cardiomyocytes.* PLoS One, 2016. **11**(5): p. e0153587.
202. Li, X., et al., *Inhibition of microRNA-497 ameliorates anoxia/reoxygenation injury in cardiomyocytes by suppressing cell apoptosis and enhancing autophagy.* Oncotarget, 2015. **6**(22): p. 18829-44.
203. Xie, S., et al., *Melatonin protects against chronic intermittent hypoxia-induced cardiac hypertrophy by modulating autophagy through the 5' adenosine monophosphate-activated protein kinase pathway.* Biochem Biophys Res Commun, 2015. **464**(4): p. 975-81.
204. Godar, R.J., et al., *Repetitive stimulation of autophagy-lysosome machinery by intermittent fasting preconditions the myocardium to ischemia-reperfusion injury.* Autophagy, 2015. **11**(9): p. 1537-60.
205. Song, H.W., et al., *ATG16L1 phosphorylation is oppositely regulated by CSNK2/casein kinase 2 and PPP1/protein phosphatase 1 which determines the fate of cardiomyocytes during hypoxia/reoxygenation.* Autophagy, 2015. **11**(8): p. 1308-1325.
206. Matsui, Y., et al., *Distinct roles of autophagy in the heart during ischemia and reperfusion: roles of AMP-activated protein kinase and Beclin 1 in mediating autophagy.* Circ Res, 2007. **100**(6): p. 914-22.
207. Senft, D. and Z.A. Ronai, *UPR, autophagy, and mitochondria crosstalk underlies the ER stress response.* Trends Biochem Sci, 2015. **40**(3): p. 141-8.

208. Rashid, H.O., et al., *ER stress: Autophagy induction, inhibition and selection.* Autophagy, 2015. **11**(11): p. 1956-1977.
209. Appenzeller-Herzog, C. and M.N. Hall, *Bidirectional crosstalk between endoplasmic reticulum stress and mTOR signaling.* Trends in Cell Biology, 2012. **22**(5): p. 274-282.
210. Sheng, R., et al., *Autophagy regulates endoplasmic reticulum stress in ischemic preconditioning.* Autophagy, 2012. **8**(3): p. 310-325.
211. Yan, W.J., H.L. Dong, and L.Z. Xiong, *The protective roles of autophagy in ischemic preconditioning.* Acta Pharmacol Sin, 2013. **34**(5): p. 636-43.
212. Gao, B., et al., *The endoplasmic reticulum stress inhibitor salubrinal inhibits the activation of autophagy and neuroprotection induced by brain ischemic preconditioning.* Acta Pharmacol Sin, 2013. **34**(5): p. 657-66.
213. Sheng, R. and Z.H. Qin, *The divergent roles of autophagy in ischemia and preconditioning.* Acta Pharmacol Sin, 2015. **36**(4): p. 411-20.
214. Petrovski, G., et al., *Cardioprotection by endoplasmic reticulum stress-induced autophagy.* Antioxid Redox Signal, 2011. **14**(11): p. 2191-200.
215. Szkudelski, T., *The mechanism of alloxan and streptozotocin action in B cells of the rat pancreas.* Physiol Res, 2001. **50**(6): p. 537-46.
216. Sambandam, N., et al., *Cardiac lipoprotein lipase in the spontaneously hypertensive rat.* Cardiovascular Research, 1997. **33**(2): p. 460-468.
217. Curaj, A., et al., *Minimal invasive surgical procedure of inducing myocardial infarction in mice.* J Vis Exp, 2015(99): p. e52197.
218. Love, M.I., W. Huber, and S. Anders, *Moderated estimation of fold change and dispersion for RNA-seq data with DESeq2.* Genome Biol, 2014. **15**(12): p. 550.
219. Wang, L., S. Wang, and W. Li, *RSeQC: quality control of RNA-seq experiments.* Bioinformatics, 2012. **28**(16): p. 2184-5.
220. Grabherr, M.G., et al., *Full-length transcriptome assembly from RNA-Seq data without a reference genome.* Nat Biotechnol, 2011. **29**(7): p. 644-52.
221. Caron, A., et al., *Loss of hepatic DEPTOR alters the metabolic transition to fasting.* Mol Metab, 2017. **6**(5): p. 447-458.
222. Pulinilkunnil, T., et al., *Lysophosphatidic acid-mediated augmentation of cardiomyocyte lipoprotein lipase involves actin cytoskeleton reorganization.* American Journal of Physiology-Heart and Circulatory Physiology, 2005. **288**(6): p. H2802-H2810.
223. Zetser, A., et al., *Heparanase affects adhesive and tumorigenic potential of human glioma cells.* Cancer Res, 2003. **63**(22): p. 7733-41.
224. Kuramochi, Y., et al., *Cardiac endothelial cells regulate reactive oxygen species-induced cardiomyocyte apoptosis through neuregulin-1beta/erbB4 signaling.* J Biol Chem, 2004. **279**(49): p. 51141-7.
225. Narmoneva, D.A., et al., *Endothelial cells promote cardiac myocyte survival and spatial reorganization: implications for cardiac regeneration.* Circulation, 2004. **110**(8): p. 962-8.
226. Hsieh, P.C., et al., *Endothelial-cardiomyocyte interactions in cardiac development and repair.* Annu Rev Physiol, 2006. **68**: p. 51-66.
227. Tirziu, D., F.J. Giordano, and M. Simons, *Cell communications in the heart.* Circulation, 2010. **122**(9): p. 928-37.
228. Ziolkowski, A.F., et al., *Heparan sulfate and heparanase play key roles in mouse beta cell survival and autoimmune diabetes.* Journal of Clinical Investigation, 2012. **122**(1): p. 132-141.

229. Hao, N.B., et al., *Hepatocyte growth factor (HGF) upregulates heparanase expression via the PI3K/Akt/NF-kappaB signaling pathway for gastric cancer metastasis.* Cancer Lett, 2015. **361**(1): p. 57-66.
230. Hammond, E., et al., *The Role of Heparanase and Sulfatases in the Modification of Heparan Sulfate Proteoglycans within the Tumor Microenvironment and Opportunities for Novel Cancer Therapeutics.* Front Oncol, 2014. **4**: p. 195.
231. Purushothaman, A., et al., *Heparanase-enhanced shedding of syndecan-1 by myeloma cells promotes endothelial invasion and angiogenesis.* Blood, 2010. **115**(12): p. 2449-57.
232. Wang, Y., et al., *Endothelial Cell Heparanase Taken Up by Cardiomyocytes Regulates Lipoprotein Lipase Transfer to the Coronary Lumen following Diabetes.* Diabetes, 2014.
233. Purushothaman, A., et al., *Heparanase-mediated loss of nuclear syndecan-1 enhances histone acetyltransferase (HAT) activity to promote expression of genes that drive an aggressive tumor phenotype.* J Biol Chem, 2011. **286**(35): p. 30377-83.
234. He, Y.Q., et al., *The endoglycosidase heparanase enters the nucleus of T lymphocytes and modulates H3 methylation at actively transcribed genes via the interplay with key chromatin modifying enzymes.* Transcription, 2012. **3**(3): p. 130-45.
235. Nobuhisa, T., et al., *Translocation of heparanase into nucleus results in cell differentiation.* Cancer Science, 2007. **98**(4): p. 535-540.
236. Wang, F., et al., *Fatty acid-induced nuclear translocation of heparanase uncouples glucose metabolism in endothelial cells.* Arterioscler Thromb Vasc Biol, 2012. **32**(2): p. 406-14.
237. Wang, Y., et al., *Endothelial Heparanase Regulates Heart Metabolism by Stimulating Lipoprotein Lipase Secretion From Cardiomyocytes.* Arterioscler Thromb Vasc Biol, 2013.
238. Nadir, Y., et al., *Heparanase induces tissue factor expression in vascular endothelial and cancer cells.* J Thromb Haemost, 2006. **4**(11): p. 2443-51.
239. Gingis-Velitski, S., et al., *Heparanase induces endothelial cell migration via protein kinase B/Akt activation.* J Biol Chem, 2004. **279**(22): p. 23536-41.
240. Poornima, I.G., P. Parikh, and R.P. Shannon, *Diabetic cardiomyopathy: the search for a unifying hypothesis.* Circulation Research, 2006. **98**(5): p. 596-605.
241. Shafat, I., et al., *Heparanase levels are elevated in the urine and plasma of type 2 diabetes patients and associate with blood glucose levels.* PLoS One, 2011. **6**(2): p. e17312.
242. Zhang, D., et al., *Hyperglycemia-induced secretion of endothelial heparanase stimulates a vascular endothelial growth factor autocrine network in cardiomyocytes that promotes recruitment of lipoprotein lipase.* Arterioscler Thromb Vasc Biol, 2013. **33**(12): p. 2830-8.
243. Zetter, B.R., *The endothelial cells of large and small blood vessels.* Diabetes, 1981. **30**(Suppl 2): p. 24-8.
244. Wang, F., et al., *Glucose-induced endothelial heparanase secretion requires cortical and stress actin reorganization.* Cardiovasc Res, 2010. **87**(1): p. 127-36.
245. Herz, J. and D.K. Strickland, *LRP: a multifunctional scavenger and signaling receptor.* Journal of Clinical Investigation, 2001. **108**(6): p. 779-84.
246. Lillis, A.P., et al., *LDL receptor-related protein 1: Unique tissue-specific functions revealed by selective gene knockout studies.* Physiol Rev, 2008. **88**(3): p. 887-918.
247. von Harsdorf, R., P.F. Li, and R. Dietz, *Signaling pathways in reactive oxygen species-induced cardiomyocyte apoptosis.* Circulation, 1999. **99**(22): p. 2934-41.
248. Chen, L. and R.D. Sanderson, *Heparanase regulates levels of syndecan-1 in the nucleus.* PLoS One, 2009. **4**(3): p. e4947.

249. Yang, Y., et al., *Nuclear heparanase-1 activity suppresses melanoma progression via its DNA-binding affinity.* Oncogene, 2015.
250. Purushothaman, A., S.K. Babitz, and R.D. Sanderson, *Heparanase enhances the insulin receptor signaling pathway to activate extracellular signal-regulated kinase in multiple myeloma.* J Biol Chem, 2012. **287**(49): p. 41288-96.
251. Boyango, I., et al., *Heparanase co-operates with Ras to drive breast and skin tumorigenesis.* Cancer Res, 2014.
252. Zetser, A., et al., *Heparanase induces vascular endothelial growth factor expression: Correlation with p38 phosphorylation levels and Src activation.* Cancer Res, 2006. **66**(3): p. 1455-1463.
253. Bhattacharjee, P.S., et al., *High-Glucose-Induced Endothelial Cell Injury Is Inhibited by a Peptide Derived from Human Apolipoprotein E.* Plos One, 2012. **7**(12).
254. Topper, J.N. and M.A. Gimbrone, *Blood flow and vascular gene expression: fluid shear stress as a modulator of endothelial phenotype.* Molecular Medicine Today, 1999. **5**(1): p. 40-46.
255. Chen, B.P.C., et al., *DNA microarray analysis of gene expression in endothelial cells in response to 24-h shear stress.* Physiological Genomics, 2001. **7**(1): p. 55-63.
256. Cai, L. and Y.J. Kang, *Cell death and diabetic cardiomyopathy.* Cardiovasc Toxicol, 2003. **3**(3): p. 219-28.
257. Gao, Q.Q., et al., *Study on the mechanism of HIF1a-SOX9 in glucose-induced cardiomyocyte hypertrophy.* Biomedicine & Pharmacotherapy, 2015. **74**: p. 57-62.
258. Chang, M.L., et al., *High Glucose Activates ChREBP-Mediated HIF-1 alpha and VEGF Expression in Human RPE Cells Under Normoxia.* Retinal Degenerative Diseases: Mechanisms and Experimental Therapy, 2014. **801**: p. 609-621.
259. Kawata, K., et al., *Role of LRP1 in transport of CCN2 protein in chondrocytes.* J Cell Sci, 2012. **125**(Pt 12): p. 2965-72.
260. Bonello, S., et al., *Reactive oxygen species activate the HIF-1 alpha promoter via a functional NF kappa B site.* Arteriosclerosis Thrombosis and Vascular Biology, 2007. **27**(4): p. 755-761.
261. Castellano, J., et al., *Hypoxia Stimulates Low-Density Lipoprotein Receptor-Related Protein-1 Expression Through Hypoxia-Inducible Factor-1 alpha in Human Vascular Smooth Muscle Cells.* Arteriosclerosis Thrombosis and Vascular Biology, 2011. **31**(6): p. 1411-1420.
262. Liu, C.C., et al., *Neuronal LRP1 Regulates Glucose Metabolism and Insulin Signaling in the Brain.* Journal of Neuroscience, 2015. **35**(14): p. 5851-5859.
263. Hong, H., et al., *Downregulation of LPR1 at the blood-brain barrier in streptozotocin-induced diabetic mice.* Neuropharmacology, 2009. **56**(6-7): p. 1054-1059.
264. Vlodavsky, I., et al., *Opposing Functions of Heparanase-1 and Heparanase-2 in Cancer Progression.* Trends Biochem Sci, 2018. **43**(1): p. 18-31.
265. Wang, F., et al., *High glucose facilitated endothelial heparanase transfer to the cardiomyocyte modifies its cell death signature.* Cardiovasc Res, 2016. **112**(3): p. 656-668.
266. Arrieta, A., E.A. Blackwood, and C.C. Glembotski, *ER Protein Quality Control and the Unfolded Protein Response in the Heart.* Curr Top Microbiol Immunol, 2018. **414**: p. 193-213.
267. Wang, X., et al., *The unfolded protein response in ischemic heart disease.* J Mol Cell Cardiol, 2018. **117**: p. 19-25.

268. Ma, S., et al., *The role of the autophagy in myocardial ischemia/reperfusion injury.* Biochim Biophys Acta, 2015. **1852**(2): p. 271-6.
269. Hetz, C., *The unfolded protein response: controlling cell fate decisions under ER stress and beyond.* Nature Reviews Molecular Cell Biology, 2012. **13**(2): p. 89-102.
270. Szegezdi, E., et al., *Mediators of endoplasmic reticulum stress-induced apoptosis.* EMBO Rep, 2006. **7**(9): p. 880-5.
271. Turer, A.T. and J.A. Hill, *Pathogenesis of myocardial ischemia-reperfusion injury and rationale for therapy.* Am J Cardiol, 2010. **106**(3): p. 360-8.
272. Elimam, H., et al., *Calcium-independent phospholipase A2gamma enhances activation of the ATF6 transcription factor during endoplasmic reticulum stress.* J Biol Chem, 2015. **290**(5): p. 3009-20.
273. Yu, Z., et al., *Activation of the ATF6 branch of the unfolded protein response in neurons improves stroke outcome.* J Cereb Blood Flow Metab, 2017. **37**(3): p. 1069-1079.
274. Naranjo, J.R., et al., *Activating transcription factor 6 derepression mediates neuroprotection in Huntington disease.* J Clin Invest, 2016. **126**(2): p. 627-38.
275. Yoshikawa, A., et al., *Deletion of Atf6alpha impairs astroglial activation and enhances neuronal death following brain ischemia in mice.* J Neurochem, 2015. **132**(3): p. 342-53.
276. Kezuka, D., et al., *Deletion of Atf6alpha enhances kainate-induced neuronal death in mice.* Neurochem Int, 2016. **92**: p. 67-74.
277. Usui, M., et al., *Atf6alpha-null mice are glucose intolerant due to pancreatic beta-cell failure on a high-fat diet but partially resistant to diet-induced insulin resistance.* Metabolism, 2012. **61**(8): p. 1118-28.
278. Cinaroglu, A., et al., *Activating transcription factor 6 plays protective and pathological roles in steatosis due to endoplasmic reticulum stress in zebrafish.* Hepatology, 2011. **54**(2): p. 495-508.
279. Lynch, J.M., et al., *A thrombospondin-dependent pathway for a protective ER stress response.* Cell, 2012. **149**(6): p. 1257-68.
280. Wang, S., et al., *ATF6 safeguards organelle homeostasis and cellular aging in human mesenchymal stem cells.* Cell Discov, 2018. **4**: p. 2.
281. Belmont, P.J., et al., *Regulation of microRNA expression in the heart by the ATF6 branch of the ER stress response.* J Mol Cell Cardiol, 2012. **52**(5): p. 1176-82.
282. Glembotski, C.C., *Roles for ATF6 and the sarco/endoplasmic reticulum protein quality control system in the heart.* J Mol Cell Cardiol, 2014. **71**: p. 11-5.
283. Paxman, R., et al., *Pharmacologic ATF6 activating compounds are metabolically activated to selectively modify endoplasmic reticulum proteins.* Elife, 2018. **7**.
284. Yan, M.M., et al., *Interplay between unfolded protein response and autophagy promotes tumor drug resistance (Review).* Oncology Letters, 2015. **10**(4): p. 1959-1969.
285. Akimoto, H., et al., *Heparin and heparan sulfate block angiotensin II-induced hypertrophy in cultured neonatal rat cardiomyocytes. A possible role of intrinsic heparin-like molecules in regulation of cardiomyocyte hypertrophy.* Circulation, 1996. **93**(4): p. 810-6.
286. Zcharia, E., et al., *Transgenic expression of mammalian heparanase uncovers physiological functions of heparan sulfate in tissue morphogenesis, vascularization, and feeding behavior.* Faseb Journal, 2004. **18**(2): p. 252-63.
287. Secchi, M.F., et al., *Recent data concerning heparanase: focus on fibrosis, inflammation and cancer.* Biomol Concepts, 2015. **6**(5-6): p. 415-21.
288. Assady, S., et al., *Nephroprotective effect of heparanase in experimental nephrotic syndrome.* PLoS One, 2015. **10**(3): p. e0119610.

289. Yang, Y., et al., *Heparanase enhances local and systemic osteolysis in multiple myeloma by upregulating the expression and secretion of RANKL.* Cancer Res, 2010. **70**(21): p. 8329-38.
290. He, X., et al., *Hypoxia increases heparanase-dependent tumor cell invasion, which can be inhibited by antiheparanase antibodies.* Cancer Res, 2004. **64**(11): p. 3928-33.
291. Navarro, F.P., et al., *Brain heparanase expression is up-regulated during postnatal development and hypoxia-induced neovascularization in adult rats (vol 105, pg 34, 2008).* Journal of Neurochemistry, 2008. **105**(4): p. 1560-1560.
292. Wu, W., et al., *Hypoxia activates heparanase expression in an NF-kappaB dependent manner.* Oncol Rep, 2010. **23**(1): p. 255-61.
293. Hu, J., et al., *Heparanase and Vascular Endothelial Growth Factor Expression Is Increased in Hypoxia-Induced Retinal Neovascularization.* Investigative Ophthalmology & Visual Science, 2012. **53**(11): p. 6810-6817.
294. Hu, J., et al., *Heparanase and vascular endothelial growth factor expression is increased in hypoxia-induced retinal neovascularization.* Invest Ophthalmol Vis Sci, 2012. **53**(11): p. 6810-7.
295. Lee, S.J., et al., *Angiopoietin-2 exacerbates cardiac hypoxia and inflammation after myocardial infarction.* J Clin Invest, 2018. **128**(11): p. 5018-5033.
296. Dhingra, S., et al., *IL-10 attenuates TNF-alpha-induced NF kappaB pathway activation and cardiomyocyte apoptosis.* Cardiovasc Res, 2009. **82**(1): p. 59-66.
297. Dhingra, S., et al., *Akt regulates IL-10 mediated suppression of TNFalpha-induced cardiomyocyte apoptosis by upregulating Stat3 phosphorylation.* PLoS One, 2011. **6**(9): p. e25009.
298. Santini, D., et al., *Surviving acute myocardial infarction: survivin expression in viable cardiomyocytes after infarction.* J Clin Pathol, 2004. **57**(12): p. 1321-4.
299. Levkau, B., et al., *Survivin determines cardiac function by controlling total cardiomyocyte number.* Circulation, 2008. **117**(12): p. 1583-93.
300. Cao, W., et al., *Burn-induced apoptosis of cardiomyocytes is survivin dependent and regulated by PI3K/Akt, p38 MAPK and ERK pathways.* Basic Research in Cardiology, 2011. **106**(6): p. 1207-1220.
301. Ueland, T., et al., *Dysregulated osteoprotegerin/RANK ligand/RANK axis in clinical and experimental heart failure.* Circulation, 2005. **111**(19): p. 2461-2468.
302. Yerlikaya, A., et al., *A proteomic analysis of p53-independent induction of apoptosis by bortezomib in 4T1 breast cancer cell line.* Journal of Proteomics, 2015. **113**: p. 315-325.
303. Haudek, S.B., et al., *TNF provokes cardiomyocyte apoptosis and cardiac remodeling through activation of multiple cell death pathways.* Journal of Clinical Investigation, 2007. **117**(9): p. 2692-2701.
304. Elmore, S., *Apoptosis: A review of programmed cell death.* Toxicologic Pathology, 2007. **35**(4): p. 495-516.
305. Crow, M.T., et al., *The mitochondrial death pathway and cardiac myocyte apoptosis.* Circulation Research, 2004. **95**(10): p. 957-970.
306. Vogler, M., *BCL2A1: the underdog in the BCL2 family.* Cell Death and Differentiation, 2012. **19**(1): p. 67-74.
307. Iwata, A., et al., *Extracellular BCL2 Proteins Are Danger-Associated Molecular Patterns That Reduce Tissue Damage in Murine Models of Ischemia-Reperfusion Injury.* Plos One, 2010. **5**(2).

308. Sheikh, M.S., et al., *p53-dependent and -independent regulation of the death receptor KILLER/DR5 gene expression in response to genotoxic stress and tumor necrosis factor alpha.* Cancer Research, 1998. **58**(8): p. 1593-1598.
309. Denes, A., G. Lopez-Castejon, and D. Brough, *Caspase-1: is IL-1 just the tip of the ICEberg?* Cell Death & Disease, 2012. **3**.
310. Aries, A., et al., *Caspase-1 cleavage of transcription factor GATA4 and regulation of cardiac cell fate.* Cell Death & Disease, 2014. **5**.
311. Schulz, R. and G. Heusch, *Tumor Necrosis Factor-alpha and Its Receptors 1 and 2 Yin and Yang in Myocardial Infarction?* Circulation, 2009. **119**(10): p. 1355-1357.
312. Chiong, M., et al., *Cardiomyocyte death: mechanisms and translational implications.* Cell Death Dis, 2011. **2**: p. e244.
313. Bajaj, G. and R.K. Sharma, *TNF-alpha-mediated cardiomyocyte apoptosis involves caspase-12 and calpain.* Biochemical and Biophysical Research Communications, 2006. **345**(4): p. 1558-1564.
314. Schott, A., et al., *Arabidopsis Stromal-derived Factor2 (SDF2) Is a Crucial Target of the Unfolded Protein Response in the Endoplasmic Reticulum.* Journal of Biological Chemistry, 2010. **285**(23): p. 18113-18121.
315. Fukuda, S., et al., *Murine and human SDF2L1 is an endoplasmic reticulum stress-inducible gene and encodes a new member of the Pmt/rt protein family.* Biochemical and Biophysical Research Communications, 2001. **280**(1): p. 407-414.
316. Lindahl, M., et al., *MANF Is Indispensable for the Proliferation and Survival of Pancreatic beta Cells.* Cell Reports, 2014. **7**(2): p. 366-375.
317. Apostolou, A., et al., *Armet, a UPR-upregulated protelin, inhibits cell proliferation and ER stress-induced cell death.* Experimental Cell Research, 2008. **314**(13): p. 2454-2467.
318. Andre, F., et al., *GILZ overexpression attenuates endoplasmic reticulum stress-mediated cell death via the activation of mitochondrial oxidative phosphorylation.* Biochem Biophys Res Commun, 2016. **478**(2): p. 513-20.
319. Tufo, G., et al., *The protein disulfide isomerases PDIA4 and PDIA6 mediate resistance to cisplatin-induced cell death in lung adenocarcinoma.* Cell Death and Differentiation, 2014. **21**(5): p. 685-695.
320. Galligan, J.J. and D.R. Petersen, *The human protein disulfide isomerase gene family.* Human Genomics, 2012. **6**.
321. Yoshida, H., et al., *XBP1 mRNA is induced by ATF6 and spliced by IRE1 in response to ER stress to produce a highly active transcription factor.* Cell, 2001. **107**(7): p. 881-891.
322. Margariti, A., et al., *XBP1 mRNA Splicing Triggers an Autophagic Response in Endothelial Cells through BECLIN-1 Transcriptional Activation.* Journal of Biological Chemistry, 2013. **288**(2): p. 859-872.
323. Vidal, R.L. and C. Hetz, *Unspliced XBP1 controls autophagy through FoxO1.* Cell Research, 2013. **23**(4): p. 463-464.
324. Liu, Y., et al., *Preventing oxidative stress: a new role for XBP1.* Cell Death Differ, 2009. **16**(6): p. 847-57.
325. Fung, T.S., Y. Liao, and D.X. Liu, *The Endoplasmic Reticulum Stress Sensor IRE1 alpha Protects Cells from Apoptosis Induced by the Coronavirus Infectious Bronchitis Virus.* Journal of Virology, 2014. **88**(21): p. 12752-12764.
326. Olivares, S. and A.S. Henkel, *Hepatic Xbp1 Gene Deletion Promotes Endoplasmic Reticulum Stress-induced Liver Injury and Apoptosis.* Journal of Biological Chemistry, 2015. **290**(50): p. 30142-30151.

327. Kurata, M., et al., *Anti-apoptotic function of Xbp1 as an IL-3 signaling molecule in hematopoietic cells.* Cell Death & Disease, 2011. **2**.
328. Lee, A.S., *The ER chaperone and signaling regulator GRP78/BiP as a monitor of endoplasmic reticulum stress.* Methods, 2005. **35**(4): p. 373-381.
329. Wang, M., et al., *Role of the Unfolded Protein Response Regulator GRP78/BiP in Development, Cancer, and Neurological Disorders.* Antioxidants & Redox Signaling, 2009. **11**(9): p. 2307-2316.
330. Zhang, X.Y., et al., *Endoplasmic reticulum chaperone GRP78 is involved in autophagy activation induced by ischemic preconditioning in neural cells.* Molecular Brain, 2015. **8**.
331. Cook, K.L., et al., *Glucose-Regulated Protein 78 Controls Cross-talk between Apoptosis and Autophagy to Determine Antiestrogen Responsiveness.* Cancer Research, 2012. **72**(13): p. 3337-3349.
332. Grkovic, S., et al., *IGFBP-3 binds GRP78, stimulates autophagy and promotes the survival of breast cancer cells exposed to adverse microenvironments.* Oncogene, 2013. **32**(19): p. 2412-2420.
333. Liu, H., et al., *Endoplasmic reticulum chaperones GRP78 and calreticulin prevent oxidative stress, Ca2+ disturbances, and cell death in renal epithelial cells.* J Biol Chem, 1997. **272**(35): p. 21751-9.
334. Bi, X., et al., *Angiopoietin-1 attenuates angiotensin II-induced ER stress in glomerular endothelial cells via a Tie2 receptor/ERK1/2-p38 MAPK-dependent mechanism.* Mol Cell Endocrinol, 2016. **428**: p. 118-32.
335. Wang, J.M., et al., *Inositol-Requiring Enzyme 1 Facilitates Diabetic Wound Healing Through Modulating MicroRNAs.* Diabetes, 2017. **66**(1): p. 177-192.
336. Wang, Y.I., et al., *Triglyceride-Rich Lipoprotein Modulates Endothelial Vascular Cell Adhesion Molecule (VCAM)-1 Expression via Differential Regulation of Endoplasmic Reticulum Stress.* Plos One, 2013. **8**(10).
337. Kawanami, D., et al., *Fasudil inhibits ER stress-induced VCAM-1 expression by modulating unfolded protein response in endothelial cells.* Biochemical and Biophysical Research Communications, 2013. **435**(2): p. 171-175.
338. Zhang, D.M., et al., *Up-regulation of VCAM1 Relates to Neuronal Apoptosis After Intracerebral Hemorrhage in Adult Rats.* Neurochemical Research, 2015. **40**(5): p. 1042-1052.
339. Eletto, D., D. Dersh, and Y. Argon, *GRP94 in ER quality control and stress responses.* Seminars in Cell & Developmental Biology, 2010. **21**(5): p. 479-485.
340. Melnick, J., S. Aviel, and Y. Argon, *The Endoplasmic-Reticulum Stress Protein-Grp94, in Addition to Bip, Associates with Unassembled Immunoglobulin-Chains.* Journal of Biological Chemistry, 1992. **267**(30): p. 21303-21306.
341. Suntharalingam, A., et al., *Glucose-regulated Protein 94 Triage of Mutant Myocilin through Endoplasmic Reticulum-associated Degradation Subverts a More Efficient Autophagic Clearance Mechanism.* Journal of Biological Chemistry, 2012. **287**(48): p. 40661-40669.
342. Dejeans, N., et al., *Overexpression of GRP94 in breast cancer cells resistant to oxidative stress promotes high levels of cancer cell proliferation and migration: implications for tumor recurrence.* Free Radic Biol Med, 2012. **52**(6): p. 993-1002.
343. Pan, Z., et al., *Silencing of GRP94 expression promotes apoptosis in pancreatic cancer cells.* International Journal of Oncology, 2009. **35**(4): p. 823-828.

344. Ostrovsky, O., N.T. Ahmed, and Y. Argon, *The Chaperone Activity of GRP94 Toward Insulin-like Growth Factor II Is Necessary for the Stress Response to Serum Deprivation.* Molecular Biology of the Cell, 2009. **20**(6): p. 1855-1864.
345. Lee, S., et al., *Thioredoxin-interacting protein regulates protein disulfide isomerases and endoplasmic reticulum stress.* Embo Molecular Medicine, 2014. **6**(6): p. 732-743.
346. Singh, S., et al., *Aldehyde dehydrogenases in cellular responses to oxidative/electrophilic stress.* Free Radical Biology and Medicine, 2013. **56**: p. 89-101.
347. Meng, E., et al., *ALDH1A1 maintains ovarian cancer stem cell-like properties by altered regulation of cell cycle checkpoint and DNA repair network signaling.* PLoS One, 2014. **9**(9): p. e107142.
348. Delgado, M.A., et al., *Toll-like receptors control autophagy.* EMBO J, 2008. **27**(7): p. 1110-21.
349. Meyer, T., et al., *Induction of apoptosis by Toll-like receptor-7 agonist in tissue cultures.* Br J Dermatol, 2003. **149 Suppl 66**: p. 9-14.
350. Guo, R., et al., *Metallothionein alleviates oxidative stress-induced endoplasmic reticulum stress and myocardial dysfunction.* Journal of Molecular and Cellular Cardiology, 2009. **47**(2): p. 228-237.
351. Yang, L.F., et al., *Heavy metal scavenger metallothionein attenuates ER stress-induced myocardial contractile anomalies: Role of autophagy.* Toxicology Letters, 2014. **225**(3): p. 333-341.
352. Ma, H.L., et al., *HMBOX1 interacts with MT2A to regulate autophagy and apoptosis in vascular endothelial cells.* Scientific Reports, 2015. **5**.
353. Ruttkay-Nedecky, B., et al., *The Role of Metallothionein in Oxidative Stress.* International Journal of Molecular Sciences, 2013. **14**(3): p. 6044-6066.
354. Shimoda, R., et al., *Metallothionein is a potential negative regulator of apoptosis.* Toxicological Sciences, 2003. **73**(2): p. 294-300.
355. Shi, C.S., et al., *Activation of autophagy by inflammatory signals limits IL-1beta production by targeting ubiquitinated inflammasomes for destruction.* Nat Immunol, 2012. **13**(3): p. 255-63.
356. Sagulenko, V., et al., *AIM2 and NLRP3 inflammasomes activate both apoptotic and pyroptotic death pathways via ASC.* Cell Death Differ, 2013. **20**(9): p. 1149-60.
357. Ho, D.V. and J.Y. Chan, *Induction of Herpud1 expression by ER stress is regulated by Nrf1.* Febs Letters, 2015. **589**(5): p. 615-620.
358. Segawa, T., et al., *Androgen-induced expression of endoplasmic reticulum (ER) stress response genes in prostate cancer cells.* Oncogene, 2002. **21**(57): p. 8749-8758.
359. Paredes, F., et al., *HERPUD1 protects against oxidative stress-induced apoptosis through downregulation of the inositol 1,4,5-trisphosphate receptor.* Free Radical Biology and Medicine, 2016. **90**: p. 206-218.
360. Kito, H., et al., *Up-regulation of K(ir)2.1 by ER stress facilitates cell death of brain capillary endothelial cells.* Biochem Biophys Res Commun, 2011. **411**(2): p. 293-8.
361. Hiroi, T., et al., *Protracted lithium treatment protects against the ER stress elicited by thapsigargin in rat PC12 cells: roles of intracellular calcium, GRP78 and Bcl-2.* Pharmacogenomics Journal, 2005. **5**(2): p. 102-111.
362. Wang, J.D., et al., *A pivotal role of FOS-mediated BECN1/Beclin 1 upregulation in dopamine D2 and D3 receptor agonist-induced autophagy activation.* Autophagy, 2015. **11**(11): p. 2057-2073.
363. Preston, G.A., et al., *Induction of apoptosis by c-Fos protein.* Molecular and Cellular Biology, 1996. **16**(1): p. 211-218.

364. Haile, Y., et al., *Rab32 connects ER stress to mitochondrial defects in multiple sclerosis.* J Neuroinflammation, 2017. **14**(1): p. 19.
365. Ao, X., L. Zou, and Y. Wu, *Regulation of autophagy by the Rab GTPase network.* Cell Death and Differentiation, 2014. **21**(3): p. 348-358.
366. Bui, M., et al., *Rab32 modulates apoptosis onset and mitochondria-associated membrane (MAM) properties.* J Biol Chem, 2010. **285**(41): p. 31590-602.
367. Olivari, S., et al., *EDEM1 regulates ER-associated degradation by accelerating de-mannosylation of folding-defective polypeptides and by inhibiting their covalent aggregation.* Biochemical and Biophysical Research Communications, 2006. **349**(4): p. 1278-1284.
368. Kosmaoglou, M., et al., *A dual role for EDEM1 in the processing of rod opsin.* Journal of Cell Science, 2009. **122**(24): p. 4465-4472.
369. Schardt, J.A., et al., *Unfolded protein response suppresses CEBPA by induction of calreticulin in acute myeloid leukaemia.* Journal of Cellular and Molecular Medicine, 2010. **14**(6b): p. 1509-1519.
370. Schardt, J., et al., *The Unfolded Protein Response (UPR) Is Activated in Human Acute Myeloid Leukemia (AML) and Suppresses Translation of the CCAAT/Enhancer Binding Protein-Alpha (CEBPA) by Induction of the RNA-Binding Protein Calreticulin.* Blood, 2008. **112**(11): p. 1009-1009.
371. Bernard-Marissal, N., et al., *Reduced calreticulin levels link endoplasmic reticulum stress and Fas-triggered cell death in motoneurons vulnerable to ALS.* J Neurosci, 2012. **32**(14): p. 4901-12.
372. Holczer, M., G. Banhegyi, and O. Kapuy, *GADD34 Keeps the mTOR Pathway Inactivated in Endoplasmic Reticulum Stress Related Autophagy.* Plos One, 2016. **11**(12).
373. Tambe, Y., et al., *The drs tumor suppressor is involved in the maturation process of autophagy induced by low serum.* Cancer Letters, 2009. **283**(1): p. 74-83.
374. Tang, Y.X., et al., *CYP1B1 expression promotes the proangiogenic phenotype of endothelium through decreased intracellular oxidative stress and thrombospondin-2 expression.* Blood, 2009. **113**(3): p. 744-754.
375. Palenski, T.L., et al., *Lack of Cyp1b1 promotes the proliferative and migratory phenotype of perivascular supporting cells.* Lab Invest, 2013. **93**(6): p. 646-62.
376. Mitsui, Y., et al., *CYP1B1 promotes tumorigenesis via altered expression of CDC20 and DAPK1 genes in renal cell carcinoma.* BMC Cancer, 2015. **15**: p. 942.
377. Wu, J., et al., *IL-33 Is Required for Disposal of Unnecessary Cells during Ovarian Atresia through Regulation of Autophagy and Macrophage Migration.* Journal of Immunology, 2015. **194**(5): p. 2140-2147.
378. Zhang, H.F., et al., *Altered serum levels of IL-33 in patients with advanced systolic chronic heart failure: correlation with oxidative stress.* Journal of Translational Medicine, 2012. **10**.
379. Seki, K., et al., *Interleukin-33 prevents apoptosis and improves survival after experimental myocardial infarction through ST2 signaling.* Circ Heart Fail, 2009. **2**(6): p. 684-91.
380. Fledderus, J.O., et al., *KLF2 primes the antioxidant transcription factor Nrf2 for activation in endothelial cells.* Arteriosclerosis Thrombosis and Vascular Biology, 2008. **28**(7): p. 1339-1346.
381. van Thienen, J.V., et al., *Shear stress sustains atheroprotective endothelial KLF2 expression more potently than statins through mRNA stabilization.* Cardiovascular Research, 2006. **72**(2): p. 231-240.

382. Birkenfeld, A.L., et al., *Influence of the Hepatic Eukaryotic Initiation Factor 2 alpha (eIF2 alpha) Endoplasmic Reticulum (ER) Stress Response Pathway on Insulin-mediated ER Stress and Hepatic and Peripheral Glucose Metabolism.* Journal of Biological Chemistry, 2011. **286**(42): p. 36163-36170.
383. Natsuizaka, M., et al., *IGFBP3 promotes esophageal cancer growth by suppressing oxidative stress in hypoxic tumor microenvironment.* American Journal of Cancer Research, 2014. **4**(1): p. 29-41.
384. Bravo, D., et al., *2-Methoxyestradiol-Mediated Induction of Frzb Contributes to Cell Death and Autophagy in MG63 Osteosarcoma Cells.* J Cell Biochem, 2017. **118**(6): p. 1497-1504.
385. Qin, S., et al., *FRZB knockdown upregulates beta-catenin activity and enhances cell aggressiveness in gastric cancer.* Oncol Rep, 2014. **31**(5): p. 2351-7.
386. Huang, J., et al., *Activation of antibacterial autophagy by NADPH oxidases.* Proceedings of the National Academy of Sciences of the United States of America, 2009. **106**(15): p. 6226-6231.
387. Meischl, C., et al., *Ischemia induces nuclear NOX2 expression in cardiomyocytes and subsequently activates apoptosis.* Apoptosis, 2006. **11**(6): p. 913-921.
388. Lei, Y., et al., *Inhibition of ANKRD1 sensitizes human ovarian cancer cells to endoplasmic reticulum stress-induced apoptosis.* Oncogene, 2015. **34**(4): p. 485-95.
389. Rutkowski, D.T., et al., *The role of p58IPK in protecting the stressed endoplasmic reticulum.* Mol Biol Cell, 2007. **18**(9): p. 3681-91.
390. van Huizen, R., et al., *P58IPK, a novel endoplasmic reticulum stress-inducible protein and potential negative regulator of eIF2alpha signaling.* J Biol Chem, 2003. **278**(18): p. 15558-64.
391. Avivar-Valderas, A., et al., *PERK Integrates Autophagy and Oxidative Stress Responses To Promote Survival during Extracellular Matrix Detachment.* Molecular and Cellular Biology, 2011. **31**(17): p. 3616-3629.
392. Huber, A.L., et al., *p58(IPK)-Mediated Attenuation of the Proapoptotic PERK-CHOP Pathway Allows Malignant Progression upon Low Glucose.* Molecular Cell, 2013. **49**(6): p. 1049-1059.
393. Zhao, L.H., et al., *Alteration of the unfolded protein response modifies neurodegeneration in a mouse model of Marinesco-Sjogren syndrome.* Human Molecular Genetics, 2010. **19**(1): p. 25-35.
394. Genereux, J.C., et al., *Unfolded protein response-induced ERdj3 secretion links ER stress to extracellular proteostasis.* Embo Journal, 2015. **34**(1): p. 4-19.
395. Nakatani, Y., et al., *Involvement of endoplasmic reticulum stress in insulin resistance and diabetes.* Journal of Biological Chemistry, 2005. **280**(1): p. 847-851.
396. Fedeles, S.V., et al., *Sec63 and Xbp1 regulate IRE1 alpha activity and polycystic disease severity.* Journal of Clinical Investigation, 2015. **125**(5): p. 1955-1967.
397. Hassan, H., et al., *Essential Role of X-Box Binding Protein-1 during Endoplasmic Reticulum Stress in Podocytes.* Journal of the American Society of Nephrology, 2016. **27**(4): p. 1055-1065.
398. Ma, R., et al., *7,8-DHF Treatment Induces Cyr61 Expression to Suppress Hypoxia Induced ER Stress in HK-2 Cells.* Biomed Res Int, 2016. **2016**: p. 5029797.
399. Borkham-Kamphorst, E., et al., *Adenoviral CCN gene transfers induce in vitro and in vivo endoplasmic reticulum stress and unfolded protein response.* Biochim Biophys Acta, 2016. **1863**(11): p. 2604-2612.

400. Cattaneo, M., et al., *Down-modulation of SEL1L, an Unfolded Protein Response and Endoplasmic Reticulum-associated Degradation Protein, Sensitizes Glioma Stem Cells to the Cytotoxic Effect of Valproic Acid.* Journal of Biological Chemistry, 2014. **289**(5): p. 2826-2838.
401. Sha, H.B., et al., *The ER-Associated Degradation Adaptor Protein Sel1L Regulates LPL Secretion and Lipid Metabolism.* Cell Metabolism, 2014. **20**(3): p. 458-470.
402. Lenna, S., et al., *The HLA-B*35 allele modulates ER stress, inflammation and proliferation in PBMCs from Limited Cutaneous Systemic Sclerosis patients.* Arthritis Res Ther, 2015. **17**: p. 363.
403. Khan, S.Y., et al., *FOXE3 contributes to Peters anomaly through transcriptional regulation of an autophagy-associated protein termed DNAJB1.* Nature Communications, 2016. **7**.
404. Cui, X., et al., *DNAJB1 destabilizes PDCD5 to suppress p53-mediated apoptosis.* Cancer Lett, 2015. **357**(1): p. 307-15.
405. Sbiera, S., et al., *Mitotane Inhibits Sterol-O-Acyl Transferase 1 Triggering Lipid-Mediated Endoplasmic Reticulum Stress and Apoptosis in Adrenocortical Carcinoma Cells.* Endocrinology, 2015. **156**(11): p. 3895-3908.
406. Shibuya, Y., et al., *Inhibiting ACAT1/SOAT1 in Microglia Stimulates Autophagy-Mediated Lysosomal Proteolysis and Increases A beta 1-42 Clearance.* Journal of Neuroscience, 2014. **34**(43): p. 14484-14501.
407. Li, B., et al., *The melanoma-associated transmembrane glycoprotein Gpnmb controls trafficking of cellular debris for degradation and is essential for tissue repair.* Faseb Journal, 2010. **24**(12): p. 4767-4781.
408. Tanaka, H., et al., *The potential of GPNMB as novel neuroprotective factor in amyotrophic lateral sclerosis.* Scientific Reports, 2012. **2**.
409. Gupta, S., et al., *NOXA contributes to the sensitivity of PERK-deficient cells to ER stress.* FEBS Lett, 2012. **586**(22): p. 4023-30.
410. Eno, C.O., et al., *Noxa couples lysosomal membrane permeabilization and apoptosis during oxidative stress.* Free Radical Biology and Medicine, 2013. **65**: p. 26-37.
411. Oda, E., et al., *Noxa, a BH3-only member of the Bcl-2 family and candidate mediator of p53-induced apoptosis.* Science, 2000. **288**(5468): p. 1053-8.
412. Rosati, A., et al., *BAG3: a multifaceted protein that regulates major cell pathways.* Cell Death & Disease, 2011. **2**.
413. Fonseca, S.G., et al., *Wolfram syndrome 1 gene negatively regulates ER stress signaling in rodent and human cells.* J Clin Invest, 2010. **120**(3): p. 744-55.
414. Yamada, T., et al., *WFS1-deficiency increases endoplasmic reticulum stress, impairs cell cycle progression and triggers the apoptotic pathway specifically in pancreatic beta-cells.* Hum Mol Genet, 2006. **15**(10): p. 1600-9.
415. Hwang, K.C., et al., *Cloning, sequencing, and characterization of the murine nm23-M5 gene during mouse spermatogenesis and spermiogenesis.* Biochemical and Biophysical Research Communications, 2003. **306**(1): p. 198-207.
416. Li, F., et al., *Identification of NME5 as a contributor to innate resistance to gemcitabine in pancreatic cancer cells.* Febs Journal, 2012. **279**(7): p. 1261-1273.
417. Chen, R., et al., *DNA damage-inducible transcript 4 (DDIT4) mediates methamphetamine-induced autophagy and apoptosis through mTOR signaling pathway in cardiomyocytes.* Toxicology and Applied Pharmacology, 2016. **295**: p. 1-11.
418. Dall'Armi, C., et al., *The phospholipase D1 pathway modulates macroautophagy.* Nat Commun, 2010. **1**: p. 142.

419. Yamada, M., et al., *Overexpression of phospholipase D prevents actinomycin D-induced apoptosis through potentiation of phosphoinositide 3-kinase signalling pathways in Chinese-hamster ovary cells.* Biochemical Journal, 2004. **378**: p. 649-656.
420. Jang, Y.H., et al., *Cleavage of phospholipase D1 by caspase promotes apoptosis via modulation of the p53-dependent cell death pathway.* Cell Death and Differentiation, 2008. **15**(11): p. 1782-1793.
421. Sun, G.D., et al., *The endoplasmic reticulum stress-inducible protein Niban regulates eIF2alpha and S6K1/4E-BP1 phosphorylation.* Biochem Biophys Res Commun, 2007. **360**(1): p. 181-7.
422. Huang, C.H., et al., *Role of HERP and a HERP-related Protein in HRD1-dependent Protein Degradation at the Endoplasmic Reticulum.* Journal of Biological Chemistry, 2014. **289**(7): p. 4444-4454.
423. Oda, Y., et al., *Derlin-2 and Derlin-3 are regulated by the mammalian unfolded protein response and are required for ER-associated degradation.* Journal of Cell Biology, 2006. **172**(3): p. 383-393.
424. Al-Furoukh, N., et al., *ClpX stimulates the mitochondrial unfolded protein response (UPRmt) in mammalian cells.* Biochimica Et Biophysica Acta-Molecular Cell Research, 2015. **1853**(10): p. 2580-2591.
425. Seo, J.H., et al., *The Mitochondrial Unfoldase-Peptidase Complex ClpXP Controls Bioenergetics Stress and Metastasis.* Plos Biology, 2016. **14**(7).
426. Kampinga, H.H. and S. Bergink, *Heat shock proteins as potential targets for protective strategies in neurodegeneration.* Lancet Neurology, 2016. **15**(7): p. 748-759.
427. McCallister, C., B. Kdeiss, and N. Nikolaidis, *HspA1A, a 70-kDa heat shock protein, differentially interacts with anionic lipids.* Biochemical and Biophysical Research Communications, 2015. **467**(4): p. 835-840.
428. Wu, F.H., et al., *Extracellular HSPA1A promotes the growth of hepatocarcinoma by augmenting tumor cell proliferation and apoptosis-resistance.* Cancer Letters, 2012. **317**(2): p. 157-164.
429. Matsumori, Y., et al., *Reduction of caspase-8 and-9 cleavage is associated with increased c-FLIP and increased binding of Apaf-1 and Hsp70 after neonatal hypoxic/ischemic injury in mice overexpressing Hsp70.* Stroke, 2006. **37**(2): p. 507-512.
430. Cheng, Y.S., D.Z. Dai, and Y. Dai, *AQP4 KO exacerbating renal dysfunction is mediated by endoplasmic reticulum stress and p66Shc and is attenuated by apocynin and endothelin antagonist CPU0213.* Eur J Pharmacol, 2013. **721**(1-3): p. 249-58.
431. Bejarano, E., et al., *Connexins modulate autophagosome biogenesis.* Nature Cell Biology, 2014. **16**(5): p. 401-U55.
432. Martins-Marques, T., et al., *Ischaemia-induced autophagy leads to degradation of gap junction protein connexin43 in cardiomyocytes.* Biochemical Journal, 2015. **467**: p. 231-245.
433. Goubaeva, F., et al., *Cardiac mitochondrial connexin 43 regulates apoptosis.* Biochemical and Biophysical Research Communications, 2007. **352**(1): p. 97-103.
434. Corum, D.G., P.N. Tsichlis, and R.C. Muise-Helmericks, *AKT3 controls mitochondrial biogenesis and autophagy via regulation of the major nuclear export protein CRM-1.* Faseb Journal, 2014. **28**(1): p. 395-407.
435. Shao, Y.P. and A.E. Aplin, *Akt3-Mediated Resistance to Apoptosis in B-RAF-Targeted Melanoma Cells.* Cancer Research, 2010. **70**(16): p. 6670-6681.
436. Wen, K.W. and B. Damania, *Hsp90 and Hsp40/Erdj3 are required for the expression and anti-apoptotic function of KSHV K1.* Oncogene, 2010. **29**(24): p. 3532-44.

437. Zimmerman, M., et al., *IFN-gamma upregulates survivin and Ifi202 expression to induce survival and proliferation of tumor-specific T cells.* PLoS One, 2010. **5**(11): p. e14076.
438. Xin, H., et al., *Increased expression of Ifi202, an IFN-activatable gene, in B6.Nba2 lupus susceptible mice inhibits p53-mediated apoptosis.* J Immunol, 2006. **176**(10): p. 5863-70.
439. Erdreich-Epstein, A., J.Y. Xu, and X.H. Ren, *Pid1 Is a Novel Sensitizer of Brain Tumor Cells to Chemotherapy.* Neuro-Oncology, 2014. **16**.
440. Jansen, P., et al., *Roles for the pro-neurotrophin receptor sortilin in neuronal development, aging and brain injury.* Nature Neuroscience, 2007. **10**(11): p. 1449-1457.
441. Ryder, C., et al., *Acidosis Promotes Bcl-2 Family-mediated Evasion of Apoptosis INVOLVEMENT OF ACID-SENSING G PROTEIN-COUPLED RECEPTOR GPR65 SIGNALING TO MEK/ERK.* Journal of Biological Chemistry, 2012. **287**(33): p. 27863-27875.
442. Hur, W., et al., *SOX4 overexpression regulates the p53-mediated apoptosis in hepatocellular carcinoma: clinical implication and functional analysis in vitro.* Carcinogenesis, 2010. **31**(7): p. 1298-307.
443. Valdearcos, M., et al., *Lipin-2 Reduces Proinflammatory Signaling Induced by Saturated Fatty Acids in Macrophages.* Journal of Biological Chemistry, 2012. **287**(14): p. 10894-10904.
444. Frigola, J., et al., *Hypermethylation of the prostacyclin synthase (PTGIS) promoter is a frequent event in colorectal cancer and associated with aneuploidy.* Oncogene, 2005. **24**(49): p. 7320-6.
445. Sakurai, D., et al., *Fc epsilon RI gamma-ITAM is differentially required for mast cell function in vivo.* Journal of Immunology, 2004. **172**(4): p. 2374-2381.
446. Swanson, M.S. and A.B. Molofsky, *Autophagy and inflammatory cell death, partners of innate immunity.* Autophagy, 2005. **1**(3): p. 174-6.
447. Dunker, N., et al., *The role of transforming growth factor beta-2, beta-3 in mediating apoptosis in the murine intestinal mucosa.* Gastroenterology, 2002. **122**(5): p. 1364-75.
448. Abedini, M.R., et al., *Cell fate regulation by gelsolin in human gynecologic cancers.* Proc Natl Acad Sci U S A, 2014. **111**(40): p. 14442-7.
449. Franke, T.F., et al., *PI3K/Akt and apoptosis: size matters.* Oncogene, 2003. **22**(56): p. 8983-98.

Appendices

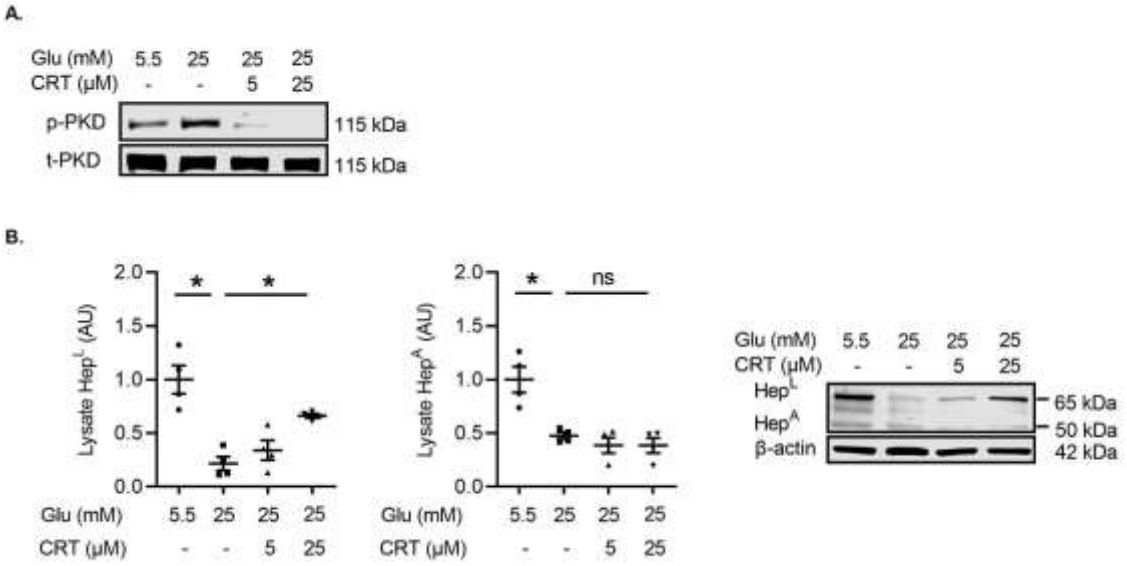

Supplementary Fig. 3.1. High glucose activation of protein kinase D promotes secretion of Hep^{L}.

RAOECs were pre-incubated with or without CRT0066101 (5 and 25 μM), a PKD specific inhibitor for 1 h prior to treatment with NG or HG for 30 min. Lysates were used to determine the activation of PKD (A) and the intracellular content of heparanase (B), n=4. Data are presented as mean ± SEM (Student's t-test). *p<0.05.

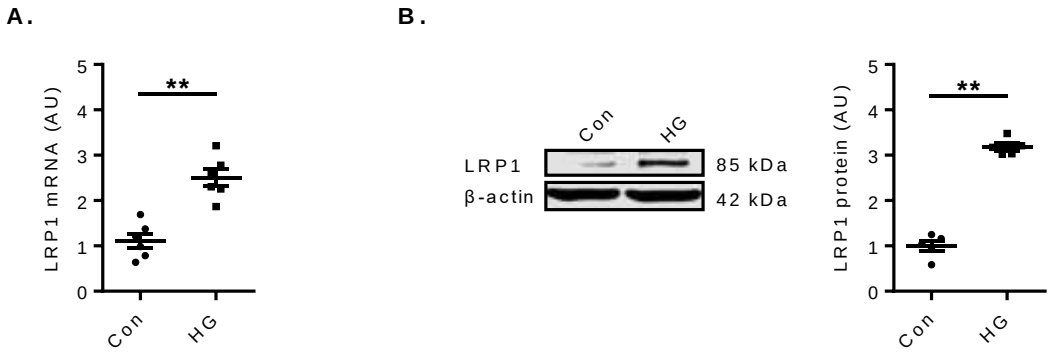

Supplementary Fig. 3.2. High glucose is a stimulus for LRP1 mRNA and protein expression.

RAOEC were incubated in HG for 6 or 12 h to determine LRP1 mRNA (A) and protein (B), respectively, n=5-6. Data are presented as mean ± SEM (Student's t-test). ***p*<0.01.

A.

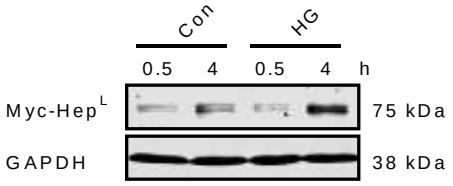
Con
HG
0.5
4
0.5
4
h
Myc-Hep^{L}
GAPDH
75 kDa
38 kDa

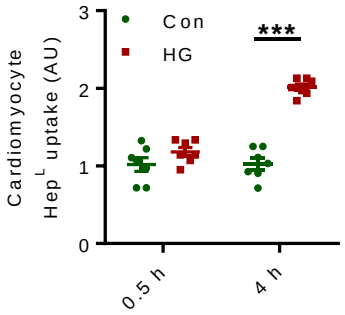
Con
HG
***
Cardiomyocyte Hep^{L} uptake (AU)
0
1
2
3
0.5 h
4 h

B.

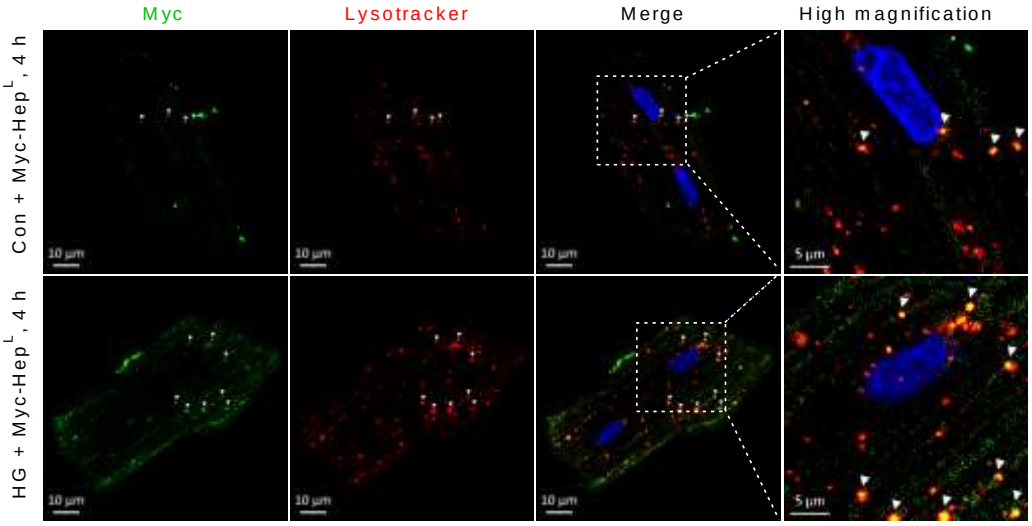
Myc
Lysotracker
Merge
High magnification
Con + Myc-Hep^{L}, 4 h
HG + Myc-Hep^{L}, 4 h
10 μm
5 μm

C.

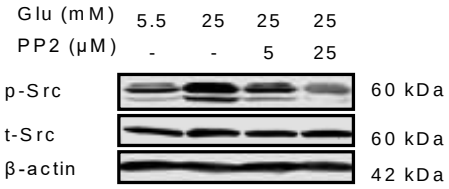
Glu (mM)
5.5
25
25
25
PP2 (μM)
-
-
5
25
p-Src
t-Src
β-actin
60 kDa
60 kDa
42 kDa

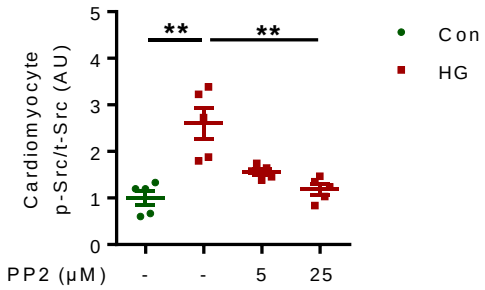
**
**
Con
HG
Cardiomyocyte p-Src/t-Src (AU)
0
1
2
3
4
5
PP2 (μM)
-
-
5
25

D.

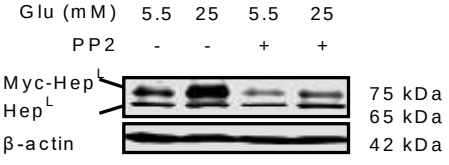
Glu (mM)
5.5
25
5.5
25
PP2
-
-
+
+
Myc-Hep^{L}
Hep^{L}
β-actin
75 kDa
65 kDa
42 kDa

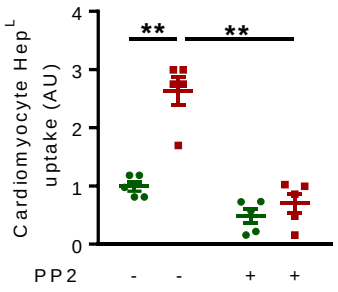
**
**
Cardiomyocyte Hep^{L} uptake (AU)
0
1
2
3
4
PP2
-
-
+
+

Supplementary Fig. 3.3. The uptake of Hep^{L} by cardiomyocytes is accelerated in high glucose in vitro

Cardiomyocytes were incubated with NG or HG in the presence of 500 ng/ml myc-Hep^{L}. Cell lysates were collected at indicated time points to measure Hep^{L} uptake (A), n=7. Cardiomyocytes seeded on slides were placed in a 6 well plate, treated with NG or HG for 4 h in the presence of 500 ng/ml myc-Hep^{L}. Lysosomes were labeled with LysoTracker (red) for 30 min prior to fixation. Anti-rabbit myc antibody (1:400) and DAPI (blue) were added, and immunofluorescence staining examined under a confocal microscope. The merged image of heparanase and lysosomes is described in the third (scale bar, 10 µm) and fourth (scale bar, 5 µm) panels from left (B) and are data from a representative experiment. Myocytes were pre-treated with or without PP2 (5-25 µM) for 15 min prior to incubation with NG or HG for 30 min. Cell lysates were collected to determine the activation of Src (C), n=5. Cardiomyocytes were pre-incubated with or without PP2 (25 µM, 15 min) prior to treatment with NG or HG in the presence of 500 ng/ml myc-Hep^{L}. Cell lysates were collected, and Western Blot used to determine the uptake of Hep^{L} (D), n=5. Data are presented as mean ± SEM (Student's t-test). ** p<0.01, *** p<0.001.

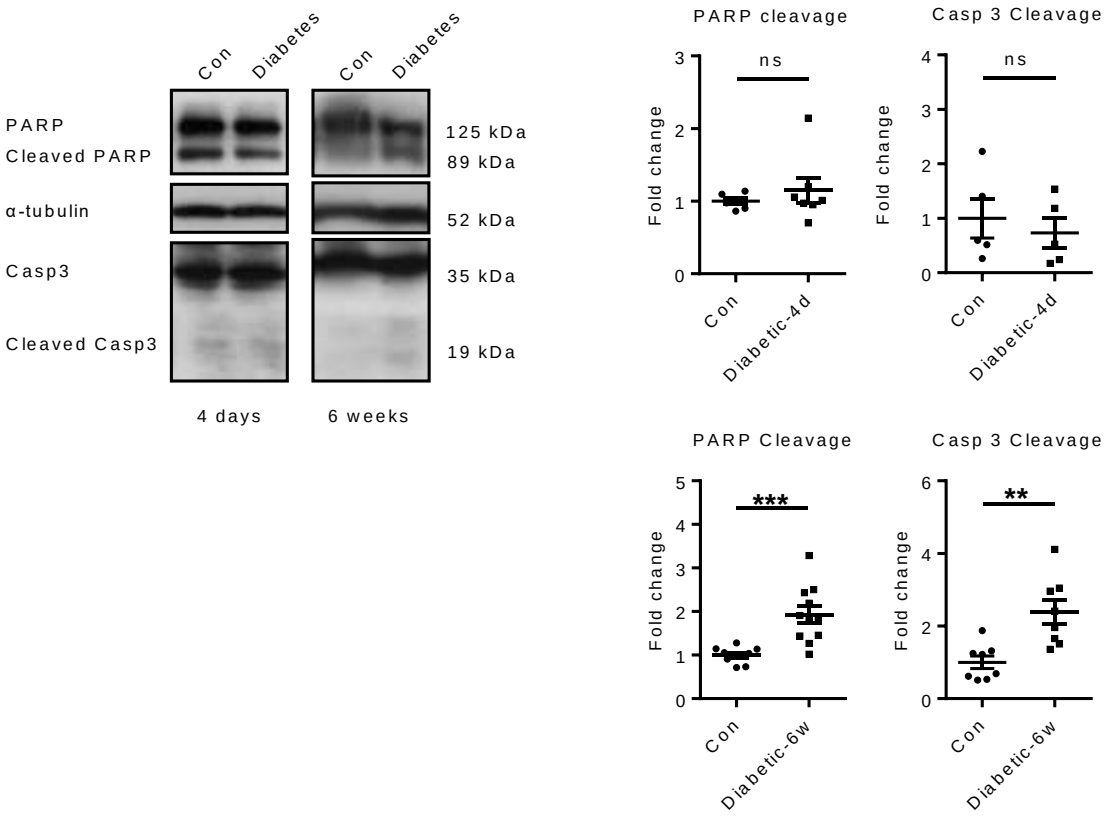

Supplementary Fig. 3.4. Chronic but not acute diabetes induces cell death in the rat heart.

Whole hearts were isolated from STZ (55 mg/kg) injected rats at the indicated times, and the cleavage of caspase 3 and PARP were determined using Western blot, n=5-11. Data are presented as mean ± SEM (Student's t-test). **p<0.01, ***p<0.001.

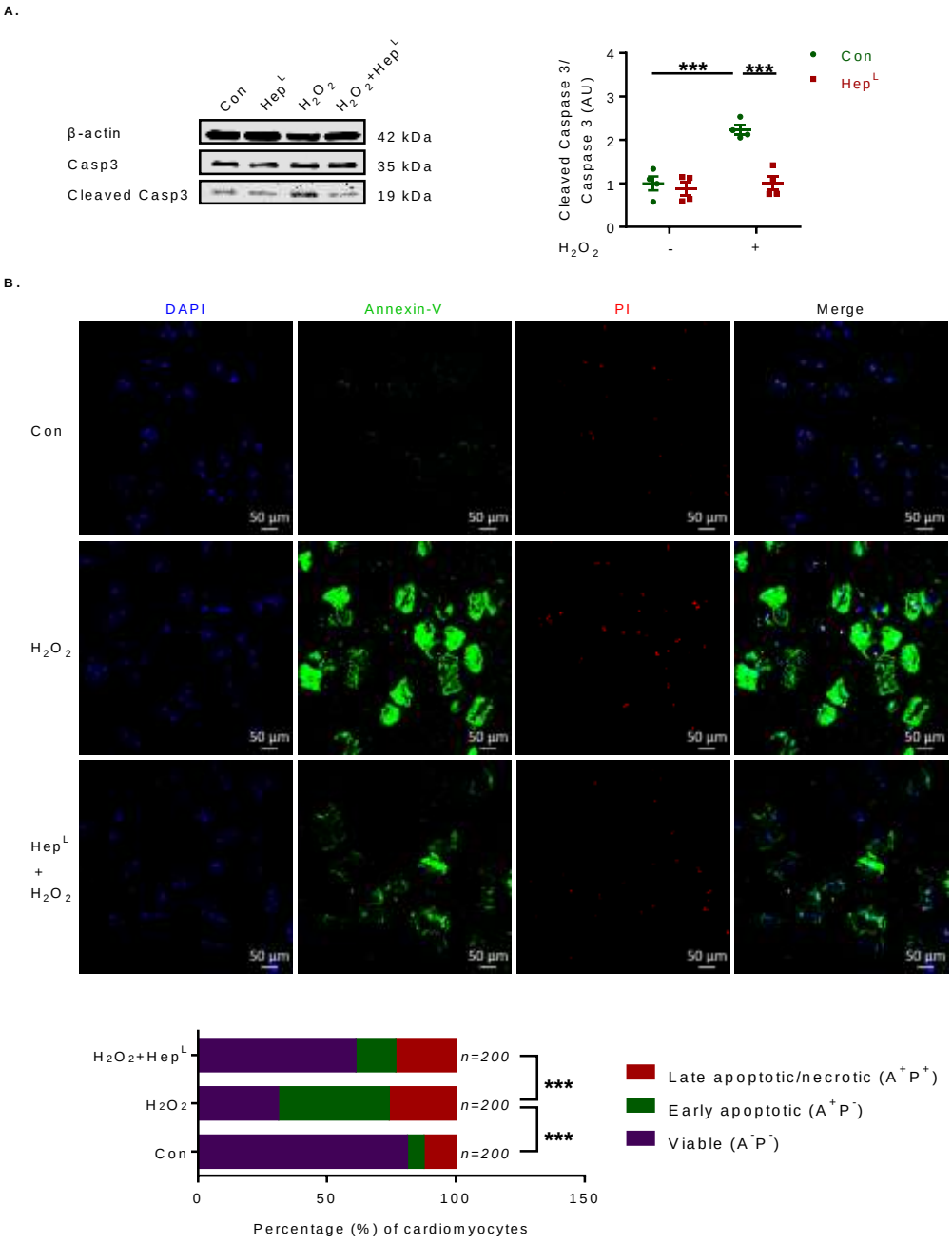

Supplementary Fig. 3.5. Hep^{L} protects cardiomyocytes from H_2O_2 induced apoptosis.

Isolated rat cardiomyocytes were incubated with 10 µM H_2O_2 and/or 500 ng/mL myc-Hep^{L} for 12 h, and caspase 3 protein measured, n=4 (A). Annexin V/PI staining, as markers of apoptosis, were also determined after cardiomyocyte incubation with H_2O_2 and/or myc-Hep^{L} (B), n=200 pooled from 4 independent experiments. Scale bar, 50 µm. Data are presented as mean ± SEM (Two-way ANOVA for A and One-way ANOVfor B). *p<0.05, ***p<0.001.

Supplementary Table 3.1

Anti-apoptotic genes					
Accession No.	**Gene Symbol/Name**	**Description**	**Aliases**	**Function**	**Fold Change**
NM_012854	Il10	Interleukin 10	CSIF	Inhibitor of TNFα induced apoptosis [296, 297]	5.4
NM_022274	Birc5	Baculoviral IAP Repeat Containing 5	API4, Survivin	Inhibitor of apoptosis [298-300]	3.2
NM_012870	**Tnfrsf11b**	Tumor Necrosis Factor Receptor Superfamily, Member 11b	Osteoprotegerin (OPG)	Decoy receptor for TRAIL activation of extrinsic pathway [301]	2.2
NM_001130554	Card10	Caspase Recruitment Domain Family, Member 10		Regulator of NF-κB and cell proliferation [302]	1.6
NM_057138	**Cflar**	CASP8 And FADD-Like Apoptosis Regulator	c-FLIP	Prevents activation of the extrinsic pathway [303, 304]	1.5
NM_031535	Bcl2l1	Bcl2-like 1	Bcl-xl	Inhibitor of intrinsic pathway [304, 305]	1.5
NM_133416	Bcl2a1	BCL2-Related Protein A1		Reduces apoptosis following I/R [306, 307]	-2.1
Pro-apoptotic genes					
Accession No.	**Gene Symbol/Name**	**Description**	**Aliases**	**Function**	**Fold Change**

NM_001108873	**Tnfrsf10b**	Tumor Necrosis Factor Receptor Superfamily, Member 10b	TRAIL-R2, DR5	Component of extrinsic pathway [304, 308]	-5.5
NM_012762	Casp1	Caspase 1	IL1β-Convertase	Involves in the signaling pathways of apoptosis, necrosis and inflammation [309, 310]	-3.4
NM_022277	Casp8	Caspase 8		Component of extrinsic pathway [304]	-3.2
NM_001100480	Tradd	TNFRSF1A-Associated Via Death Domain		Component of extrinsic pathway [304]	-2.6
NM_053704	Bik	BCL2-Interacting Killer		Component of intrinsic pathway [304]	-1.8
NM_022260	Casp7	Caspase 7		Apoptosis effector [304]	-1.8
NM_130426	Tnfrsf1b	Tumor Necrosis Factor Receptor Superfamily, Member 1B	TNF-R2	Component of extrinsic pathway [311, 312]	-1.7
NM_145681	**Tnfsf10**	Tumor Necrosis Factor (Ligand) Superfamily, Member 10	TRAIL, Apo-2L	Activator of extrinsic pathway [304]	-1.5
NM_022698	Bad	BCL2-Associated		Component of intrinsic	-1.5

		Agonist Of Cell Death		pathway [304]	
NM_012908	Faslg	Fas Ligand	CD95-L, Tnfsf6	Activator of extrinsic pathway [304, 308]	3.6
NM_130422	Casp12	Caspase 12		Mediates TNFa induced apoptosis [313]	3.7

Supplementary Table 3.1. Apoptosis-related genes that show at least a 1.5-fold dysregulation (up- or downregulation) in the Hep^{L}-treated primary rat cardiomyocyte samples compared with control.

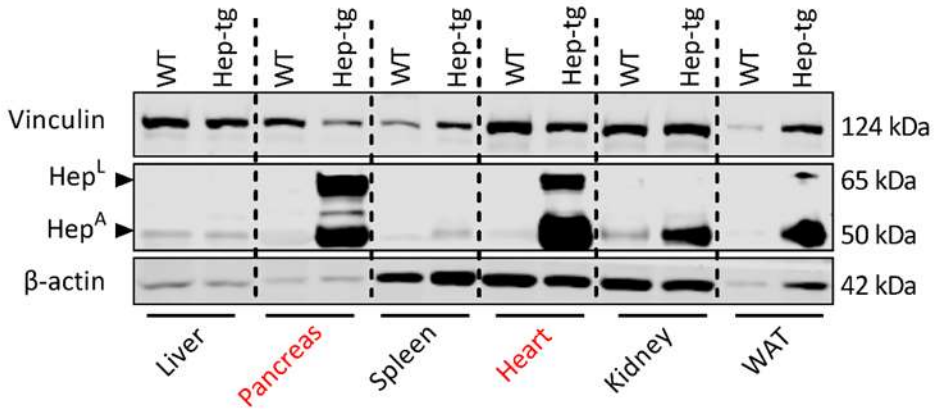

Supplementary Fig 4.1. Differential expression of heparanase.

Protein expression of heparanase in 6 tissues from WT and Hep-tg mice (n=6).

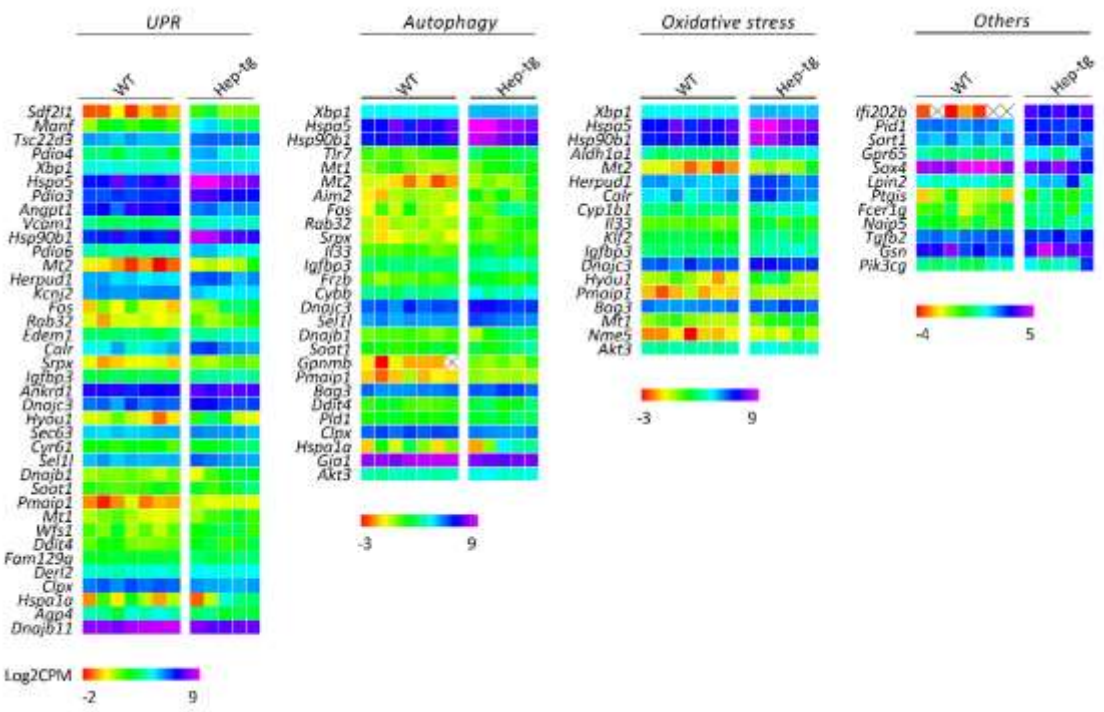

Supplementary Fig 4.2. Heat map highlighting differentially regulated genes involved in different mechanisms of cell survival.

Cladogram shows clustering of biological replicates from WT (n=7) and Hep-tg (n=5) mice ventricle.

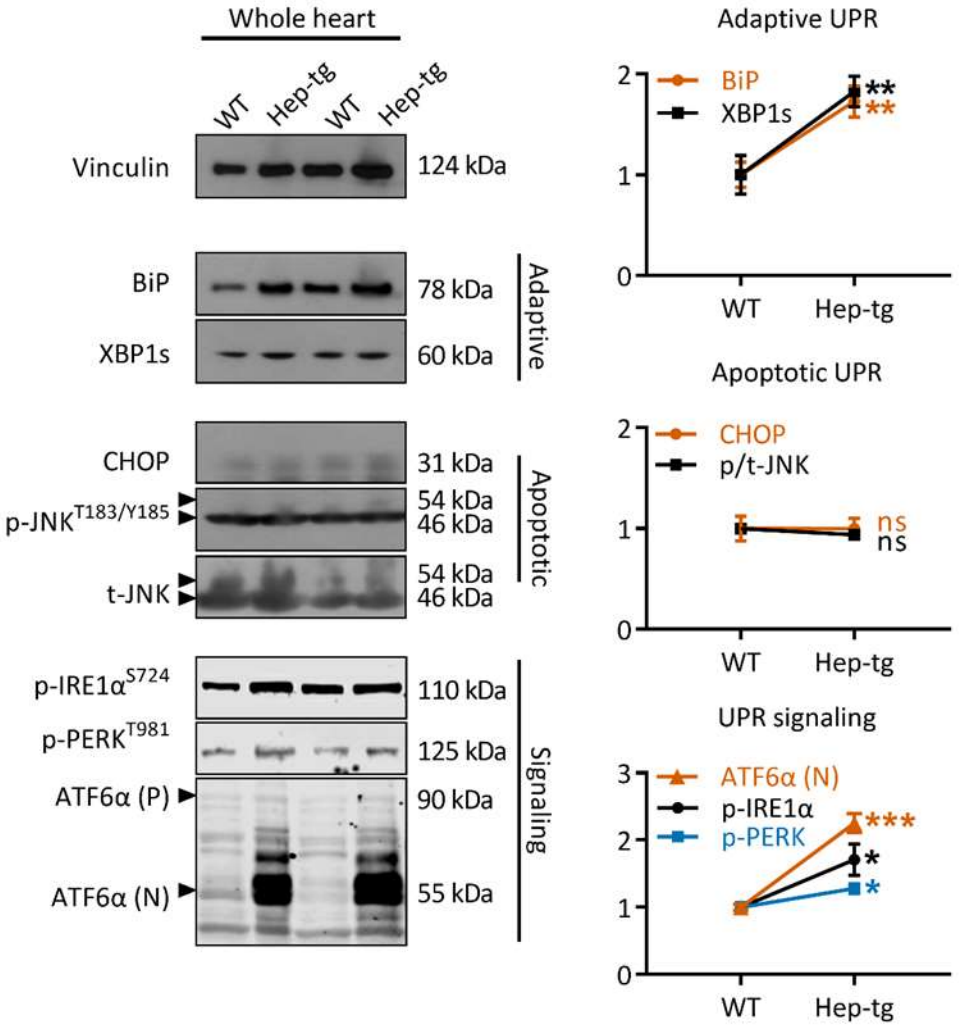

Supplementary Fig 4.3. Protein expression of representative UPR related proteins in WT and Hep-tg mice whole heart (n=5-23).

Data are presented as mean ± SEM (Student's t-test). *p<0.05, **p<0.01, ***p<0.001.

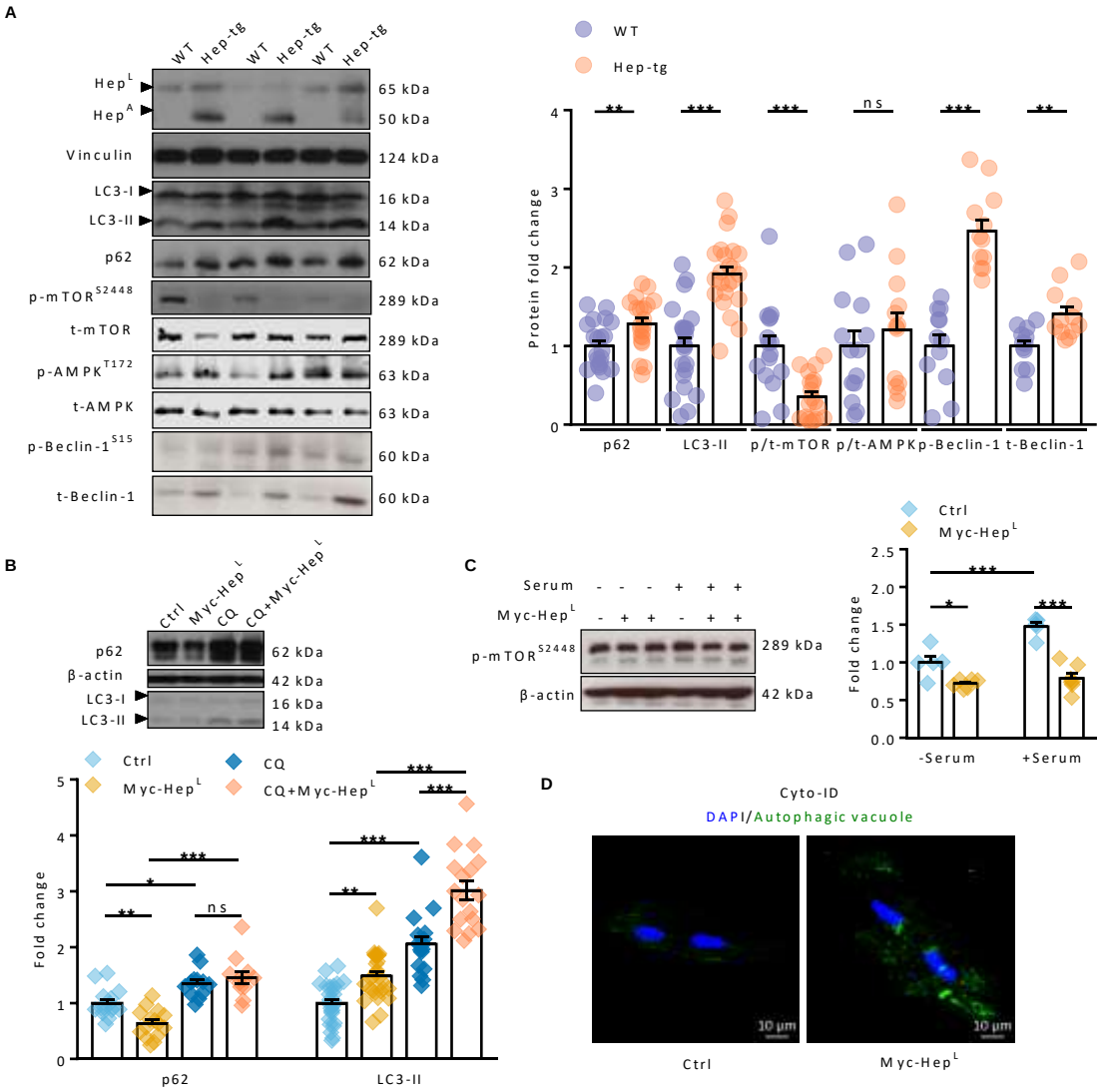

Supplementary Fig 4.4. Autophagy in Hep-tg whole heart and cardiomyocytes treated with recombinant Hep^{L}.

A: Measurement of autophagy markers in whole heart by Western blot (n=12-23). B: Isolated rat cardiomyocytes were treated with Myc-HepL (500 ng/mL) and/or CQ (10 µM) and autophagy proteins p62 and LC3 measured (n=15). C: Isolated mouse cardiomyocytes were incubated with or without serum (0.1% FBS) and treated with 500 ng/mL recombinant Myc-HepL for 12 h, followed by determination of mTOR phosphorylation (n=5-7). D: Immunofluorescence was used to observe autophagic vacuole in rat cardiomyocytes treated with or without recombinant Myc-HepL (n=5). Data are presented as mean ± SEM (Student's t-test for A and Two-way ANOVA for B and C). *p<0.05, **p<0.01, ***p<0.001.

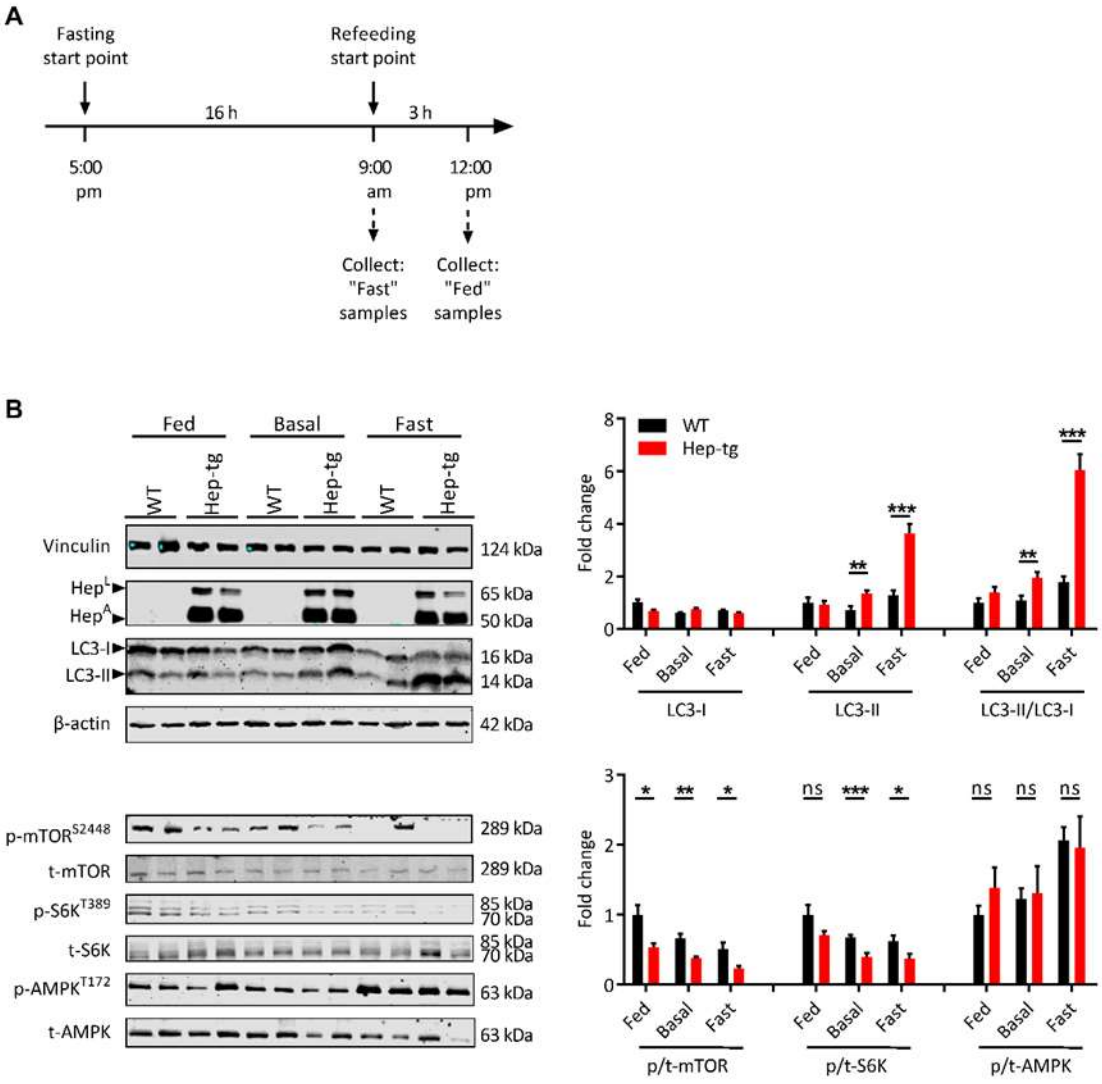

Supplementary Fig 4.5. Autophagy in fasting and re-fed WT and Hep-tg mouse heart.

A: Diagram describing the fasting/refeeding procedure. B: Protein expression of LC3 and mTOR signalling molecules in WT and Hep-tg mice heart under fed, basal, and fasting conditions (n=6-12). Data are presented as mean ± SEM (Student's t-test). **p*<0.05, ***p*<0.01, ****p*<0.001.

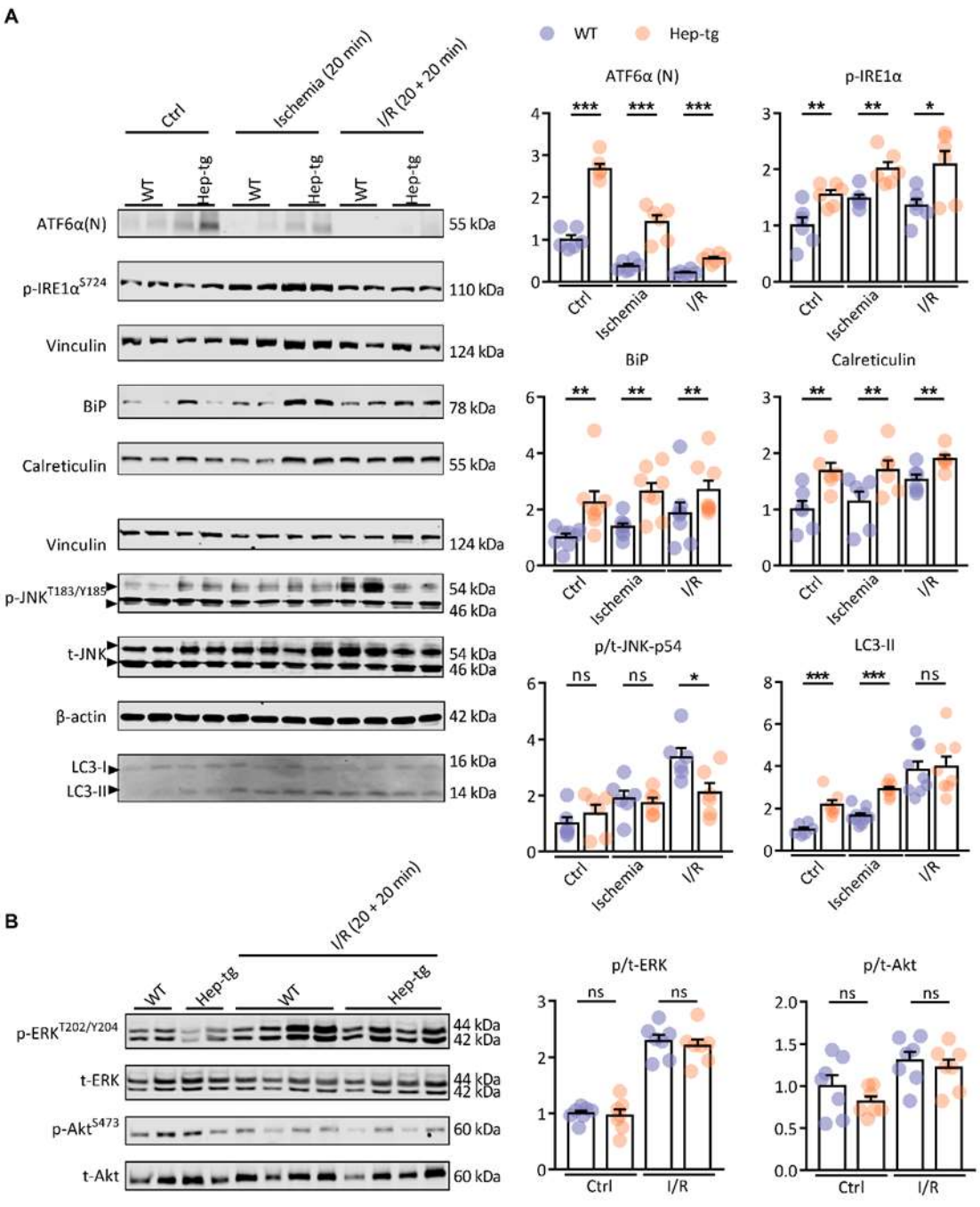

Supplementary Fig 4.6. UPR and RISK signalling during I/R.

Measurement of A: UPR signalling and autophagy (n=6-18) and B: RISK pathway markers (n=7) after 20 min ischemia and I/R. Data are presented as mean ± SEM (Two-way ANOVA). *p<0.05, **p<0.01, ***p<0.001.

Supplementary Table 4.1. Complete list of genes that are differentially expressed in Hep-tg mice ventricle.

	gene_id	gene_name	log2FoldChange	log2CPM
1	ENSMUSG00000026535	Ifi202b	7.73	2.99
2	ENSMUSG00000035273	Hpse	5.14	3.7
3	ENSMUSG00000046805	Mpeg1	2.29	3.87
4	ENSMUSG00000090015	Gm15446	4.3	2.57
5	ENSMUSG00000026532	Spta1	-2.57	3.96
6	ENSMUSG00000026675	Hsd17b7	-3.16	3.69
7	ENSMUSG00000026605	Cenpf	-2.47	4.27
8	ENSMUSG00000073491	Ifi213	-3.27	0.99
9	ENSMUSG00000020120	Plek	1.51	3.73
10	ENSMUSG00000024471	Myot	0.98	5.34
11	ENSMUSG00000038147	Cd84	2.19	2.58
12	ENSMUSG00000022865	Cxadr	-1.28	6.34
13	ENSMUSG00000073489	Ifi204	1.33	4.21
14	ENSMUSG00000053062	Jam2	0.77	7.63
15	ENSMUSG00000022769	Sdf2l1	2.39	1.19
16	ENSMUSG00000069792	Wfdc17	2.17	1.67
17	ENSMUSG00000032575	Manf	2.01	3.83
18	ENSMUSG00000073490	Ifi207	1.22	3.76
19	ENSMUSG00000031431	Tsc22d3	0.8	6.16
20	ENSMUSG00000038521	C1s1	0.99	3.61
21	ENSMUSG00000025823	Pdia4	1.68	4.54
22	ENSMUSG00000023349	Clec4n	2.05	0.65
23	ENSMUSG00000020484	Xbp1	0.83	5.14
24	ENSMUSG00000079105	C7	1.5	2.01
25	ENSMUSG00000074102	Rbm15b	1.41	2.89
26	ENSMUSG00000026864	Hspa5	1.62	8.83
27	ENSMUSG00000027248	Pdia3	1	7.64
28	ENSMUSG00000024672	Ms4a7	1.7	1.86
29	ENSMUSG00000043613	Mmp3	2.12	0.82
30	ENSMUSG00000015396	Cd83	1.45	1.59
31	ENSMUSG00000022309	Angpt1	-1.18	7.24
32	ENSMUSG00000020044	Timp3	0.84	7.97
33	ENSMUSG00000027962	Vcam1	1.03	4.25
34	ENSMUSG00000020048	Hsp90b1	1.35	8.4
35	ENSMUSG00000020571	Pdia6	1	4.92
36	ENSMUSG00000040181	Fmo1	0.79	4.49
37	ENSMUSG00000040170	Fmo2	1.15	5.27
38	ENSMUSG00000053279	Aldh1a1	0.82	4.04

39	ENSMUSG00000101389	Ms4a4a	1.73	0.87
40	ENSMUSG00000022148	Fyb	1.73	0.8
41	ENSMUSG00000044583	Tlr7	1.09	2.33
42	ENSMUSG00000031762	Mt2	1.79	0.48
43	ENSMUSG00000037860	Aim2	1.59	1.14
44	ENSMUSG00000040552	C3ar1	1.13	2.83
45	ENSMUSG00000031770	Herpud1	1.15	5.89
46	ENSMUSG00000041695	Kcnj2	-0.73	5.96
47	ENSMUSG00000021250	Fos	1.78	2.12
48	ENSMUSG00000019832	Rab32	1.27	1.24
49	ENSMUSG00000043004	Gng2	0.99	3.57
50	ENSMUSG00000025351	Cd63	1.07	3.55
51	ENSMUSG00000029919	Hpgds	1.77	2.17
52	ENSMUSG00000048120	Entpd1	0.67	3.77
53	ENSMUSG00000069516	Lyz2	1.35	5.35
54	ENSMUSG00000030104	Edem1	0.66	3.75
55	ENSMUSG00000033777	Tlr13	1.47	1.07
56	ENSMUSG00000049037	Clec4a1	1.52	1.88
57	ENSMUSG00000089672	NA	0.99	2.99
58	ENSMUSG00000043336	Filip1l	0.63	4.92
59	ENSMUSG00000003814	Calr	1.21	6.04
60	ENSMUSG00000029675	Eln	-1.28	2.68
61	ENSMUSG00000038642	Ctss	1.17	4.69
62	ENSMUSG00000041616	Nppa	1.78	2.96
63	ENSMUSG00000022372	Sla	1.32	0.5
64	ENSMUSG00000063383	Zfp947	-1.42	2.2
65	ENSMUSG00000015852	Fcrls	1.67	1.33
66	ENSMUSG00000090084	Srpx	1.25	0.95
67	ENSMUSG00000028868	Wasf2	0.8	4.07
68	ENSMUSG00000040888	Gfer	-2.05	0.26
69	ENSMUSG00000043832	Clec4a3	1.36	2.26
70	ENSMUSG00000028967	Errfi1	0.77	3.92
71	ENSMUSG00000022742	Cpox	-1.06	6.48
72	ENSMUSG00000010080	Epn3	1.39	1.51
73	ENSMUSG00000023828	Slc22a3	0.97	3.26
74	ENSMUSG00000029321	Slc10a6	1.44	1.22
75	ENSMUSG00000026674	Ddr2	0.6	4.66
76	ENSMUSG00000024087	Cyp1b1	0.8	3.95
77	ENSMUSG00000053347	Zfp943	-0.93	6.52
78	ENSMUSG00000039252	Lgi2	1.42	0.92
79	ENSMUSG00000033544	Angptl1	-1.85	1.59
80	ENSMUSG00000055541	Lair1	1.39	1.53
81	ENSMUSG00000087141	Plcxd2	1.71	0.89

82	ENSMUSG00000024810	Il33	0.87	1.98
83	ENSMUSG00000055148	Klf2	0.86	3.31
84	ENSMUSG00000042156	Dzip1	1.27	0.59
85	ENSMUSG00000036552	Ermard	0.97	2.37
86	ENSMUSG00000045658	Pid1	0.78	3.17
87	ENSMUSG00000027524	Edn3	1.02	1.84
88	ENSMUSG00000020427	Igfbp3	0.71	3.82
89	ENSMUSG00000027004	Frzb	1	1.89
90	ENSMUSG00000078185	Chml	-0.83	5.23
91	ENSMUSG00000016194	Hsd11b1	0.81	3.58
92	ENSMUSG00000027799	Nbea	-0.71	4.31
93	ENSMUSG00000015340	Cybb	0.83	4
94	ENSMUSG00000021750	Fam107a	1.23	1.74
95	ENSMUSG00000059142	Zfp945	0.72	5.48
96	ENSMUSG00000018401	Mtmr4	0.72	3.99
97	ENSMUSG00000021866	Anxa11	0.9	1.92
98	ENSMUSG00000024803	Ankrd1	0.65	8.15
99	ENSMUSG00000022136	Dnajc3	0.78	7.05
100	ENSMUSG00000032115	Hyou1	1.51	1.63
101	ENSMUSG00000025154	Arhgap19	1.11	1.42
102	ENSMUSG00000026650	Meig1	1.23	0.61
103	ENSMUSG00000028339	Col15a1	-0.87	4.47
104	ENSMUSG00000019802	Sec63	0.61	5.87
105	ENSMUSG00000034442	Trmt5	-0.64	4.38
106	ENSMUSG00000043263	Ifi209	-1.39	1.2
107	ENSMUSG00000028195	Cyr61	0.8	2.87
108	ENSMUSG00000020964	Sel1l	0.62	5.8
109	ENSMUSG00000074622	Mafb	0.91	2.72
110	ENSMUSG00000014959	Gorasp2	0.99	3.91
111	ENSMUSG00000068747	Sort1	0.8	2.84
112	ENSMUSG00000028497	Hacd4	0.7	2.98
113	ENSMUSG00000032802	Srxn1	1.04	1.48
114	ENSMUSG00000031972	Acta1	0.93	2.57
115	ENSMUSG00000038175	Mylip	0.73	3.43
116	ENSMUSG00000031375	Bgn	0.96	4.28
117	ENSMUSG00000021665	Hexb	0.81	4.33
118	ENSMUSG00000041773	Enc1	0.99	1.84
119	ENSMUSG00000031596	Slc7a2	0.82	1.9
120	ENSMUSG00000028581	Laptm5	0.94	0.64
121	ENSMUSG00000017466	Timp2	1.05	3.68
122	ENSMUSG00000051853	Arf3	1.06	1.98
123	ENSMUSG00000005483	Dnajb1	1.12	2.03
124	ENSMUSG00000033972	Zfp944	-0.79	5.09

125	ENSMUSG00000090035	Galnt4	0.79	2.77
126	ENSMUSG00000030737	Slco2b1	1.03	2.26
127	ENSMUSG00000026600	Soat1	0.85	2.64
128	ENSMUSG00000021886	Gpr65	1.1	1.54
129	ENSMUSG00000029816	Gpnmb	1.4	0.56
130	ENSMUSG00000044067	Gpr22	-0.77	7.22
131	ENSMUSG00000068270	Shroom4	0.64	4.24
132	ENSMUSG00000099398	Ms4a14	1.19	1.24
133	ENSMUSG00000042331	Specc1	1.26	1.06
134	ENSMUSG00000076431	Sox4	-0.91	4.22
135	ENSMUSG00000022667	Cd200r1	1.21	1.12
136	ENSMUSG00000024521	Pmaip1	1.12	0.22
137	ENSMUSG00000042254	Cilp	-1.31	0.34
138	ENSMUSG00000030847	Bag3	0.56	6.42
139	ENSMUSG00000024066	Xdh	1.11	2.99
140	ENSMUSG00000058503	Fam133b	-0.96	4.07
141	ENSMUSG00000031765	Mt1	1.07	1.66
142	ENSMUSG00000033949	Trim36	-1.23	1.06
143	ENSMUSG00000039474	Wfs1	1.02	2.39
144	ENSMUSG00000041540	Sox5	1.02	1.37
145	ENSMUSG00000068856	Sf3b4	1.04	1.49
146	ENSMUSG00000021234	Fam161b	0.85	2.64
147	ENSMUSG00000020431	Adcy1	-1.32	1.56
148	ENSMUSG00000038463	Olfml2b	0.95	2.75
149	ENSMUSG00000069833	Ahnak	0.52	7.13
150	ENSMUSG00000030218	Mgp	1.03	2.91
151	ENSMUSG00000047648	Fbxo30	-0.69	6.4
152	ENSMUSG00000063919	Srrm4	0.74	2.01
153	ENSMUSG00000019188	H13	1.25	1.36
154	ENSMUSG00000047330	Kcne4	0.95	0.77
155	ENSMUSG00000060771	Tsga10	-1.08	2.92
156	ENSMUSG00000044033	Ccdc141	-0.48	7.26
157	ENSMUSG00000060244	Alyref2	-1.39	0.36
158	ENSMUSG00000035984	Nme5	1.15	0.58
159	ENSMUSG00000024052	Lpin2	1.03	2.08
160	ENSMUSG00000025283	Sat1	0.57	4.35
161	ENSMUSG00000020823	Sec14l1	0.64	3.23
162	ENSMUSG00000027712	Anxa5	0.55	5.04
163	ENSMUSG00000020108	Ddit4	0.93	2.41
164	ENSMUSG00000036896	C1qc	0.97	2.12
165	ENSMUSG00000027695	Pld1	0.63	2.59
166	ENSMUSG00000026483	Fam129a	0.49	3.36
167	ENSMUSG00000030317	Timp4	0.78	3.57

168	ENSMUSG00000003617	Cp	0.42	6.77
169	ENSMUSG00000018442	Derl2	0.5	4.82
170	ENSMUSG00000049791	Fzd4	0.65	4.57
171	ENSMUSG00000053199	Arhgap20	0.49	5.13
172	ENSMUSG00000075232	Amd1	0.62	7.18
173	ENSMUSG00000053963	Stum	1.32	0.47
174	ENSMUSG00000062593	Lilrb4a	0.77	3.01
175	ENSMUSG00000022146	Osmr	0.59	3.61
176	ENSMUSG00000004609	Cd33	1.01	2.02
177	ENSMUSG00000024664	Fads3	0.99	3
178	ENSMUSG00000021248	Tmed10	0.51	6.84
179	ENSMUSG00000041012	Cmtm8	-1.25	1.88
180	ENSMUSG00000026670	Uap1	0.66	4.09
181	ENSMUSG00000017969	Ptgis	1.2	0.43
182	ENSMUSG00000000278	Scpep1	0.89	1.74
183	ENSMUSG00000015880	Ncapg	-1.15	0.72
184	ENSMUSG00000058715	Fcer1g	1.16	0.51
185	ENSMUSG00000095930	Nim1k	1.01	0.79
186	ENSMUSG00000064210	Ano6	0.73	2.65
187	ENSMUSG00000019848	Popdc3	0.66	3.29
188	ENSMUSG00000042129	Rassf4	1.04	1.82
189	ENSMUSG00000036155	Mgat5	0.71	2.87
190	ENSMUSG00000045690	Wdr89	-1.02	0.57
191	ENSMUSG00000020034	Tcp11l2	-0.62	6.76
192	ENSMUSG00000042379	Esm1	0.91	0.78
193	ENSMUSG00000024304	Cdh2	-0.54	8.22
194	ENSMUSG00000061762	Tac1	-1.15	0.72
195	ENSMUSG00000006014	Prg4	0.78	2.04
196	ENSMUSG00000035783	Acta2	0.66	2.48
197	ENSMUSG00000056492	Adgrf5	0.64	6.26
198	ENSMUSG00000048865	Arhgap30	0.71	1.57
199	ENSMUSG00000039982	Dtx4	0.97	1.75
200	ENSMUSG00000098134	Rnf113a2	-0.99	1.67
201	ENSMUSG00000040848	Sft2d2	0.54	4.1
202	ENSMUSG00000015357	Clpx	-0.46	6.13
203	ENSMUSG00000029135	Fosl2	0.54	4.17
204	ENSMUSG00000036594	H2-Aa	1.06	2.34
205	ENSMUSG00000025893	Kbtbd3	-0.68	5.17
206	ENSMUSG00000020589	Fam49a	0.57	3.38
207	ENSMUSG00000026062	Slc9a2	0.95	1.35
208	ENSMUSG00000091971	Hspa1a	1.61	2.69
209	ENSMUSG00000020676	Ccl11	1.01	0.73
210	ENSMUSG00000053063	Clec12a	1.21	1.19

211	ENSMUSG00000021903	Galnt15	0.51	4.27
212	ENSMUSG00000037071	Scd1	0.72	3.44
213	ENSMUSG00000026043	Col3a1	-0.71	6.96
214	ENSMUSG00000064061	Dzip3	-0.66	4.37
215	ENSMUSG00000033147	Slc22a15	-0.78	1.13
216	ENSMUSG00000024411	Aqp4	-0.77	4.08
217	ENSMUSG00000050953	Gja1	-0.51	9.07
218	ENSMUSG00000049130	C5ar1	0.97	0.8
219	ENSMUSG00000030062	Rpn1	0.61	3.6
220	ENSMUSG00000029217	Tec	0.76	2.31
221	ENSMUSG00000053769	Lysmd1	-1.24	0.5
222	ENSMUSG00000026986	Hnmt	-0.6	4.63
223	ENSMUSG00000079419	Ms4a6c	0.81	3.65
224	ENSMUSG00000045868	Gvin1	-0.83	5.44
225	ENSMUSG00000019699	Akt3	0.52	4.2
226	ENSMUSG00000071203	Naip5	0.87	0.55
227	ENSMUSG00000039239	Tgfb2	0.6	2.94
228	ENSMUSG00000045078	Rnf216	-0.8	4.15
229	ENSMUSG00000000976	Heatr6	-0.86	1.76
230	ENSMUSG00000041189	Chrnb1	0.88	1.36
231	ENSMUSG00000020422	Tns3	0.63	3.05
232	ENSMUSG00000026879	Gsn	0.8	3.96
233	ENSMUSG00000022901	Cd86	0.8	1.5
234	ENSMUSG00000048787	Dcun1d3	0.53	3.11
235	ENSMUSG00000004460	Dnajb11	0.77	3.47
236	ENSMUSG00000027540	Ptpn1	0.78	1.55
237	ENSMUSG00000020573	Pik3cg	1.03	1.49
238	ENSMUSG00000020027	Socs2	0.6	4.46
239	ENSMUSG00000051341	Zfp52	-0.76	4.35
240	ENSMUSG00000072623	Zfp9	0.77	3.16

Supplementary Table 4.2. Detailed functional description of the differentially expressed genes that are related to cell survival.

Rank #	ensembl_id	Mgi_symbol	Full name (other name)	Log_2CPM	Fold Change	Process involved			Effect: S=survival A=apoptotic	Note1	Note2
						UPR	Autophagy	Oxidative stress			
	ENSMUSG00000035273	*Hpse*	*heparanase*	3.70	35.26						*Hep-tg*
Cell survival genes related to UPR, autophagy, or oxidative stress											
1	ENSMUSG00000022769	Sdf2l1	stromal cell-derived factor 2-like 1	1.19	5.24	U [314, 315]			S [314, 315]	ER (chaperone)	1.Interacts with BiP, defensin ERAD
2	ENSMUSG00000032575	Manf	mesencephalic astrocyte-derived neurotrophic factor (Armet)	3.83	4.03	U [316, 317]			S [316, 317]	ER, Golgi, ECM	1.Interacts with BiP
3	ENSMUSG00000031431	Tsc22d3	TSC22 domain family member 3	6.16	1.74	U [318]			S [318]		Osmotic stress transcription factor 1
4	ENSMUSG00000025823	Pdia4	protein disulfide isomerase associated 4	4.54	3.20	U [319, 320]			S [319, 320]	ER (PDI chaperone)	1.Protein folding
5	ENSMUSG00000020484	Xbp1	X-box binding protein 1	5.14	1.78	U [321]	A [322, 323]	O [324]	S [325-327]	ER	1.ATF6/IRE1-mediated UPR 2. Both unspliced and spliced XBP1 induce autophagy
6	ENSMUSG00000026864	Hspa5	heat shock protein 5 (Grp78, Bip)	8.83	3.07	U [328, 329]	A [330-332]	O [333]	S [329, 331, 332]	ER (general chaperone)	1.Help protein folding 2. Induce protective autophagy

										Hsp70 machine	
7	ENSMUSG00000027248	Pdia3	protein disulfide isomerase associated 3	7.64	2.00	U [320]			S [320]	ER (PDI chaperone)	1.Protein folding
8	ENSMUSG00000022309	Angpt1	angiopoietin 1	7.24	-2.27	U [334, 335]			S [334]		1.IRE1 induce the expression of Angpt1 1&4. Angpt1 attenuates ER stress induced apoptosis
9	ENSMUSG00000027962	Vcam1	vascular cell adhesion molecule 1	4.25	2.04	U [336, 337]			A [338]		1&3. High expression correlated with apoptosis
10	ENSMUSG00000020048	Hsp90b1	heat shock protein 90, beta member 1 (Grp94)	8.40	2.55	U [339, 340]	A [341]	O [342]	S [343, 344]	ER (general chaperone) Hsp90 machine	1.Protein folding & ERAD
11	ENSMUSG00000020571	Pdia6	protein disulfide isomerase associated 6	4.92	2.00	U [319, 320, 345]			S [319, 320]	ER (PDI chaperone)	1.Protein folding
12	ENSMUSG00000053279	Aldh1a1	aldehyde dehydrogenase family 1, subfamily A1	4.04	1.77			O [346]	S [347]		1&2&4. Protective against oxidative/heavy metal-induced ER stress and apoptosis; modulates autophagy
13	ENSMUSG00000044583	Tlr7	toll-like receptor 7	2.33	2.13		A [348]		A [349]		

14	ENSMUSG00000031765	Mt1	metallothionein 1	1.66	2.10	U [350]	A [351, 352]	O [353]	S [352, 354]	Mitochondrion	1.Expression necessary for induction of BiP 2.Upregulates Beclin 1
15	ENSMUSG00000031762	Mt2	metallothionein 2	0.48	3.46						
16	ENSMUSG00000037860	Aim2	absent in melanoma 2	1.14	3.01		A [355]		A [356]		
17	ENSMUSG00000031770	Herpud1	homocysteine-inducible, endoplasmic reticulum stress-inducible, ubiquitin-like domain member 1	5.89	2.22	U [357, 358]		O [359]	S [359]	ER	1.PERK-mediated UPR & ERAD
18	ENSMUSG00000041695	Kcnj2	potassium inwardly-rectifying channel, subfamily J, member 2	5.96	-1.66	U [360]			A [360]	PM	1.Upregulation by ER stress correlates with cell death
19	ENSMUSG00000021250	Fos	FBJ osteosarcoma oncogene	2.12	3.43	U [361]	A [362]		A [363]		1.Expression necessary for induction of BiP 2.Upregulates Beclin 1
20	ENSMUSG00000019832	Rab32	RAB32, member RAS oncogene family	1.24	2.41	U [364]	A [365]		S [366]		2.Autophagosome formation
21	ENSMUSG00000030104	Edem1	ER degradation enhancer, mannosidase alpha-like 1	3.75	1.58	U [367]			S [368]	ER	1.IRE1-mediated UPR, ubiquitin-dependent ERAD pathway

22	ENSMUSG00000003814	Calr	calreticulin	6.04	2.31	U [369, 370]		O [333]	S [333, 371]	ER (lectin chaperone)	1.ATF6-mediated UPR
23	ENSMUSG00000090084	Srpx	sushi-repeat-containing protein	0.95	2.38	U [372]	A [372, 373]		A [373]	ER, ECM	1.Interacts with GADD34
24	ENSMUSG00000024087	Cyp1b1	cytochrome P450, family 1, subfamily b, polypeptide 1	3.95	1.74			O [374]	S [375, 376]	Cytoplasm, Nucleus ER	4. Reduction of CYP1B1 increase oxidative stress and apoptosis
25	ENSMUSG00000024810	Il33	interleukin 33	1.98	1.83		A [377]	O [378]	S [379]		
26	ENSMUSG00000055148	Klf2	Kruppel like factor 2	3.31	1.82			O [380]	S [380, 381]		3&4. Enhances antioxidant activity of Nrf2 in response to shear stress
27	ENSMUSG00000020427	Igfbp3	insulin-like growth factor binding protein 3	3.82	1.64	U [382]	A [332]	O [383]	S [332]	ECM	2.Binds to BiP
28	ENSMUSG00000027004	Frzb	frizzled-related protein	1.89	2.00		A [384]		A [384, 385]	ECM	2&4. Apoptotic autophagy
29	ENSMUSG00000015340	Cybb	cytochrome b-245, beta polypeptide	4.00	1.78		A [386]		A [387]		
30	ENSMUSG00000024803	Ankrd1	ankyrin repeat domain 1 (cardiac muscle)	8.15	1.57	U [388]			S [388]	Cytoplasm, Nucleus	1&4. Inhibition of ANKRD1 sensitizes cells to ER stress-induced apoptosis. Response to multiple stress and stimuli

											Apoptosis marker
31	ENSMUSG00000022136	Dnajc3	DnaJ heat shock protein family (Hsp40) member C3	7.05	1.72	U [389, 390]	A [391]	O [391]	S [389, 392]	ER (Cochaperone) Hsp70 machine	1&4. Inhibition of PERK mediated ER stress and apoptosis
32	ENSMUSG00000032115	Hyou1	hypoxia up-regulated 1 (Grp170)	1.63	2.85	U [393, 394]		O [395]	S [393]	ER (general chaperone) Hsp70 machine	1.Protein folding
33	ENSMUSG00000019802	Sec63	SEC63 homolog, protein translocation regulator	5.87	1.53	U [396, 397]			S [397]	Hsp70 machine	Interacts with XBP1
34	ENSMUSG00000028195	Cyr61	cysteine rich protein 61	2.87	1.74	U [398, 399]			S [398, 399]	ECM	1&4. Prevention of apoptosis via UPR induction
35	ENSMUSG00000020964	Sel1l	SEL1L ERAD E3 ligase adaptor subunit	5.80	1.54	U [400]	A [401]		S [400]		Interacts with Derl2
36	ENSMUSG00000005483	Dnajb1	DnaJ heat shock protein family (Hsp40) member B1	2.03	2.17	U [402]	A [403]		S [403, 404]	Chaperone Hsp70 machine	
37	ENSMUSG00000026600	Soat1	sterol O-acyltransferase 1	2.64	1.80	U [405]	A [406]		S [405]		
38	ENSMUSG00000029816	Gpnmb	glycoprotein (transmembrane) nmb	0.56	2.64		A [407]		S [407, 408]	PM	2.Recruit LC3 to phagosome

39	ENSMUSG00000024521	Pmaip1	phorbol-12-myristate-13-acetate-induced protein 1 (Noxa)	0.22	2.17	U [409]	A [140]	O [410]	A [140, 411]	Mitochondrion	1&2&4. Contributes to ER stressed induced and autophagy mediated apoptosis
40	ENSMUSG00000030847	Bag3	BCL2 Associated Athanogene 3	6.42	1.47		A [191, 412]	O [191]	S [191, 412]	Cytoplasm Hsp70 machine	
41	ENSMUSG00000039474	Wfs1	Wolfram syndrome 1 homolog (human)	2.39	2.03	U [413, 414]			S [413, 414]	ER	1&4. Loss of Wfs1 increases ER stress and apoptosis & involved in ERAD
42	ENSMUSG00000035984	Nme5	NME/NM23 family member 5	0.58	2.22			O [415]	S [416]	Cytoplasm	4. Confer resistance to cell death in multiple cancer types
43	ENSMUSG00000020108	Ddit4	DNA damage inducible transcript 4	2.41	1.91	U [208]	A [417]		A [417]		Inhibitors of mTOR signaling
44	ENSMUSG00000027695	Pld1	phospholipase D1	2.59	1.55		A [418]		S [419, 420]		2.Promotes autophagy 4.Loss of Pld1 promotes apoptosis Induced by oxidative stress.
45	ENSMUSG00000026483	Fam129a	family with sequence similarity 129, member A	3.36	1.40	U [421]			S [421]		

46	ENSMUSG00000018442	Derl2	Der1-like domain family, member 2	4.82	1.41	U [422, 423]			S [423]		1&4. IRE1 branch, interacts with Sel1l, help protein folding and ERAD
47	ENSMUSG00000015357	Clpx	caseinolytic mitochondrial matrix peptidase chaperone subunit	6.13	-1.38	U [424, 425]	A [425]		S [425]	Mitochondrion	1&2. Loss of Clpx induce protein misfolding and Autophagy
48	ENSMUSG00000091971	Hspa1a	heat shock protein 1A	2.69	3.05	U [426]	A [427]		S [428, 429]	Chaperone Hsp70 machine	
49	ENSMUSG00000024411	Aqp4	aquaporin 4	4.08	-1.71	U [430]			S [430]	PM	1.AQP4 KO induce UPR and downregulate connexion 43 Osmotic stress downregulates aqp4
50	ENSMUSG00000050953	Gja1	gap junction protein, alpha 1 (Connexin 43)	9.07	-1.42		A [431, 432]		A [433]	PM	2.Gja1 KO increases autophagy; autophagy increase Gja1 degradation Upregulates by mechanical stress
51	ENSMUSG00000019699	Akt3	AKT serine/threonine kinase 3	4.20	1.43		A [434]	O [434]	S [435]		
52	ENSMUSG00000004460	Dnajb11	DnaJ heat shock protein family (Hsp40) member B11 (Erdj3)	3.47	1.71	U [394]			S [436]	Hsp70 machine	
[23]Other cell survival related genes											

1	ENSMUSG00000026535	Ifi202b	interferon activated gene 202B	2.99	212.31				S [437, 438]		
2	ENSMUSG00000045658	Pid1	phosphotyrosine interaction domain containing 1	3.17	1.72				A [439]		
3	ENSMUSG00000068747	Sort1	sortilin 1	2.84	1.74				A [440]		
4	ENSMUSG00000021886	Gpr65	G-protein coupled receptor 65	1.54	2.14				S [441]		
5	ENSMUSG00000076431	Sox4	SRY-box 4	4.22	-1.88				S [442]		
6	ENSMUSG00000024052	Lpin2	lipin 2	2.08	2.04				S [443]		
7	ENSMUSG00000017969	Ptgis	prostaglandin I2 synthase	0.43	2.30				A [444]		
8	ENSMUSG00000058715	Fcer1g	Fc fragment of IgE receptor Ig	0.51	2.23				S [445]		
9	ENSMUSG00000071203	Naip5	NLR family, apoptosis inhibitory protein 5	0.55	1.83				S [446]		
10	ENSMUSG00000039239	Tgfb2	transforming growth factor beta 2	2.94	1.52				A [447]		
11	ENSMUSG00000026879	Gsn	gelsolin	3.96	1.74				S [448]		
12	ENSMUSG00000020573	Pik3cg	phosphatidylinositol-4,5-bisphosphate 3-kinase catalytic subunit gamma	1.49	2.04				S [449]		

Red: gene expression alteration implicates pro-apoptosis effect.